Comparative Biochemical Analysis of the Major Yolk Protein in the Sea Urchin Egg and Coelomic Fluid

by

Shemul Dev

A Thesis submitted to the

School of Graduate Studies

in partial fulfillment of the requirements for the degree of

Master of Science

Department of Biochemistry

Memorial University of Newfoundland

May, 2014

St. John's Newfoundland

ABSTRACT

The sea urchin major yolk protein (MYP) is localized in nutritive phagocytes in the testis and ovary, as well as the egg and coelomic fluid of the adult sea urchin. We and others have shown that the egg MYP can drive calcium-dependent, membrane-membrane interactions. However, much less is known about the coelomic fluid-localized MYP. Therefore, we have begun a comparative biochemical analysis of the egg and coelomic fluid MYPs. Sucrose density gradient ultracentrifugation revealed unique elution profiles for the MYP species present in the egg and coelomic fluid. Under reducing conditions, there were two species of MYP both in the egg and the coelomic fluid. Sodium dodecyl sulfate polyacrylamide gel electrophoresis (SDS-PAGE) of the egg and coelomic fluid MYPs under reducing and non-reducing conditions revealed that under reducing conditions, there are two species in each fraction, 170- nad 240 kDa in the egg and 180- and 250 kDa in the coelomic fluid. However, under non-reducing conditions only one species is present in each fraction, 240 kDa in the egg and 250 kDa in the coelomic fluid. In addition, V8 protease peptide mapping showed that all four polypeptide species have very similar primary structures. Further analysis with circular dichroism (CD) revealed that the purified 170- and 180 kDa species possess different secondary structural features. Endogenous tryptophan fluorescence measurements in the presence of different concentrations of calcium showed a notable difference in apparent dissociation constants (calcium); 245- and 475 μM for the egg and coelomic fluid MYPs, respectively. Interestingly, there was no notable difference in the apparent dissociation constants for zinc. Additional assays revealed that both the 170- and 180 kDa species have different

calcium requirements for binding to liposomal membranes, with an apparent dissociation constants (calcium) of 10- and 290 μM for the 170- and 180 kDa species, respectively. In addition, both the 170- and 180 kDa species have different calcium requirement to induce vesicular aggregation, which is correlated with the calcium induced tertiary structural change in both polypeptides. Collectively, these results identify structural differences between the egg and coelomic fluid MYPs which may reflect different functional capabilities between these species.

ACKNOWLEDGEMENTS

I would like to thank my supervisor, Dr. John Robinson, Department of Biochemistry, Memorial University of Newfoundland, for his guidance and encouragement during the course of this project. I appreciate his advice on various research techniques and for the suggestions he made during the preparation of this thesis. Without his supervision and constant help this thesis would not have been possible.

I would like to thank my committee members, Dr. Ross McGowan, Department of Biochemistry, Memorial University of Newfoundland and Dr. Philip Davis, Department of Biochemistry, Memorial University of Newfoundland for their useful suggestions throughout this project.

In addition, I would also like to thank Dr. Michael Hayley for helpful advice during designing different experiments.

I also want to thank to School of Graduate Studies, Memorial University of Newfoundland for their financial support granted through fellowship.

I thank my parents for their constant support.

Table of Contents

List of Tables

List of Figures

Chapter 1: Introduction

1.1 The sea urchin:

The sea urchin is a spiny, hard-shelled animal that lives on the rocky seafloor, from shallow waters to great depths. It is a globular marine invertebrate under the phylum echinodermata, which also includes sea stars, sea cucumbers, brittle stars, and crinoids. There are about 950 different species of sea urchins worldwide. Sea urchins are omnivorous animals and therefore eat both plant and animal matter. The sea urchin mainly feeds on algae, along with decomposing matter such as dead fish, mussels, sponges and barnacles. The main predators of the sea urchin are crabs, large fish, sea otters, eels, birds and humans. In some countries, certain species of the sea urchin are harvested and served as a sushi delicacy. There are black and dull shades of green, olive, brown, purple, blue, and red colored sea urchins.

The sea urchin larvae have bilateral symmetry, but the adult sea urchins have fivefold symmetry (pentamarism), with five equally sized parts radiating out from their central axes (Fig.1.1 A and B). The mouth (known as the Aristotle's lantern) is located in the middle of the lower surface of the sea urchin and has five tooth-like structures for feeding. The anus of the sea urchin is located on the apical surface of the body. The internal organs are enclosed in a hard test composed of fused plates of calcium carbonate covered by a thin dermis and epidermis.

Fig.1.1: Internal structure of a sea urchin. A) Lateral view (from Petrunkevitch, 1875) and B) Top view.

A)

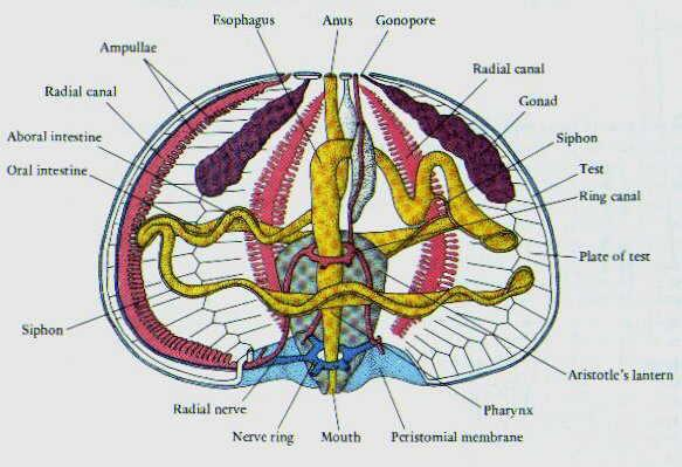
Esophagus
Anus
Gonopore
Ampullae
Radial canal
Radial canal
Gonad
Aboral intestine
Siphon
Oral intestine
Test
Ring canal
Plate of test
Siphon
Aristotle's lantern
Radial nerve
Pharynx
Nerve ring
Mouth
Peristomial membrane

B)

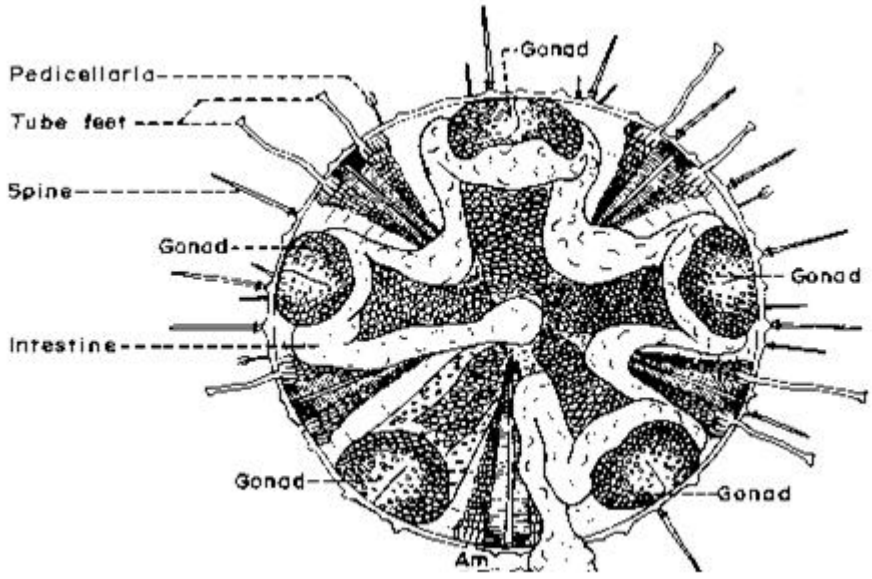
Gonad
Pedicellaria
Tube feet
Spine
Gonad
Gonad
Intestine
Gonad
Gonad
Am

The sea urchins have a round shaped body with long spines. The spines of the sea urchin are used for protection and to trap food particles that are floating around in the water. The spines are controlled by two rings of muscle and are covered with a layer of epithelium. They have small pinching appendages called pedicellaria at the base of spines. Sea urchins also have five paired rows of tiny tube feet which are found amongst the spines. The tube feet of the sea urchin have suction pads which help the sea urchin to move about, capture food, and to hold onto the ocean floor. The sea urchins have a vascular system comprised of water-filled channels that run through the body. Sea urchins have five gonads, and the female sea urchins releases millions of eggs into the water that are then fertilized by the sperm of the male sea urchins.

1.2 The sea urchin as a model organism for developmental studies.

The sea urchin has been most intensely used as a model system for research not only in gene regulation, molecular biology, molecular embryology, fertilization biology, cell biology, and evolutionary biology, but also in other areas like marine population genetics, toxicology and immunity. For more than a century, the sea urchin embryo has been used as an important model organism in developmental biology, due to their relatively simple construction, ease of spawning fertilization and growth of embryos, translucent appearance, and the ease of following the fate of individual cells as development proceeds.

Moreover, sea urchins belong to the deuterostome lineage, which also includes hemichordate (including starfish, sand dollars, and sea cucumbers) and chordates, including humans (Fig. 1.2). Consequently sea urchins are more closely related to vertebrates than fruit flies or worms. It also helps to use the sea urchin as a research model for the analysis of genes that are ancient within the regulatory architecture of human genome, genes that are chordate specific and modified due to evolution. For example, a molecular linkage has been established between a number of genes from the genome of S. purpuratus and mammalian major histocompatibility complex (MHC), even though sea urchins lack MHC genes (Sodergren et al., 2006).

In the past, detailed gene expression analysis of mesoendoderm specification was performed in sea urchin, which has been the basis for the most comprehensive dissection of gene regulatory networks in metazoans (Davidson et al., 2002; Pederson, 2006). The sea urchin has contributed much as a research model in the area of gene expression and gene regulation in development. For example, the discovery of maternal mRNA and pronuclear fusion at fertilization were first recognized in sea urchin eggs. Moreover, the first measurement that established the complexity and distribution of mRNAs, the transcription rates, average and specific mRNA turnover rates, as well as protein synthesis rates, in embryos were first carried out on sea urchin embryos. Extensive characterization of actin genes (Crain et al., 1981, Cooper and Crain, 1982; Overbeek et al., 1981; Schuler et al., 1983; Lee et al., 1984) and identification of specific probes for each gene (Lee et al., 1984) made the sea urchin embryo an advantageous system for early studies of the diversity of expression patterns of individual actin genes (Cox et al., 1986).

Fig. 1.2: The phylogenetic position of the sea urchin relative to other model systems and humans. (Sodergren et al., 2006)

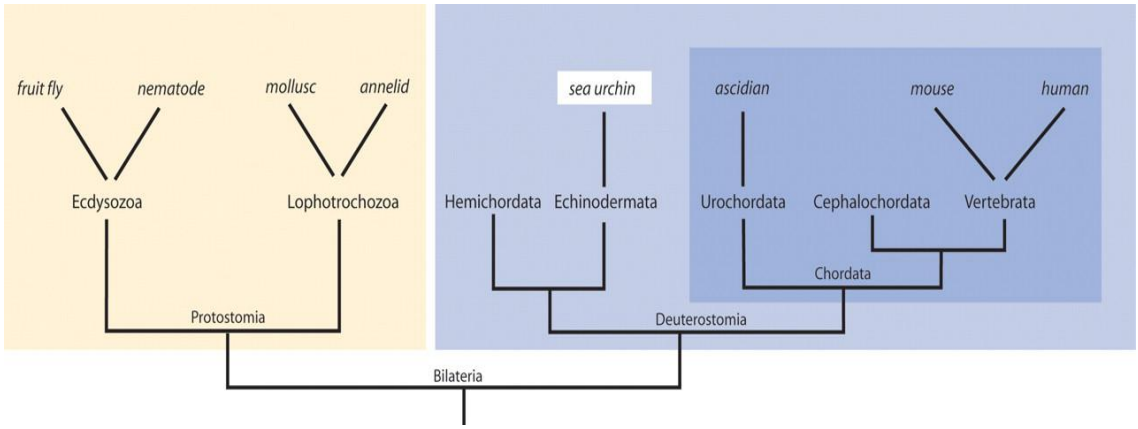
fruit fly
nematode
mollusc
annelid
sea urchin
ascidian
mouse
human
Ecdysozoa
Lophotrochozoa
Hemichordata
Echinodermata
Urochordata
Cephalochordata
Vertebrata
Chordata
Protostomia
Deuterostomia
Bilateria

The sequencing and annotation of the sea urchin genome is also enhancing the utility of this embryo for developmental studies.

The 814-megabase genome of the sea urchin Strongylocentrotus purpuratus has been sequenced using whole genome shotgun and bacterial artificial choromosome (BAC) sequences (Sodengren et al., 2006). Among the 23,300 genes in the sea urchin genome nearly all are related to vertebrate gene families including genes previously thought to be vertebrate specific. An extensive defensome was identified in sea urchin genome. The sea urchin genome also includes orthologs of genes associated with vision, hearing, balance and chemosensation in vertebrates.

In the sea urchin, around 12,000 to 13,000 genes were expressed during the early stages of development, indicating that about 52% of the entire protein coding capacity of the sea urchin genome is expressed during development to the mid–late gastrula stage (Sodengren et al., 2006). About 80% of the sea urchin regulome were expressed during 48 hr of embryogenesis. In addition, more than 1200 genes involved in signal transduction were also identified, including 353 genes for protein kinases. In the sea urchin embryo 87% of signaling kinases and 80% of phosphatases were expressed, confirming the importance of signaling pathways in embryonic development. In addition, more than 90% of the GTPases are also expressed during embryogenesis. The sea urchin embryo also expresses genes encoding proteins like 14-3-3 epsilon and PI-nectin (Russo et al., 2010; Zito et al., 2010). The 14-3-3 epsilon is responsible for many cellular events including stress response, survival and apoptosis (Russo et al., 2010). This protein

expression in the sea urchin embryo increases with stress, indicating its role as a molecular biomarker for the dangerous effects of sunlight occurring in marine organisms living in shallow water.

The sea urchin genome has been sequenced and it encodes about 23,300 genes, which have homology to nearly all vertebrate gene families (Sodergren et al., 2006). Although they are invertebrates, sea urchins share a common ancestor with humans and have more than 7,000 genes orthologs of known human disease-associated genes, including genes associated with Parkinson's, Alzheimer's and Huntington's diseases, as well as muscular dystrophy. Moreover, between 4 and 5% of the genes in the sea urchin genome are related to genes responsible for immune function in humans, including 222 Toll-like receptors and a large family of scavenger receptor cysteine rich proteins (Rast et al., 2006; Pancer, 2000). A complex immune system in purple sea urchin is likely to be controlled by gene expression in coelomocytes similar to vertebrates. Earlier studies on the sea urchin immune system showed the presence of a complement system similar to the chordate alternative complement pathway (Gross et al., 1999; Smith et al., 2006), antibacterial molecules (Haug et al., 2002; Li et al., 2008) and the expression of a large array of scavenger receptor cystein rich proteins (Pancer, 2000). These findings make the sea urchin a model system for studies on human disease and immune system.

There are also many additional reasons why the sea urchin embryo is useful as a research model in the study of developmental gene regulation. Technologies have been established in sea urchins allowing for very high throughput gene transfer, stable nuclear extract

production as well as methods for whole mounts in situ hybridization and immunocytology. As a result we now know a great detail about the signaling and transcription control processes (e.g; cis-regulatory elements) leading to cell specification in this embryo. The sea urchin research has also contributed to our understanding of the cell biology and biochemistry of eggs and the fertilization process. For example: Cyclins were first observed in sea urchin eggs, the role of cell adhesion was also first analyzed in sea urchins and cytonemes were also discovered in sea urchin embryos.

The sea urchin embryo is also used as a model organism for biomineralization research due to the presence of spicules (tiny calcitic skeletal elements in Fig. 1.3). To date, 231 spicule matrix proteins have been identified in S. purpuratus (Mann et al., 2010). These proteins play important roles in matrix assembly and mineralization.

Sea urchin embryos have been successfully used in studies of the effects of various antiproliferative, antimitotic and cytotoxic agents e.g; anti-cancer drug testing and identification of anti-mitotic molecules that affect tubulin dynamics (Nishioka et al., 2003, Semenova et al., 2006). During early embryogenesis, the series of successive cell divisions occurring at approximately 30 min intervals and the cilliary swimming ability of hatched P. lividus embryos within 9-12 h after fertilization can be easily monitored and quantified, making the sea urchin embryo an important model to screen molecules affecting microtubule structure and function (Semenova et al., 2006).

Fig.1.3: Scanning electron microscopy of the purified S. purpuratus spicules (Man et al., 2010).

A. Section showing fragments of spicules prepared from pluteus larvae. B. Higher magnification showing the clean surfaces of spicule fragments. C. Cross-section of a fractured spicule. D. Deeper etching and higher magnification picture.

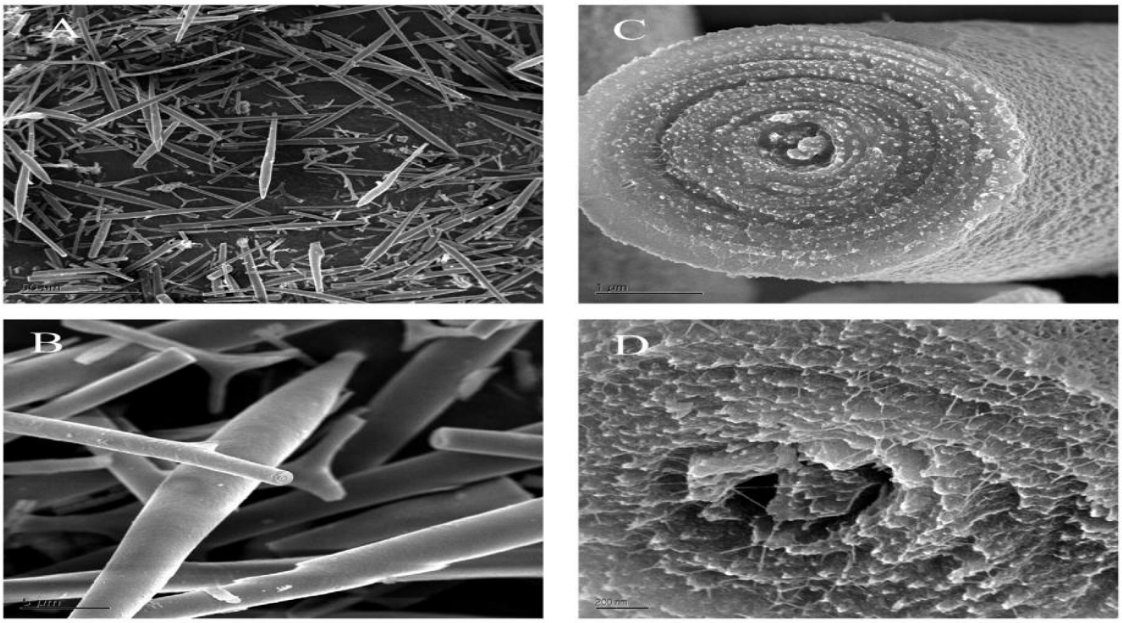
A
C
B
D

The sea urchin is also widely used as a model organism for the study of the composition and functions of egg yolk granules, an abundant organelle in the sea urchin egg and embryo (Armant et al., 1986, Scott et al., 1990), and also for the major yolk protein present in the yolk granules (Perera et al., 2004, Hayley et al., 2006). The yolk granule is the primary membrane-bound organelle present in the eggs, embryos and larvae, occupying approximately one-third of the cytoplasmic volume and more than 50 % of the total yolk protein present in yolk granule is the major yolk protein (Kari and Rottmann, 1985). This makes the sea urchin an appropriate model organism for large scale biochemical studies during development.

Recently, the sea urchin has been also used as a tool to monitor environmental hazards e.g; sea water pollution. The teratogenic effects of various chemical agents and drugs on embryo development have been extensively studied (Kobayashi, 1980; Ozretic et al., 1985, Sconzo et al., 1995, Morale et al., 1998). A recent study has shown that the coelomocytes, cells of the sea urchin coelomic fluid, can be used as a bioindicator for sea water pollution (Matranga et al., 2000). The number of coelomocytes increases with the level of sea water pollution.

1.3 Sea urchin gametogenesis:

In the sea urchin, the major yolk protein is mainly synthesized in the digestive tract and accumulates in the nutritivie phagocytes before gametogenesis to supply nutrients for the developing gamets (Unuma et al., 2002). In the sea urchin, reproduction, gametogenesis

and intra-gonadal nutrient storage and utilization are linked processes. During gametogenesis, the size of the sea urchin gonads increases due to the increase of size and/or number of germinal and somatic cells (nutritive phagocytes) present in the germinal epithelium of gonads. Nutritive phagocytes in both sexes play an important role in gametogenesis by supplying required nutrients, such as protein, lipid and glycogen (Walker, 1982; Walker et al., 2005 & 2007). Here, I describe the structural changes that occur inside the gonads during different stages of gametogenesis as determined by Fuji et al., (1960) and Unuma et al., (1996 & 2002) (Fig. 1.4).

Stage 1 Immature gonad before gametogenesis. Abundant amounts of the major yolk protein (MYP) are stored in the immature gonads of both sexes of sea urchins. However, as gametogenesis proceeds the amount of the major yolk protein decreases (Unuma et al., 1998). The amount of MYP decreased rapidly in male but decreased gradually in female. In stage 1, nutritive phagocytes filled the gonadal acinus of both sexes of sea urchins. A few young oocytes are present in the periphery of the gonadal acini of ovaries whereas, in this stage detection of spermatogenic cells was difficult in testes (Unuma and Walker, 2010). The ovarian lumen is occasionally filled with hematoxylin-stained round spots, residue from phagocytized ova (Masuda and Dan, 1977; Tominaga & Takashima, 1987), whereas, hematoxylin-stained amorphous shaped speckles, residues from phagocytized spermatozoa are often present in nutritive phagocytes of testes (Kato & Ishikawa, 1982, Reunov et al., 2004).

Fig. 1.4: Representative morphology in the ovary (A—D) and testis (E—H) of P. depressus at different stages.

At stage 1 (A,E), nutritive phagocytes filled the gonadal lumina. At stage 2 (B,F), the periphery is filled with many developing oocytes or clusters of spermatogonia. At stage 3 (C,G), the center of the lumina is filled with ripe ova or spermatozoa by replacing nutritive phagocytes. At stage 4 (D,H; fully mature gonad), the lumina are filled with ripe ova or spermatozoa. NP, nutritive phagocyte; OC, oocyte; OV, ripe ovum; SG, spermatogonium; SC, spermatocyte; SZ, spermatozoon. Scale bar, 100 μm. (Unuma et al., 2003)

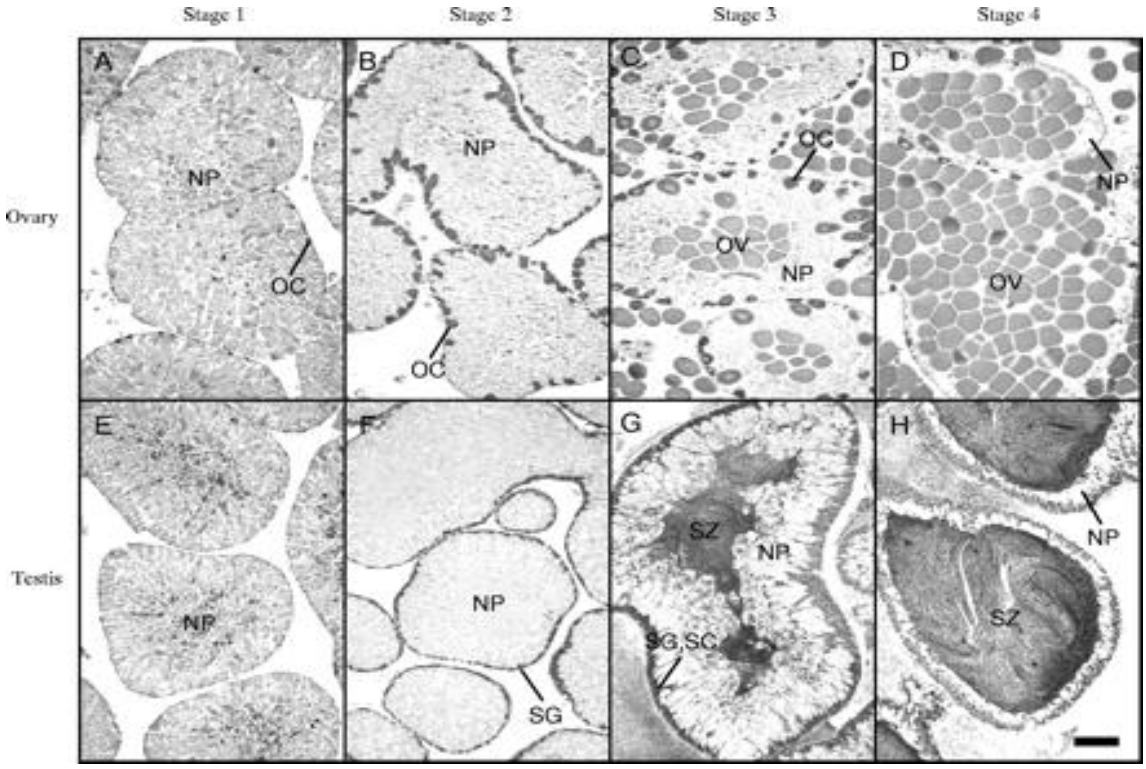
Stage 1
Stage 2
Stage 3
Stage 4
Ovary
Testis
A
B
C
D
E
F
G
H
NP
OC
OV
SZ
SG
SG,SC

Stage 2 Beginning of spermatogenesis. In this stage the periphery of gonadal acini of both sexes is filled with clusters of developing oocytes and spermatogonia, but the gonadal lumina are still filled with nutritive phagocytes. The membrane-bound vesicles or cytoplasm of nutritive phagocytes in both sexes is filled with a variety of proteins, carbohydrates and lipids. The principle protein accumulated in this stage is the major yolk protein, a glycoprotein with a native molecular weight of about 1020 kDa (Unuma et al., 1998, 2003). In the gonads of both sexes more than 80% of the total protein is MYP.

Stage 3 Middle of gametogenesis. The center of gondal lumina are filled with ripe ova or spermatozoa by replacing nutritive phagocytes. In this stage, mobilization of nutrients from nutritive phagocytes and gonadal cell mitosis begins. The periphery of gonadal acini becomes filled with numerous developing oocytes or clusters of spermatogonia and spermatocytes (Ward & Nishioka, 1993; Walker et al., 2005). In this stage nutritive phagocytes gradually decreased in size. As gametogenesis proceeds a quantitative decrease in MYP with an increase in nucleic acids and proteins other than MYP was observed in both sexes (Unuma et al., 2003). It was suggested that, the MYP stored in both ovarian and testicular nutritive phagocytes are utilized to synthesis amino acids, that in turn provides materials to synthesis new proteins, nucleic acids and other nitrogenous substances that constitute eggs and sperm. The MYP presents in the yolk granules also degrades to provide nutrient for the larval stage (Scott et al., 1990). In this stage, numerous ovary specific proteins such as hyaline, glycosaminoglycans, serine proteases, ovoperoxidase and proteoliaisin, YP39 are synthesized in the oocytes and are later found in the cortical granules of fully mature ova (Wessel et al., 1998, Schuel et al., 1974,

Haley and Wessel 1999, Sommers et al., 1989; Nomura et al., 1999; Berg and Wessel, 2003). Moreover, testes specific proteins including histone H1, H2B-1, and H2B-2 are produced in spermatogonial cells of testes (Poccia et al., 1989).

Stage 4 Fully-mature gonads at the end of gametogenesis. In this stage the gonadal lumen is filled with fully differentiated gametes in both sexes. The shrunken nutritive phagocytes have already lost their nutrients and are located at the periphery of the gonadal acini. In this stage, gamete storage and spawning are the major activities of the gonads in both sexes. During spawning, the male spawns spermatozoa, which are activated and begin to swim upon contact with sea water and the female releases ova into a cloud of actively moving spermatozoa. The factors that influence spawning are still unknown but a study reported that a small molecular weight protein resulting from phytoplankton blooms initiate spawning in both sexes of S. droebachiensis (Himmelman, 1975; Starr et al., 1992).

Stage 5 After spawning. Nutritive phagocytes gradually phagocytize the residual ova or spermatozoa in the gonadal lumina and grow in size by accumulating nutrients. After this gonads return to Stage 1 and a new cycle begins.

1.4 Properties of the yolk granules

Yolk granules are large membrane-bound organelles comprising approximately 28-38 % of the egg cytoplasmic volume and are found in eggs, embryos and early larvae of the sea

urchin (Harvey, 1932; Costello, 1939). The yolk granule is a spherical or oval shaped organelle, with a diameter of 1-1.7 µm (Gross et al., 1960; Monroy and Maggio, 1964; Armant et al., 1986). It can be separated into two density classes by sucrose density gradient ultracentrifugation. The low density yolk granule fraction contains an acid phosphatase activity and is covered with an approximately 9 nm thick membrane. However, the purified, high density yolk granule is often slightly contaminated with mitochondria. During different stages of development, the chemical composition of the yolk granules also remained unchanged, but the major yolk protein undergoes proteolytic processing (Kari and Rottmann, 1985; Armant et al., 1986; and Harrington and Easton, 1982).

Electron microscopic examination revealed that, yolk granules of sea urchin also have some membrane-bound substructures with a diameter of 20- 30 nm (Takashima, 1971). After osmotic lysis and negative staining, it was revealed that those sub particles are lipoproteins, present throughout development and varying in diameter from about 10-50 nm (Ichio et al., 1978).

Most of the water-soluble lipoproteins in sea urchin eggs are localized in yolk granules (Ichio et al., 1978). Schuel et al., (1975) found that several lysosomal enzymes are also present within yolk granules of sea urchin eggs. The study done by Yokota et al. (1993) revealed that, the yolk granule undergoes morphological changes throughout embryonic development. However, the number and mass of yolk granules do not change. Yolk granules can be classified into four types, according to their structural characteristics

observed in electron microscope. They are dense, intermediate, sparse and lysosomal yolk granules (Fig. 1.5).

During the course of development, the dense granules are replaced by the sparse granules via an intermediate state. The dense type yolk granules are mostly observed in unfertilized eggs but they are rarely observed in the gastrula stage. These morphological changes are due to the biochemical changes occurring in the yolk granules. Yolk granules are also involved in protein export to the extracellular matrix, this process may be also responsible for the morphological changes in yolk granules during embryonic development (Gratwohl et al., 1991; Mayne and Robinson 1998, 2002). For example, 41 kDa collagenase/gelatinase and HLC-32 are localized in yolk granules of unfertilized eggs but later as development proceeds they are found on the embryonic cell surface. The functional role of the yolk granules in sea urchin embryogenesis is still unknown. Previously, yolk granules were thought to serve as a storage compartment for nutrients required for embryogenesis.

However, throughout development yolk granules remain unchanged, even during nutrient deprivation, and are only metabolized in 7 day old larvae (Ichio IL et al., 1978; Armant et al., 1986; Scott et al., 1990). This indicates a non-nutritional role for these membrane-bound organelles. Studies done by Liao and Wang (1994) and Wang et al. (1995) revealed the dynamic nature of yolk granules. Localization of RNase to yolk granules in bullfrog oocytes suggests that yolk granules contain a cellular compartment that regulates the cytoplasmic access of some intracellular enzymes.

Fig. 1.5: Different morphological features of yolk granules.

a) Dense type. b) Intermediate type c) Sparse type and d) & e) Lysosomal type yolk granules. Arrows indicate the small membrane-bounded particles. (Yokota et al., 1993).

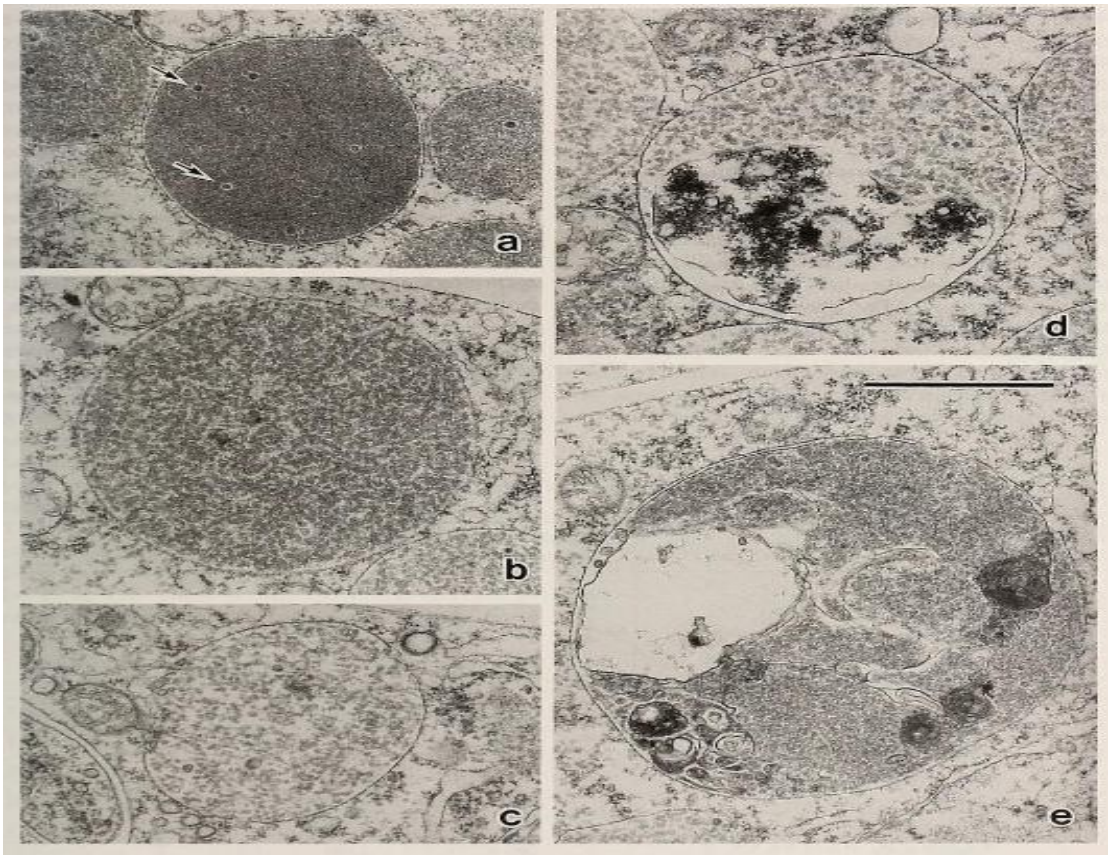
a
b
c
d
e

Yolk granules were also reported to be a storage compartment for proteins destined for transport to the cell surface (Grathwohl et al., 1991). For example, toposome, a glycoprotein, is destined for export from the yolk granule to the plasma membrane, where it may play a role in cell adhesion (Noll et al., 1985; Matranga et al., 1986; Cervello & Matranga, 1989; Grathwohl et al., 1991). Yolk granules may also play a role in plasma-membrane repair. Studies done by McNeil et al. (2000) showed that yolk granules fuse with plasma-membrane in a rapid, chaotic manner in the presence of high concentrations of calcium.

1.5 Yolk storage proteins

Vitellogenesis is a process by which yolk proteins are synthesized and accumulated in growing oocytes to make the yolk of the mature eggs. The majority of the oocyte yolk proteins in different species are imported into the oocytes and the major sites of synthesis are also different such as liver for vertebrates, the fat body in insects and intestine in echinoderms.

The yolk is a mixture of proteins, lipids and carbohydrates used for embryogenesis. In oviparous animals, accumulation of yolk proteins into yolk granules is a prerequisite for reproduction and oocyte growth and maturation. The yolk storage proteins are mainly vitellogenin (Vg), yolk proteins (YPs) and the major yolk protein (MYP). The vitellogenin is present in frog, chicken, nematode, fish and some insects such as mosquito, whereas the yolk proteins are found in dipteran insects such as fruitfly,

housefly, and the fleshfly (Brook and Wessel, 2003) (Table. 1.1). The major yolk protein (MYP) is present in the echinoderms, for example sea urchins. In oviparous animals, vitellogenin (Vg) and yolk proteins (YPs) are both female specific-proteins, whereas the major yolk protein in sea urchin is present in both sexes (Shyu et al., 1986; Unuma et al., 2001). There is no sequence homology between vitellogenin and yolk proteins. Major yolk protein cDNA sequencing of several species of sea urchins revealed that the MYP does not have sequence homology with any known vitellogenin (Unuma et al., 2001; Brooks and Wessel, 2002; Yokota et al., 2003; Noll et al., 2007). To date, three genes have been identified to encode vitellogenin-like proteins in Strongylocentrotus purpuratus (Song et al., 2006). In addition to vitellogenin and yolk proteins, other proteins are also packaged into the yolk granules. For example, hemolymph proteins in insects and vitellogenic cathepsin B (VCB) thiol protease in yellow fever mosquito (Aedes aegypti) (Cho et al., 1999).

Sea urchin yolk proteins are mostly N-linked glycoproteins, comprising about 10- 15% of the egg proteins and ranging in size from 35-300 kDa (Ichio et al., 1978; Ozaki, 1980; Harrington and Easton, 1982; Kari & Rottmann, 1985). There are striking similarities in their amino acid and monosaccharide compositions and pI values among different species of sea urchin (Scott & Lennarz, 1989).

Table 1.1: Yolk Proteins in different phyla (Brook and Wessel, 2003).

Protein name	Organism	Size	Sex-specific	Site of synthesis	Processing	Receptor	Function
Vitellogenin (Vg)	Frog, chicken, fish, nematode, some insects	400-500 kDa	Yes, females only	Vertebrate: Liver Nematode: Intestine Insects: Fat body	Large precursor is cleaved into smaller units, prior to yolk packaging	LDLr-like Vertebrate: 95-115 kDa Insedcts: 180-240 kDa	Nutrition and carrier protein for hormones and micronutrients
Yolk proteins (YP)	Dipteran insects (ex, Drosophila)	46-50 kDa	Yes, females only	Fat body overian filllicle cells	No difference between hemolymph and yolk form	LDLr-Like 210 kDa	Nutrition & carrier protein for ecdysone.
Major yolk protein (MYP)	Echinoderms (ex- ea urchin)	180-200 kDa	no	Intestine and nutritive phagocytes if ovary and testis	Slight difference between coelomic fluid and yolk form	???	???

1.6 Major yolk protein in egg and coelomic fluid.

A 22-27 S particle was identified from the sea urchin eggs as a major component of the yolk granules (Malkin et al., 1965; Infanate and Nemer, 1968; Ichio et al., 1978). Later, Kari & Rotmann, 1980, identified a glycoprotein with an apparent molecular weight of 200 kDa as the major protein component. Moreover, this protein species accounts for 10-15% of the total egg protein and for about 50% of the yolk and coelomic fluid proteins, and it was named the major yolk protein (MYP).

The major yolk protein (MYP) which was previously known as toposome, is the major protein component of the yolk granule present in the eggs, embryos and larvae of the sea urchin. This protein is peripherally associated with the yolk granule membrane (Kari & Rottmann, 1985; Perera et al., 2004; Hayley et al., 2006) and is a calcium binding, hexameric glycoprotein. Under reducing conditions, each subunit appears with an apparent molecular weight of 170 kDa and is characterized by intrachain disulfide bonds and stabilized by calcium.

A non nutritional role for this protein in the developing embryo and larvae has been suggested since during embryogenesis and starvation its abundance remains unchanged (Armant et al., 1986, Scott et al., 1990). The major yolk protein is also present in the coelomic fluid and nutritive phagocytes of the gonad of both sexes (Unuma et al., 2010, 2011). More than 80% of the stored proteins in nutritive phagocytes are MYPs. It is stored in the nutrititive phagocytes and is suggested to supply nutrients for gametogenesis

and embryogenesis (Scott et al., 1990; Unuma et al., 1998, 2003). It is also believed to transport iron and zinc in the developing oocytes. However, the structure of MYP is different from the other transferrin family proteins (Brooks & Wessel, 2002; Unuma et al., 2007; Lambert et al., 2005; Noll et al., 2007). In addition, during embryogenesis the egg MYP may also function as a cell-adhesion molecule and may participate in membrane repair in embryo and larvae (Noll et al., 1985; Matranga et al., 1986; Perera et al., 2004; Hayley et al., 2006, 2008).

Prior to gametogenesis MYP is stored in ovarian and testicular nutritive phagocytes to supply nutrients for gametogenesis (Ozaki et al., 1986; Unuma et al., 1998, 2003). Under reducing conditions, the apparent molecular weight of MYP is 170-180 kDa in nutritive phagocytes. The yolk granules of egg also accumulate MYP, which in turn may supply nutrient for the larval stage after fertilization (Scott et al., 1990). Major yolk protein mRNA expression profile studies showed that, in the adult sea urchin the MYP is predominantly synthesized in the inner epithelium of the digestive tract and the nutritive phagocytes in both sexes (Unuma et al., 2010). Noll et al. (2007) reported that the cDNA of the precursor major yolk protein (180-190 kDa) in gut and gonads of adult sea urchins undergoes a proteolytic removal of the N terminal WAP domain to generate the mature major yolk protein (170 kDa) in oocytes. The cleavage site is between amino acids 86 and 87 of the precursor MYP.

There are two isoforms of MYP. Under reducing conditions, the egg contains the 170 kDa species (egg MYP) and the coelomic fluid contains 180 kDa species (Coelomic fluid

MYP) (Unuma et al., 2011) and both species are present in nutritive phagocytes. Genome analysis of Strongylocentrotus purpuratus showed that, both species of MYP are encoded by the same gene (Song et al., 2006). Major yolk protein was previously thought to be a vitellogenin-like protein (Shyu et al., 1986; Cervello et al., 1994; Unuma et al., 2001; Yokota et al., 2003). However, to date three genes that encode vitellogenine-like proteins have been discovered in the sea urchin, S. purpuratus. The major yolk protein coding region encodes 1344 amino acids and cDNA sequencing of Pseudocentrolus depresssus and other species revealed that the MYP does not have any sequence homology with any known vertebrate vitellogenin, but is slightly homologus to transferrin family proteins (Fig. 1.6) (Unuma et al., 2001; Brook & Wessel, 2002; Yokota et al., 2003; Noll et al., 2007). The precursor of the major yolk protein shows some special structural features: 1) a protease-inhibiting WAP domain, whose removal generates the mature major yolk protein in oocytes: 2) a 280 amino acid modified cysteine-less insertion in the C-lobe and: 3) a 240 residue C-terminal extension with a modified cystine knot motif found in multisubunit external cell surface glycoproteins. The cystine knot motif is important to stabilize the cell-bound trimers upon calcium dependent cell dissociation of hexamer linked cells.

1.7 Synthesis, transport and packaging of egg major yolk protein in the Sea Urchin.

The major yolk protein is predominantly synthesized in the digestive tract (stomach, intestine and rectum) of the adult sea urchin as a slightly higher molecular weight component than the egg localized form (Shyu et al., 1986).

Fig. 1.6: Amino acid sequence derived from T. gratilla cDNA encoding toposome precursor (Noll et al.., 2007). The sequence homologous to the transferrin family is framed. The canonical cysteines (1–6, 8, 10–12 in the N-lobe and 1′–6′, 9′,–12′ in the C-lobe of the transferrin part of the toposome) are indicated, and the positions corresponding to the iron-binding ligand amino acids in the diferric transferrins are marked by asterisks.

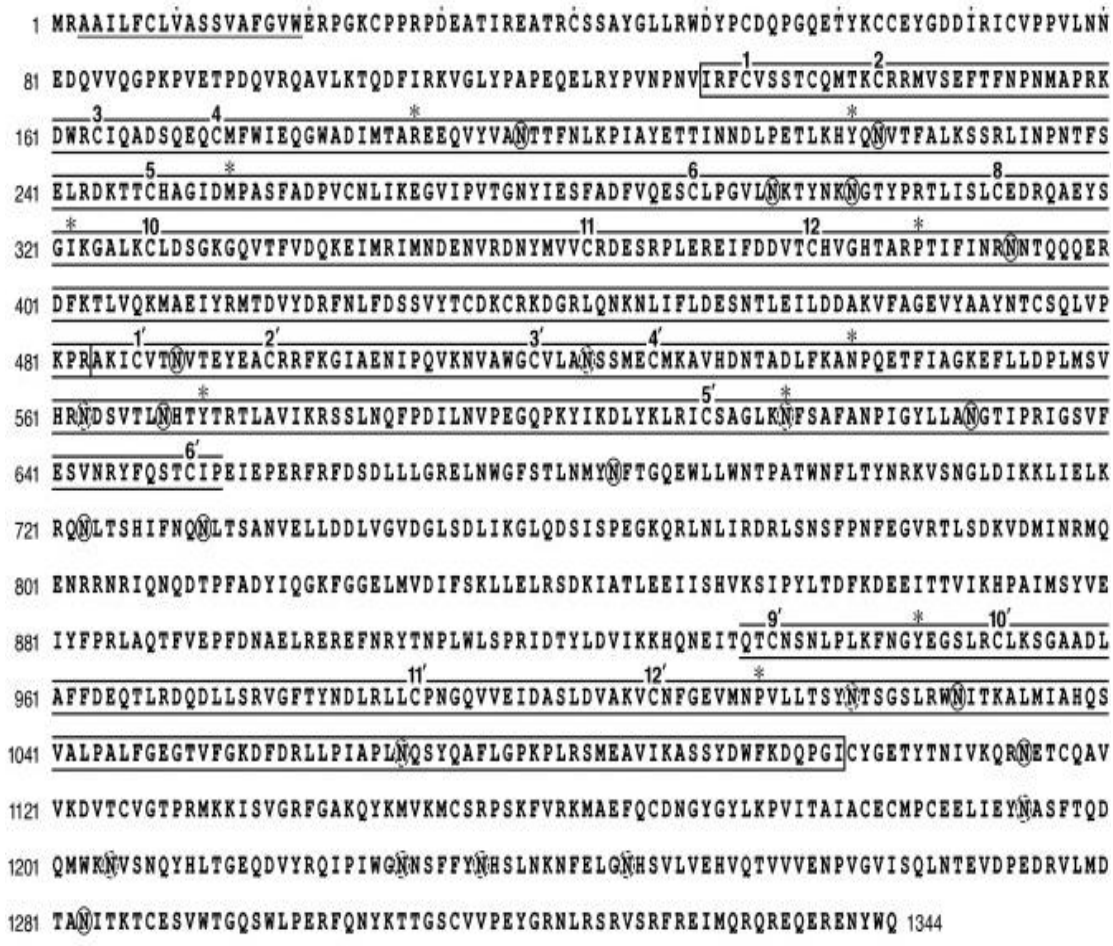

An mRNA expression study done by Unuma et al. (2001) showed that the MYP is also synthesized in the gonads of immature sea urchin. The MYP synthesized in the digestive tract, is then secreted into the coelomic fluid, transverses the two epithelial layers of the ovarian capsule and is absorbed by the nutritive phagocytes (Shyu et al., 1986). Later the MYP is localized peripherally on the oocyte, where a dynamin-dependent mechanism is involved in the endocytosis of MYP into the ova (Brooks & Wessel, 2004). Expression of a protein named YP 30 with an apparent molecular weight 30 kDa has been reported only in the oocytes, where it may play a role in the storage or packaging of MYP during oogenesis and/or utilization of the MYP in development (Wessel et al., 2000). Nutritive phagocytes provide nutrition for gametogenesis and also recycle nutrients by absorbing any unshed or degenerating germ cells at the end of the gametic cycle (Fuji, 1969; Walker, 1982; Harrington & ozaki, 1986; Unuma et al., 1998, 2001).

1.8 Proteolytic processing of egg major yolk protein.

The sea urchin yolk granules contain a large number of lysosomal hydrolases, which are optimally active at low pH (Schuel et al., 1975). A study done by Yokota & Kato (1988) showed that, under acidic condition (pH 4.2) the major yolk protein of both unfertilized and fertilized eggs undergoes proteolytic processing to lower molecular weight species of 114, 94, 72 and 61 kDa, with a concomitant disappearance of the high molecular weight major yolk protein. The study done by Perera et al. (2004) also supports the idea of proteolytic processing of MYP. In vivo radiolabelling experiments also showed that, the lower molecular weight protein species were not a result of de novo protein synthesis but

due to the proteolytic processing of major yolk protein (Armant et al., 1986). The protease responsible for proteolytic processing is a cysteine protease (Cathepsin B) (Yokota and Kato, 1988; Scott et al., 1990a; Mallaya et al., 1992) or serine protease (Giga and Ikai, 1985; Lee et al., 1989). This protease becomes active due to mild acidification of yolk granules after fertilization (Medina et al., 1988; Mallaya et al., 1992; Fausto et al., 2001). However, the structural integrity and the function of the major yolk protein remain intact after proteolytic cleavage through the maintenance of the disulfide-linked cleavage products (Perera et al., 2004; Noll et al., 1981; Matranga et al., 1986).

Yokota et al. (2003) studied the overall cDNA sequence of the precursor of MYP and suggested a cysteine-less region is the site of proteolytic cleavage. There is no cysteine between amino acids 653 and 938 in H. pulcherrimus, between 656 and 941 in P. depressus (Unuma et al., 2001) and between 661 and 944 in S. purpuratus (Brooks & Wessel, 2002). This region is a unique feature of sea urchin

1.9 Proposed functions of MYP.

1.9.1 Role of MYP as iron transporter.

Iron is an important nutrient for a number of protein functions and physiological processes. Most organisms have special cofactors and proteins to absorb and transport iron by maintaining iron in a water soluble state, as free iron can generate oxidative radicals that damage lipids, proteins and DNA (Yoshiga et al., 1999; Boldt, 1999; Nappi

& Vass, 2000; Brooks & Wessel, 2002). Transferrins reversibly bind iron. Vertebrate transferrins are monomeric glycoproteins (~80 kDa) that consist of two domains with similar amino acid sequences, each with a single iron-binding site (Backer & Lindley, 1992). These iron binding sites are stabilized by intrachain disulfide bonds. In vertebrates and invertebrates most of the transferrins function as iron transporters (Crichton & Charloteaux-Wauters, 1987; Bartfeld & Law, 1990; Kurama et al., 1995). The MYP can bind metals such as calcium, magnesium, barium, cadmium and manganese as well as iron in vitro (Brooks & Wessel, 2002; Hayley et al., 2008).

In vitro iron binding assays with the major yolk protein in coelomic fluid also supported the idea that the coelomic fluid MYP can bind with iron. It was suggested that, the MYP can act as a shuttle to transport iron to support embryogenesis and gametogenesis (Fig. 1.7). The coleomic fluid localized MYP may bind iron and deliver it to the developing oocyte (Brooks & Wessel 2002). It was suggested that, the transported iron may remain associated with MYP or may be transferred to the other metalloproteins of egg such as ovorperoxidase. Iron can also be transferred to the iron storage protein ferritin and nutritive phagocytes by MYP. Cervello et al. (1994) suggested that the coleomic fluid MYP may have bacteriostatic function by scavenging iron ions from bacterial pathogens.

Fig. 1.7: Proposed model of MYP function (Brooks & Wessel, 2002). The coelomic fluid MYP is an iron transporter, Delivery of iron to the ovary and testis may support gametogenesis and the packaging of MYP into yolk granules may serve as a mechanism of iron delivery during embryogenesis. The major yolk protein packaging in coelomocytes could have a dual function of providing a bacteriostatic function in coleomic fluid as well as MYP-Fe delivery to the gonad

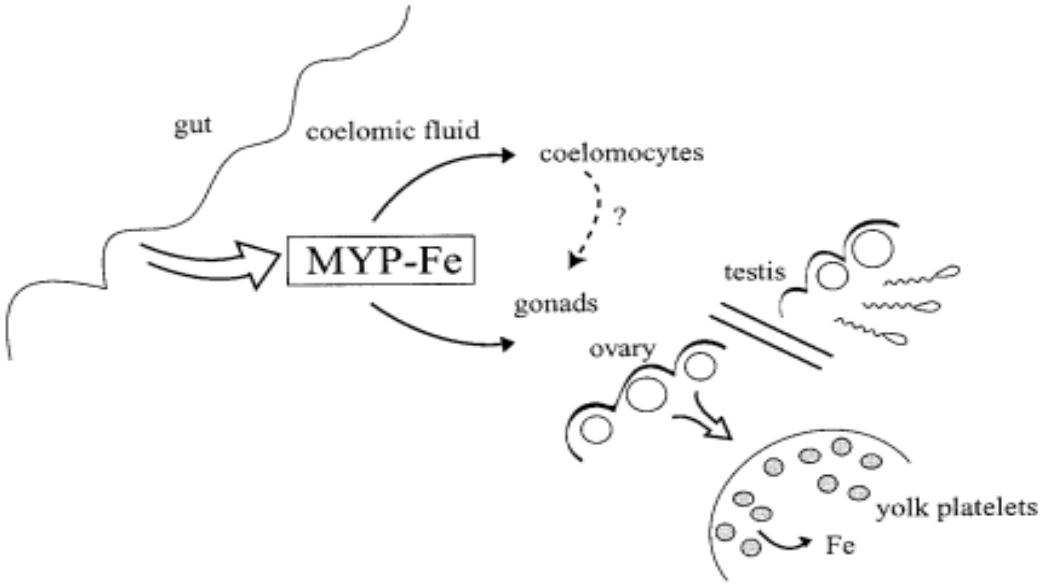
gut
coelomic fluid
coelomocytes
?
MYP-Fe
gonads
testis
ovary
yolk platelets
Fe

However, Hayley et al. (2008) suggested that though the MYP is transferrin-like in sequence, it is unlikely to function as an iron transporter in the developing sea urchin eggs and embryos. Functional transferrins bind iron as Fe^{3+} and are able to transport iron at or below nano-molar concentrations (Baker et al., 2003). Binding data suggested that the apparent dissociation constant of the egg MYP for Fe^{3+} is 275 μM, which indicates the egg MYP is insensitive to low concentrations of iron (Hayley et al., 2008).The strongest evidence against iron binding by the MYP is the absence of any canonical ligand amino acids (Noll et al., 2007). Furthermore, five iron binding amino acids e.g; two Y, one D, one R and one H are also absent in the egg MYP (Noll et al., 2007; Backer et al., 1987; Legrand et al., 1988; Baker and Lindley, 1992).

1.9.2 Role of the MYP as a zinc transporter.

Zinc is an essential trace element for gametogenesis (Falchuk & Montorzi, 2001; Yamaguchi et al., 2009). The structural integrity of chromatin and the functional states of many enzymes and gene regulatory proteins are also dependent on zinc (Fulchuk & Montorzi, 2001). The S. purpuratus genome also contains many genes encoding many zinc binding proteins that are expressed during embryogenesis (Materna et al., 2006; Angerer et al., 2006; Howard-Ashby et al., 2006).

The sea urchin gonads contain both the germ cell and nutritive phagocytes (somatic cells). Both sexes of the sea urchin store nutrients for gametogenesis in the nutritive phagocytes (Walker, 1982; Walker et al., 2006). Unuma et al. (2011) studied MYP accumulation and

its relationship to zinc content in sea urchin gonads during the non-reproductive season. Accumulation of the MYP in the agametogenic gonads suggests a role as a zinc transporter during the non-reproductive season.

The MYP may also transport zinc from the digestive tract to the ovary and testis through the coelomic fluid to supply nutrients during gametogenesis and thus act as a zinc transporter throughout the reproductive season (Unuma et al., 1998, 2003 & 2007) Zinc transport is more active in female than male sea urchins.

The major yolk protein can bind with other trace metals including calcium, magnesium, barium, cadmium and manganese as well as iron in vitro (Hayley et al., 2008). Unuma et al. (2007) reported that the MYP loses its zinc binding capacity after transport from the coelomic fluid into the gonads of sea urchins suggesting that the coelomic fluid-localized MYP may have a greater zinc binding ability than the MYP localized in eggs. The gonad also increases in size by accumulating MYP and zinc. These results indicate that, during the reproductive season and before metamorphosis in the larvae, the coelomic fluid-localized MYP transports zinc to the gonads (Unuma et al., 2007, 2009). Unuma et al. (2007) suggested that the MYP synthesized in the digestive tract binds zinc derived from ingested food and transports it through the coelomic fluid to the nutritive phagocytes in agametogenic gonads (Fig. 1.8). The nutrititive phagocytes store the MYP and zinc for future usage. Oogenesis in the sea urchin required more zinc than spermatogenesis, indicating that the sea urchin eggs contain a higher level of zinc than sperm (Unuma et al., 2007).

Fig. 1.8: Proposed model for the synthesis and accumulation of the MYP and its involvement in zinc transport in male and female sea urchins (Unuma et al., 2007).

There are two possible fates for the amino acids synthesized in the digestive tract to MYP in the gonad. (1) Amino acids from the digestive tract are transported to the nutritive phagocytes to produce the MYP (coelomic fluid MYP or egg MYP or both) in these cells (open arrows). (2) Amino acids from digestive tract may also synthesize coelomic fluid MYP, which may bind with zinc and then transported to the gonad, playing a role as zinc transporter (closed arrows). Incorporation of some coelomic fluid MYPs into the nutritive phagocytes form egg MYPs, with a loss of zinc binding ability.

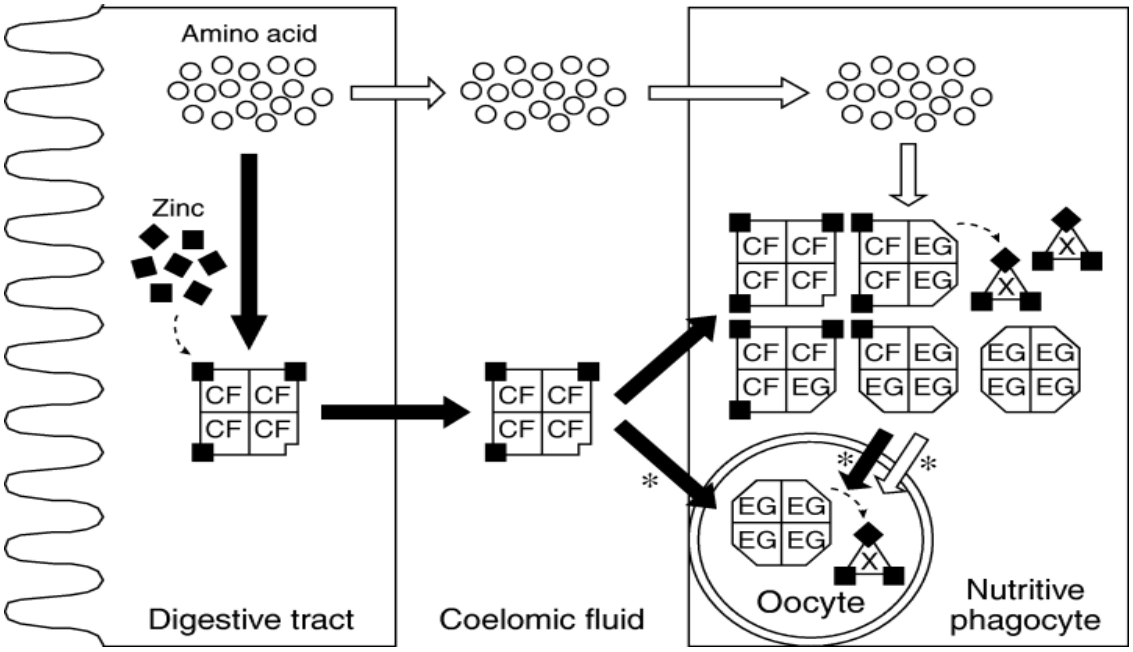
Amino acid
Zinc
CF CF
CF CF
CF CF
CF CF
CF CF
CF EG
CF CF
CF EG
CF EG
EG EG
EG EG
EG EG
X
X
X
*
*
*
EG EG
EG EG
Digestive tract
Coelomic fluid
Oocyte
Nutritive
phagocyte

1.9.3 Role of the egg major yolk protein in mediating cell-cell adhesion and plasma membrane repair in eggs and embryo.

Cell adhesion is required in many cellular processes like embryonic development, tissue formation and signal transduction. In general, there are two classes of cell adhesion molecules; one is calcium-dependent like integrins, cadherins, selectins and the other group is calcium-independent like immunoglobulin superfamily.

The egg MYP is localized to the yolk granule, cortical granule and plasma membrane in the unfertilized sea urchin egg (Gratwohl et al., 1991). During embryogenesis, the proteolytically processed, yolk granule-localized MYP is transported to the plasma membrane and the cortical granule-localized MYP is released into the extracellular matrix (Noll et al., 1985; Matranga et al., 1986). In addition, yolk granules also have a large amount of membrane required for patching lesions in the plasma membrane of sea urchin eggs and embryos (Terasaki et al., 1997; McNeil et al., 2000). The major yolk protein plays a role in plasma membrane yolk granule interaction by associating with yolk granule and may also be important in expressing positional information (Perera et al., 2004; Hayley et al., 2006; Noll et al., 1985; Matranga et al., 1986; Cervello & matranga, 1989).

Plasma membrane disruption is a normal event in many cells. Plasma membrane fusion is an important and ubiquitous process that is required by all types of cells. It may occur extracellularly such as during fertilization, organ development and also during viral

infection. Intracellularly membrane-membrane fusion occurs in such processes as exocytosis and membrane trafficking (Tamm et al., 2003). In the sea urchin membrane-membrane interaction is required for membrane repair and to export protein. Sea urchins spawn in open sea water and embryogenesis occurs in a hostile marine environment. Plasma membrane damage results in the influx of sea water with a high concentration of calcium (10 mM), and results in yolk granule aggregation and fusion with the plasma membrane in a rapid and organized manner that patches the damaged area (McNeil et al., 1997, 2000).

In the sea urchin, the egg MYP and calcium are required to initiate cell-cell interaction (Noll et al., 1985; Matranga et al., 1986). In the developing embryo exogenously added egg MYP stimulates the re-aggregation of dissociated blastula cells, depleted of MYP by butanol extraction (Matranga et al., 1986, Cervello & Matranga, 1989). This process is calcium-dependent. Calcium induces secondary and tertiary structural changes in the egg MYP to trigger the plasma membrane repair in the sea urchin egg and embryo (Fig. 1.9) (Hayley et al., 2006).

The NMR study done by Hayley et al. (2006) indicated that the egg MYP interacts peripherally with the membrane in the presence of 100 μM calcium, and this interaction is not further modified with the increasing concentration of calcium. The egg major yolk protein undergoes a calcium-dependent two step structural change, one required for MYP-membrane binding and the other facilitating an MYP-dependent membrane-membrane interaction (Perera et al., 2004 and Hayley et al., 2006).

Fig. 1.9: Putative role of the egg MYP in the patch hypothesis of membrane repair (McNeil et al.. 2000).

(A) A normal egg or embryonic cell. The egg MYP is peripherally associated with the yolk granule membrane (Perera et al.. 2004).

(B) The plasma membrane of the egg or embryonic cell undergoes damage, resulting in an influx or extracellular calcium.

(C) This influx of calcium is more than sufficient to cause a change in the tertiary structure of the egg MYP, which could then mediate membrane–membrane interaction between the yolk granule and plasma membranes, resulting in repair.

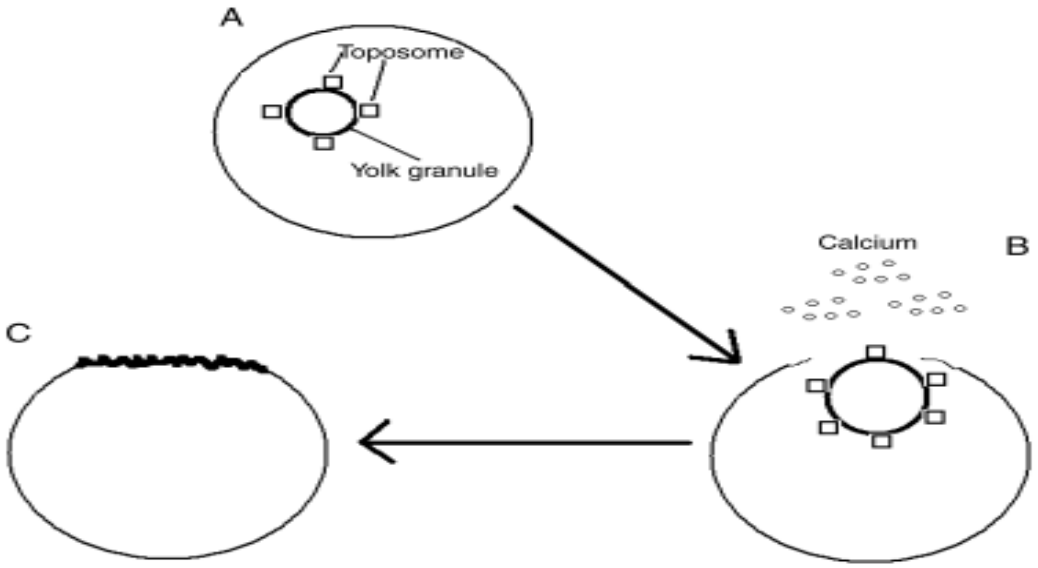
A
Toposome
Yolk granule
Calcium
B
C

In the trace of increasing concentrations of calcium, a secondary structural change occurred with an apparent dissociation constant (k_d) of 25 μM, responsible for the binding of the egg MYP to the membrane. This is followed by a tertiary structural change with an apparent k_d (calcium) of 240 μM, which was responsible for triggering MYP-dependent membrane-membrane interaction.

Perara et al. (2004) have also shown that the egg MYP can induce yolk granule aggregation. 1) Yolk granules lose their calcium-dependent aggregation activity after the addition of EGTA. In the presence of EGTA, the egg MYP is dissociated from the isolated yolk granule and the aggregation activity can be restored by addition of purified egg MYP to the EGTA-treated yolk granules. 2) The EGTA-treated yolk granules also lose aggregation activity if the added, purified egg MYP is preincubated with anti-egg MYP antibody. 3) Trypsin-treated yolk granules no longer aggregate in the presence of calcium. Again, incubation with purified egg MYP restores calcium-dependent aggregation. 4) Preincubation of purified yolk granules with anti-egg MYP antibody followed by an assay for calcium-dependent aggregation also shows the loss of aggregation activity.

1.9.4 Importance of coelomic fluid major yolk protein and coelomic fluid.

Coelomic fluid is a suspension that occupies the coelomic cavity of the sea urchin, mainly used to wrap and protect the inner organs and to mediate interactions between different regions of the cavity. The coelomic fluid contains a large number of cells (about 1-5 X

10^6/ ml) named coelomocytes that take part in the sea urchin immune response (Smith et al., 2006). The sea urchin coelomocytes have been classified into four types: phagocytes, vibratile cells and red and white morula cells, Fig. 1.10 (Bertheussen and Selijelid, 1978; Gerardi et al., 1990). Coelomocytes are the immune cells of echinoderms, due to their ability to respond to injuries, host invasion and cytotoxic agents. About 33% of the coelomocytes are involved in phagocytosis and the rest of the cells initiate clotting and antibacterial activity by releasing specific molecules (Smith et al., 1996; Stabili et al., 1996; Terwilliger et al., 2006; Dheilly et al., 2009). Coelomic fluid contains proteins responsible for cell adhesion and cytoskeleton organization e.g; the cytoskeletal actin and profilin (Fasoli et al., 2012). Profilin is responsible for changes in the coelomocyte shape in the sea urchin. Moreover, a calcium binding protein, calmodulin-2 and the complement, C3 were identified in the coelomic fluid, indicating the presence of an innate immune response in the sea urchin.

Harrington & Ozaki (1986) identified the major yolk protein in cultured coelomocytes using an anti-egg MYP antibody. They suggested that the coelomocytes produce the MYP and secret it into the coelomic fluid. A later study done by Cervello et al. (1994) also suggested that the white morula cells produce the MYP and release it under stress conditions such as in response to injury or host invasion, indicating a role for the coelomic fluid MYP in the clotting phenomena. The coelomic fluid MYP concentration was high in sea urchins infected with bacteria, which indicates a bacteriostatic role for this protein (Unuma et al., 2010).

Fig. 1.10: Morphology of four types of coelomocytes in the coelomic fluid of P. depressus (Unuma et al., 2010).

A, phagocyte; B, vibratile cell; C, white morula cell and D, red morula cell.

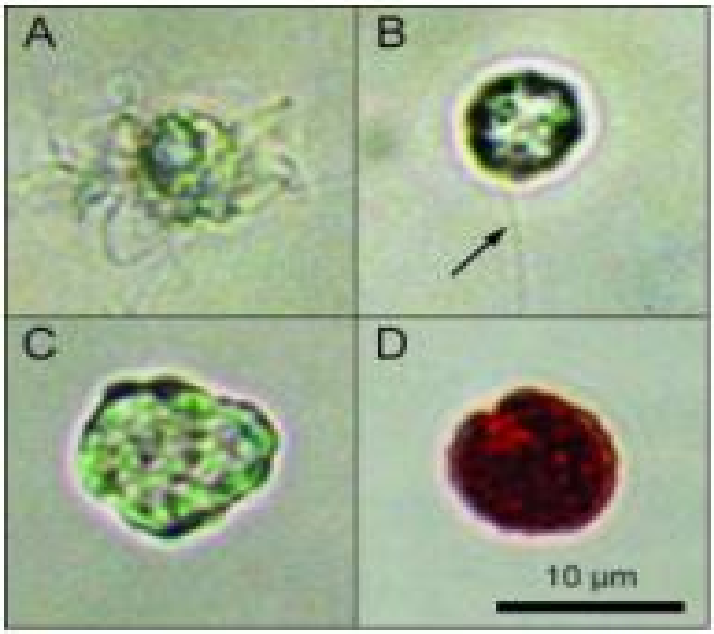
A
B
C
D
10 µm

It was also observed in sea star Asterias rubens that coleomocyte numbers increase in the post-traumatic stress period suggesting a defensive role (Pinsino et al., 2007). It was found that the coelomocytes aggregate in response to stress conditions such as wound healing in A. rubens (Smith, 1981; Moss et al., 1998). In echinoderms, wound repair and encapsulation of invasive materials require an adhesive activity in coelomic fluid (Pinsino et al., 2007). In the sea urchin, both the coelomic fluid and coelomocytes contain major yolk protein, which is an adhesive protein molecule (Matranga et al., 1986; Perera et al., 2004; Hayley et al., 2006, 2008). Under conditions of stress such as unusual temperature, acidic pH, heavy metals and other pollutants, the sea urchin also produces Hsp 70, which is responsible for a number of intracellular processes such as chaperone guidance, protein folding, and protection against apoptosis (Matranga et al., 2000, 2002, 2005, 2006; Becker & Craig 1994; Buchner 1996; Parcellier et al., 2003). Interestingly, an increased number of coelomocytes and increased concentrations of Hsp 70 were also reported for sea urchins in polluted sea water, suggesting that sea urchin coelomocytes can be utilized as bio-indicators of environmental stress (Matranga et al., 2000). Other studies also suggested that coelomocytes can respond to injury by activating a series of genes related to the immune response (Smith et al., 1996).

1.10 Purpose of study.

We were interested in a comparative biochemical analysis of the egg and coelomic fluid MYPs. Both the coelomic fluid MYP and the egg MYP are products of the same gene, while the coelomic fluid MYP is 10 kDa higher in molecular mass and considered to be a

precursor of the egg MYP (Harrington and Easton, 1982). Moreover, a proteolytical removal of the N-terminal domain from the coelomic fluid MYP generates the egg MYP (Noll et al., 2007). These observations indicate that the egg MYP and coelomic fluid MYP may be different in their biological functions. However, the biological functional difference between the coelomic fluid MYP and the egg MYP have yet to be identified. Unuma et al., (2007) showed that the coelomic fluid MYP has a higher zinc binding capacity than the egg MYP. Moreover, the egg MYP is peripherally located to the plasma membrane which is important for its biological function. In contrast, the ability of the coelomic fluid localized MYP to bind with plasma membrane is still unknown.

In this study, I compared the structural and biological properties of both the egg and coelomic fluid localized forms of MYP. Initially I employed sucrose density gradient ultracentrifugation both in the presence and absence of Triton X-100, to study the elution profile of both the egg and coelomic fluid MYPs. Sodium dodecyl sulfate polyacrylamide gel electrophoresis (SDS-PAGE) and Native-PAGE were employed both in the presence and absence of reducing agents, to identify the apparent molecular mass differences between both the reducible and non-reducible forms of the major yolk protein present in both the egg and coelomic fluid. A partial V8 protease peptide map analysis was done to probe the primary structural relationship between the egg MYP and coelomic fluid MYP. Circular dichroism and fluorescence spectroscopy were utilized to probe the secondary and tertiary structure in a calcium-dependent manner. To investigate the calcium-dependent phospholipid binding and vesicular aggregation capacity of these proteins, I performed liposome binding assay and liposome aggregation assay, respectively.

Chapter 2: Materials and Methods

2.1 Preparation of the egg yolk granule protein extracts and coelomic fluid protein extracts.

Strongylocentrotus droebachiensis were collected off the east coast of Newfoundland and induced to release eggs by intracoelomic injection of 0.5 M KCl. Preparation of the yolk granule protein extracts followed the procedure described previously with some modifications (Perera et al., 2004). The eggs were suspended in a solution containing 0.5 M KCl, 10 mM Tris, pH 8.0, and homogenized in a hand-held Dounce homogenizer in the presence of protease inhibitor (Sigma Chemical Co.) at 0°C. The homogenate was then fractionated by centrifugation at 400xg for 10 min at 4°C and the pellet was discarded. The supernatant then underwent fractionation by centrifugation at 2400xg for 10 min at 4°C. The final pellet was incubated for 30 min in the presence of protease inhibitor (Sigma Chemical Co.) in a solution containing 20 mM Tris, 2 mM EDTA, pH 8.0 followed by ultracentrifugation at 50,000xg for 1 h at 4°C by using 70 Ti rotor. The supernatant was collected and further purified by using anion exchange chromatography.

The coelomic fluid was collected from different individuals of Strongylocentrotus droebachiensis and protease inhibitor (Sigma Chemical Co.) was added. The fluid was then centrifuged at 15,000xg for 30 min at 4°C to remove the coelomocytes and other insoluble materials. The supernatant was collected and further purified by anion exchange chromatography.

2.2 Purification of major yolk proteins from the egg and coelomic fluid extracts by anion exchange chromatography.

The aliquots containing the egg MYP and coelomic fluid MYP were dialyzed against the starting buffer (10 mm Tris-HCl, pH 8.0) and loaded onto a Q-Sepharose Fast Flow column (Amersham Pharmacia, Uppsala, Sweden) that had been previously equilibrated with the starting buffer. The column was washed three times to remove any unbound proteins followed by the elution of bound proteins with a NaCl step gradient, prepared in sstarting buffer. To purify the egg MYP a 0.2 M to 0.4 M NaCl gradient, and a 0.1 M to 1 M NaCl gradient were used to purify the coelomic fluid MYP. The eluted proteins were then analyzed on an 8% (w/v) polyacrylamide gel by sodium dodecyl sulfate polyacrylamide gel electrophoresis (SDS–PAGE) and the gel was stained with CBB R-250 (Laemmli, 1970).

2.3 Sucrose density gradient centrifugation.

The aliquots containing the egg MYP and coelomic fluid MYP were further fractionated using sucrose density gradient ultracentrifugation to analyze the elution profiles of the proteins present in the egg and coelomic fluid extracts. We used sucrose density gradient centrifugation as described previously (Mayne et al., 2002). Aliquots of the resuspended pellet were loaded on to discontinuous sucrose gradients composed of 30%, 25%, 20% and 15% (w/v) sucrose in 20 mM Tris pH 8.0, followed by ultracentrifugation at 100,000xg by using an SW 28 rotor for 18 hours at 15°C. The gradients were fractionated

from the bottom of the tubes using a peristaltic pump and 600 µl fractions were collected. The collected fractions were further analyzed by performing sodium dodecyl sulfate polyacrylamide gel electrophoresis (SDS-PAGE) using an 8% (w/v) polyacrylamide gel under reducing conditions as described by Laemmli (1970) and stained with Coomassie Brilliant Blue (CBB) R-250. The separated protein bands were excised and incubated overnight with 25% (v/v) pyridine. The proteins were quantified by measuring absorbance at 650 nm.

2.4 Sodium dodecyl sulphate polyacrylamide gel electrophoresis

Electrophoresis was carried out using a mini gel electrophoretic apparatus (ThermoEC) in 1.5 mm thick 8% (w/v) polyacrylamide, [30% (w/v) acrylamide, 0.8% (w/v) bisacrylamide] slab gels (Laemmli, 1970). Protein samples were precipitated with an equal volume of 20% (w/v) TCA on ice for 30 min, centrifuged in an eppendrof centrifuge at 16000xg for 3 min and the supernatant were discarded. Pellets were resuspended in solubilizing solution [0.4 M Tris, 2% (w/v) SDS, 32 % glycerol, 0.1 M DTT and 0.1 % bromophenol blue]. Protein samples were boiled for 2 min and separated by electrophoresis at 20 mA. The electrophoresis buffer contained 25 mM Tris, 200 mM glycine and 0.1% (w/v) SDS. After electrophoresis, the gels were stained with 0.25% (w/v) CBB R-250 in 45% (v/v) methanol and 10% (v/v) acetic acid for 15 min at 37 °C, followed by destaining with a solution containing 10% (w/v) acetic acid and 7% (w/v) methanol at 37°C. Alternatively, some gels used in peptide mapping and two-dimensional SDS-PAGE was stained with silver by using silver staining kits (BIO-RAD). The gels

were photographed by using the ChemiImager software program of Gel Documentation System (Alpha Innotech Corporation).

2.5 Two dimensional gel electrophoresis.

In the first-dimension gel, the aliquots containing the egg and coelomic fluid proteins were fractionated in a 3-12% (w/v) gradient gel with 3% (w/v) stacking gel (Laemmli, 1970) in the absence of the reducing agent DTT. The protein bands corresponding to the egg and coelomic fluid proteins were excised and stored at -20 °C. Prior to second-dimension separation, the stored protein bands were incubated for 1 hr in a shaking water bath at 37 °C in an equilibrium buffer containing 50 mM Tris, 2% SDS and 20 mM DTT, pH 6.8. The gel slices were then placed at the bottom of the wells of a 3% (w/v) stacking gel on a 3-12% (w/v) gradient gel of polyacrylamide (Laemmli, 1970). The second-dimension electrophoresis was performed at 10 mA until the tracker dye reached the gel interface. The elecrtrophoresis was then increased to 20 mA and allowed to run for an extra hour until the tracker dye came out. This was followed by silver staining of the gel.

2.6 Peptide mapping analysis:

Peptide mapping analysis was performed as described by Cleveland et al. (1977). Aliquots containing the egg and coelomic fluid proteins were fractionated in a 3-12% (w/v) gradient gel containing a 3% (w/v) stacking gel (Laemmli, 1970) and stained by using CBB R-250 to visualize the protein bands. The appropriate protein bands were

excised and shaken at room temperature for 30 min in a solution containing 0.125M Tris-HCl, 0.1% (W/V) sodium dodecyl sulfate (SDS) and 1 mM EDTA, pH 6.8. The gel slices were then placed at the bottom of the wells of a 3% (w/v) stacking gel of polyacrylamide with different concentrations of acrylamide (7-12% and 3-12%) (Laemmli, 1970). Different concentrations of Staphylococcis aureus-V8 protease were overlayed on the gel slices and electrophoresis was performed at 10 mA and stopped for 45 min when the protein substances and the protease fully entered into the stacking gel. The electrophoretic separation was then resumed at 20 mA and the gel was stained with silver.

2.7 Determination of protein concentration by Lowry assay.

Aliquots of protein were precipitated with an equal volume of 20 % (w/v) TCA for 30 min on ice followed by centrifugation in an eppendorf centrifuge at 16,000xg for 10 min and the supernatants were discarded. The protein concentrations were determined by using BSA as a standard (Lowry et al., 1951). Absorbance was measured at 750 nm in a spectrophotometer (Spectronic 601, Milton Roy)

2.8 Circular dichroism spectrometry measurements.

Circular dichroism (CD) spectra measurements in the far ultraviolet (190-230 nm) were performed on a Jasco-810 spectrapolarimeter. Aliquots of purified major yolk proteins both in the egg and coelomic fluid were dialyzed against the starting buffer, 20 mM Tris, pH 8.0, and the absorbance of the protein/reagents mixture was checked at 222nm to ensure that it did not exceed 1.0. A CTC-345 circulating water bath was used to control

the temperature at 15°C. The scanning speed of the instrument was set at 100 nm/min with normal sensitivity. A water-jacketed cell (light path = 5 mm) was used and spectra were collected between 190 and 300 nm. Baselines were established using the appropriate buffers and 5 spectra were collected for each sample and averaged. Prior to the collection of spectra, the purified major yolk protein of both the egg and coelomic fluid was incubated with 200 µM of calcium for 30 min at 15°C.

The raw elipticity (mdeg) values were transformed in mean residue molar ellipticity ($deg.cm^2.dmol^{-1}$) by using the following equation.

$$\text{Mean residue molar elipticity } [\Theta] = \frac{\Theta_{abs} \text{ X } 115 \text{ g/ mole}}{10 \text{ X } l_{cm} \text{ X } C}$$

Where 115 g/ mole is the mean residue weight, l is the path length of the CD cell in cm, Θ_{abs} is the elipticity in mdeg and $[\Theta]$ is the mean residue molar elipticity in $deg.cm^2.dmol^{-1}$. The secondary structural features were calculated from the collected spectra using the computer program K2d3 (Louis-Jeune et al., 2011). This program can be accessed at http://www.ogic.ca/projects/k2d3.

2.9 Endogenous tryptophan fluorescence measurements.

Tryptophan fluorescence was measured for the major yolk protein in both the egg and coelomic fluid in the absence and presence of different concentrations of calcium or zinc at room temperature in a Shimadzu Model RF-540 spectrofluorimeter. The excitation wavelength was 287 nm and emission spectra were measured between 300 and 400 nm.

In all cases, the aliquots of major yolk protein of both the egg and coelomic fluid were dissolved in 20 mm Tris-HCl, pH 8.0.

2.10 Preparation of multilammellar liposomes.

Brain lipid extract (10% (w/w) PI, 50% (w/w) phosphatidyl serine and several other lipids; Sigma-Aldrich Canada) were used to prepare multilammellar liposomes. The lipid was solubilized in chloroform: methanol (2:1) by vortexing for 4 min, evaporated to dryness under nitrogen gas and dried under vacuum for 1 h. The dried lipid film was resuspended in the liposome binding buffer (50 mm Imidazole, 150 mm NaCl, 0.1 mm EDTA, pH 7.4) to a final concentration of 5 mg/ml and five freeze-thaw cycles were done by dipping the lipid into liquid nitrogen for rapid cooling followed by a transfer at a temperature of 45°C for thawing.

2.11 Liposome binding assay.

Liposome binding assays were performed following the method of Spenneberg et al. (1998) with some modifications. The aliquots of purified major yolk protein of both the egg and coelomic fluid were incubated with multilammilar brain lipid liposomes (10% (w/w) PI, 50% (w/w) phosphatidyl serine and several other lipids; Sigma-Aldrich Canada, Oakville, Ontario, Canada) in the presence of different concentrations of free calcium for 30 min at room temperature. The online software program WEBMAXC STANDARD (http://www-leland.stanford.edu/~cpatton/webmaxc/webmaxcE.htm) was used to

determine the free calcium concentrations. After the 30 min incubation, the liposome pellets and supernatants were harvested by centrifugation. Both the liposome pellet and corresponding supernatant were fractionated in an 8% (w/v) SDS–PAGE gel, which was stained with Coomassie Brilliant Blue R-250. The corresponding major yolk protein bands from the egg (170 kDa) and coelomic fluid (180 kDa) were excised and incubated with 25% (v/v) pyridine overnight. The proteins were quantified by measuring the absorbance at 650 nm. The percentage of bound protein was calculated and plotted against calcium concentrations.

2.12 Liposome aggregation assays.

Liposome aggregation assays were performed as described by Lee et al. (1997). Liposome aggregation assays were performed with a fixed amount (5 µg) of toposome and varying amounts of calcium. Aliquots of both the egg and coelomic fluid MYPs were incubated in the aggregation buffer, 40 mM histidine, 300 mM sucrose and 0.5 mM $MgCl_2$, pH 6.0, containing different concentrations of calcium for 10 min at room temperature. In the meantime, we measured the absorbance of the multilammellar liposome (10 mg/ml) alone and also in the presence of different concentrations of calcium to determine the effect of calcium on liposome aggregation. After 10 min at room temperature, protein pre-incubated with different concentrations of calcium was added to the liposome to determine the effect of protein alone on liposome aggregation. The optical density at 350 nm was monitored per min for a total period of 25 min. The initial

rates of aggregation (ΔOD_{350}/min) were determined and plotted against calcium concentration.

Chapter 3: Results

3.1 Purification of the major yolk proteins from the egg and coelomic fluid extracts by using anion exchange chromatography:

The prepared egg extract was fractionated by 8% (w/v) SDS-PAGE (Fig. 3.1 A). The apparent molecular mass of the major polypeptides present in the egg extract were 240 kDa, 170 kDa and 32 kDa. For further analysis the 170 kDa complex was purified by using an ion exchange chromatographic technique. An anion exchange resin, Q-sepharose fast flow (fast-Q) (Pharmacia Biotech) and a step gradient of NaCl ranging from 0.2 M to 0.4 M were used to achieve a fractionation of the proteins present in the egg extract. After loading the column with the egg extract, the bound proteins were eluted with a step gradient of 0.2 M, 0.25 M, 0.3 M, 0.35 M and 0.4 M NaCl (Fig. 3.1 B). We again combined the 0.2 M (lanes 3 and 4) and 0.25 M (lanes 5 and 6) fractions followed by anion exchange chromatography using the fast-Q resin (Pharmacia Biotech) with the same step gradient of NaCl to get the purified 170 kDa species. The eluted fractions were than analyzed in an 8% (w/v) polyacrylamide gel followed by CBB staining (Fig. 3.2).

The prepared coelomic fluid extract was fractionated in a 10% (w/v) polyacrylamide gel under reducing conditions (Fig. 3.3 A) followed by CBB staining. The collected coelomic fluid extract contains mainly 250 kDa, 180 kDa and a low molecular weight (LMW) polypeptides. For further analysis the 180 kDa complex was purified by using an ion exchange chromatographic technique. An anion exchange resin, Q-sepharose fast flow (fast-Q) (Pharmacia Biotech) and a step gradient of NaCl ranging from 0.1 M to 1 M were used to fractionate the proteins present in the coelomic fluid extract.

Fig. 3.1: Sodium dodecyl sulfate polyacrylamide gel electrophoresis of the egg yolk granule extract and the fractions eluted from the anion exchange resin.

A) Aliquots of the egg extract were fractionated in an 8% (w/v) polyacrylamide gel followed by CBB staining. The egg extract mainly contains polypeptides of 240 kDa, 170 kDa and 32 kDa.

B) Anion exchange resin, Q-Sepharose fast flow (fast-Q) was equilibrated with 0.15 M NaCl, 10 mM tris, pH 8.0, at 4 °C and protein containing egg extract was loaded onto the column. Aliquots of the first wash (lane 1), unbound fraction (lane 2) and elution from 0.2 M (lanes 3 and 4), 0.25 M (lanes 5 and 6), 0.3 M (lanes 7 and 8), 0.35 M (lane 9) and 0.4 M NaCl (lane 10) were fractionated in an 8% (w/v) polyacrylamide gel followed by CBB staining.

A)

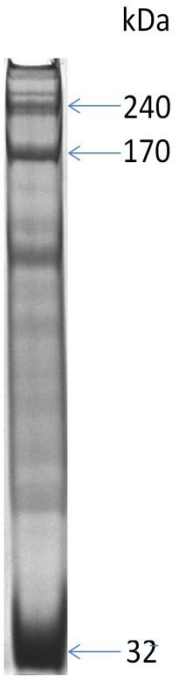

B)

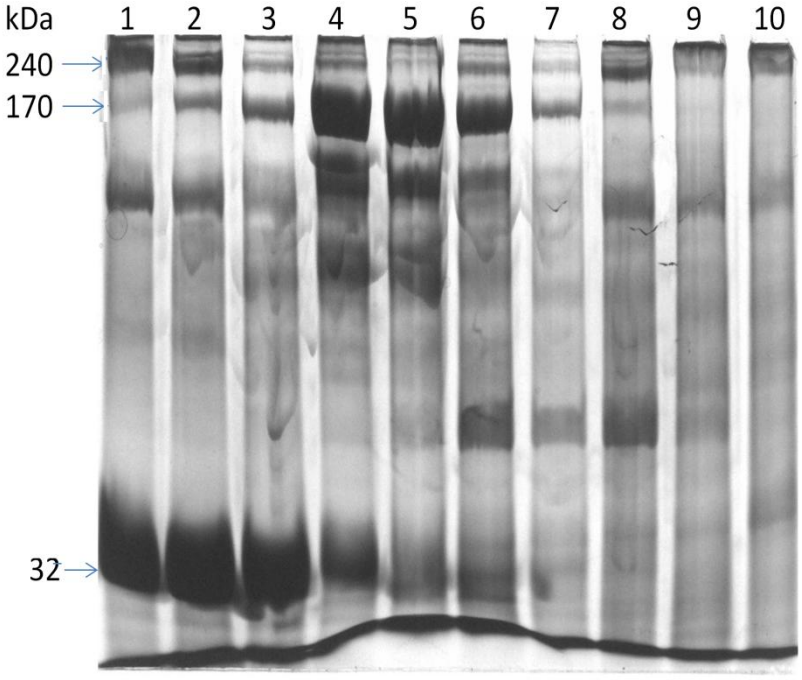

Fig. 3.2: Sodium dodecyl sulfate polyacrylamide gel electrophoresis of the combined fraction of 0.2 M and 0.25 M NaCl, 10 mM Tris, pH 8.0 (Fig. 3.1, panel B, lane 3 to 6) eluted from the anion exchange resin.

The anion exchange resin, Q-Sepharose fast flow (fast-Q) (Pharmacia Biotech) was equilibrated with 0.15 M NaCl, 10 mM tris, pH 8.0, at 4 °C and the aliquots of combined NaCl fractions of 0.2 M and 0.25 M NaCl, 10 mM Tris pH 8.0 (Fig. 3.1, panel B, lanes 3 to 6) was loaded onto the column. The column was washed with same equilibration buffer and the bound proteins were eluted with a 0.2 M, 0.25 M, 0.3 M, 0.35 M and 0.4 M step gradient of NaCl in the same buffer. Aliquots of the first wash (lane 1), unbound fraction (lane 2) and elution from 0.2 M (lanes 3 and 4), 0.25 M (lanes 5 and 6), 0.3 M (lanes 7 and 8), 0.35 M (lane 9) and 0.4 M NaCl (lane 10) were fractionated in an 8% (w/v) polyacrylamide gel followed by CBB staining.

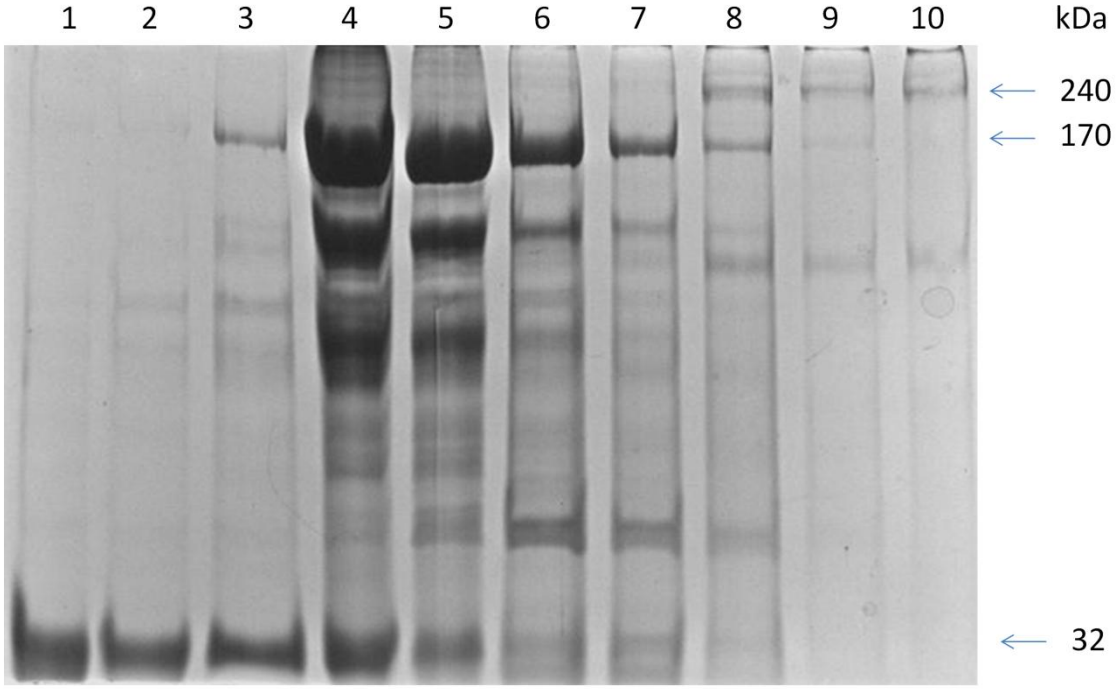
1
2
3
4
5
6
7
8
9
10
kDa
240
170
32

Fig. 3.3: Sodium dodecyl sulfate polyacrylamide gel electrophoresis of the coelomic fluid extract and the fractions eluted from the anion exchange resin.

A) Aliquots of the coelomic fluid extract were fractionated in a 10% (w/v) polyacrylamide gel followed by CBB staining. The coelomic fluid extract contains polypeptides of 250 kDa, 180 kDa and low molecular weight (LMW). The coelomic fluid is enriched with 180 kDa species.

B) Anion exchange resin, Q-Sepharose fast flow (fast-Q) (Pharmacia Biotech) was equilibrated with 10 mM tris, pH 8.0, at 4 °C and protein containing coelomic fluid extract was loaded onto the column. Aliquots of the first wash (lane 1), unbound fraction (lane 2) and elution from 0.1 M to 1 M (lanes 3 to lane 8, respectively) were fractionated in an 8% (w/v) polyacrylamide gel followed by CBB staining.

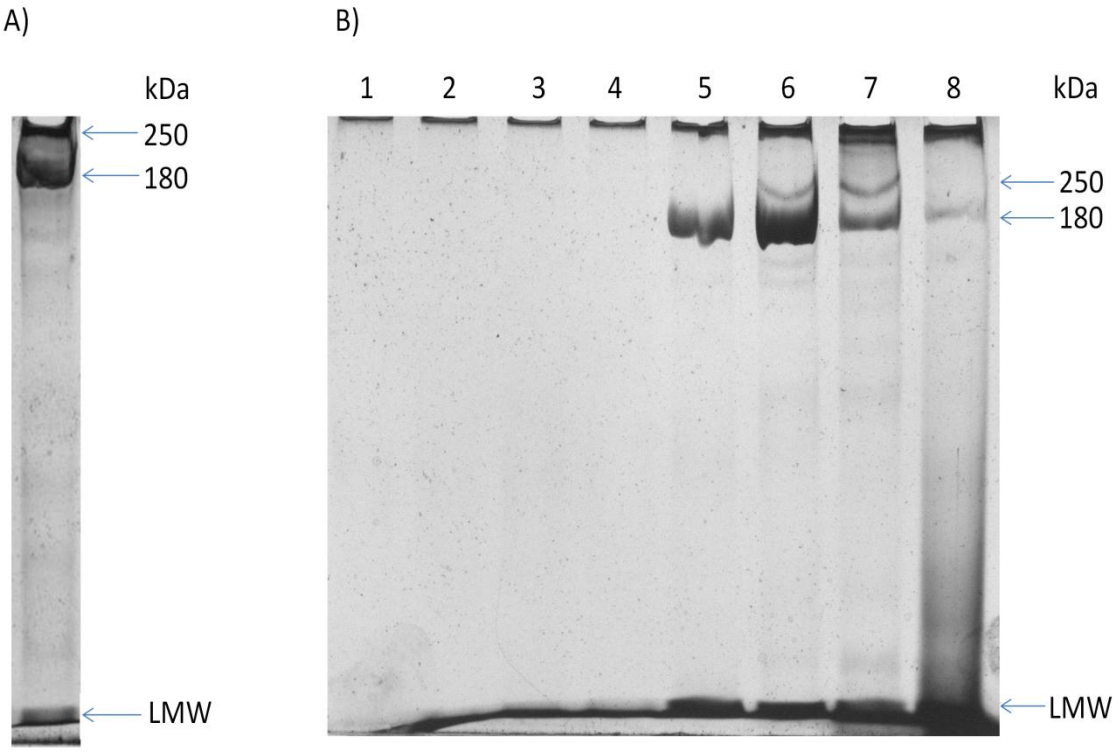
A)
kDa
250
180
LMW
B)
1
2
3
4
5
6
7
8
kDa
250
180
LMW

After loading the column with the coelomic fluid extract, the bound proteins were eluted with a step gradient of 0.1 M, 0.2 M, 0.3 M, 0.4 M, 0.5 M and 1 M NaCl, 10 mM Tris, pH8.0 (Fig. 3.3 B). The eluted fractions were than analyzed in an 8% (w/v) polyacrylamide gel followed by CBB staining.

Most of the 170 kDa species eluted in the 0.25 M (Fig. 3.2, lanes 5 and 6) and 0.3 M (Fig.3.2, lane 7) NaCl fractions from the Q-resin. However, most of the 180 kDa species eluted in 0.3 M (Fig. 3.3, Panel B, lane 5) and 0.4 M (Fig. 3.3, Panel B, Lane 6) fractions. Those fractions were further used for structural and functional analysis of the egg and coelomic fluid MYPs.

3.2. Sucrose density gradient ultracentrifugation analysis of the proteins present in the egg and coelomic fluid extracts, both in the absence and presence of Triton X-100.

Sucrose density gradient ultracentrifugation was performed to examine the elution profile of the polypeptide species present in both the egg and coelomic fluid extracts in the absence of Triton X-100. Aliquots of the egg and coelomic fluid extracts were loaded on to a discontinuous sucrose gradients composed of 30%, 25%, 20% and 15% (w/v) sucrose in 20 mM Tris pH 8.0, followed by ultracentrifugation at 100,000xg by using an SW 28 rotor for 18 hours at 15°C. The eluted fractions were collected from the bottom by using a peristaltic pump and further fractionated in by 8% (w/v) SDS-PAGE under reducing conditions. The gel was stained with CBB, and the corresponding bands for the 240-,

170- and 32 kDa from the egg extract and the 250 kDa, 180 kDa, and LMW from the coelomic fluid extract were excised and incubated overnight with 25% (v/v) pyridine to further quantify the proteins by measuring absorbance at 650 nm. The elution profile of the egg extract revealed that the majority of the 240 kDa, 170 kDa and 32 kDa polypeptides eluted in fraction 28, 17 and 27, respectively (Fig. 3.4 A). Similarly, the majority of the 250 kDa, 180 kDa and low molecular weight (LMW) species in the coelomic fluid extracts eluted in fraction 21, 13 and 19, respectively (Fig. 3.4 B).

We also analyzed the elution profile of all the polypeptides present in the egg and coelomic fluid extracts in the presence of 0.5% Triton X-100 using sucrose density gradient ultracentrifugation. Triton X-100 is a non-ionic surfactant, mainly used to solubilize membrane proteins. We used the same sucrose-Tris step gradient as in the fractions separated for both the egg and coelomic fluid extracts, followed by ultracentrifugation at 100,000xg by using an SW 28 rotor for 18 hours at 15°C. We collected the separated fractions and analyzed them in an 8% (w/v) polyacrylamide gel. The gel was stained with CBB and the corresponding bands for proteins present in both egg and coelomic fluid extracts were excised and incubated overnight with 25% (w/v) pyridine to further quantify the proteins by measuring absorbance at 650 nm. The elution profile revealed that in the egg extract most of the 240 kDa, 170 kDa and 32 kDa eluted in fraction 23, 17 and 29, respectively (Fig. 3.5 A). Whereas, most of the 250 kDa, 180 kDa and LMW species eluted in fraction 23, 17 and 21, respectively (Fig. 3.5 B).

Fig. 3.4: Sodium dodecyl sulfate gel electrophoretic analysis of separated fractions of the egg and coelomic fluid extracts after sucrose density gradient ultracentrifugation in the absence of Triton X-100 and under reducing conditions.

A) Fractions collected from the egg extract after ultracentrifugation on a discontinuous sucrose gradients composed of 30%, 25%, 20% and 15% (w/v) sucrose in 20 mM Tris pH 8.0 for 18 hours at 15°C. The fractions were separated in an 8% (w/v) SDS-PAGE followed by CBB staining. The specific polypeptide bands were excised and incubated overnight with 25% (v/v) pyridine. The proteins were quantified by measuring absorbance at 650 nm. Most of the 240 kDa, 170 kDa and 32 kDa polypeptides eluted in fraction 28, 17 and 27, respectively.

B) Fractions collected from the coelomic fluid extract after ultracentrifugation on a discontinuous sucrose gradients composed of 30%, 25%, 20% and 15% (w/v) sucrose in 20 mM Tris pH 8.0 for 18 hour at 15°C. The fractions were separated in an 8% (w/v) SDS-PAGE followed by CBB staining. The specific polypeptide bands were excised and incubated overnight with 25% (v/v) pyridine. The proteins were quantified by measuring absorbance at 650 nm. Most of the 250 kDa, 180 kDa and a Low molecular weight (LMW) polypeptide eluted in fraction 21, 13 and 19, respectively.

A) **Egg**

Fraction no:

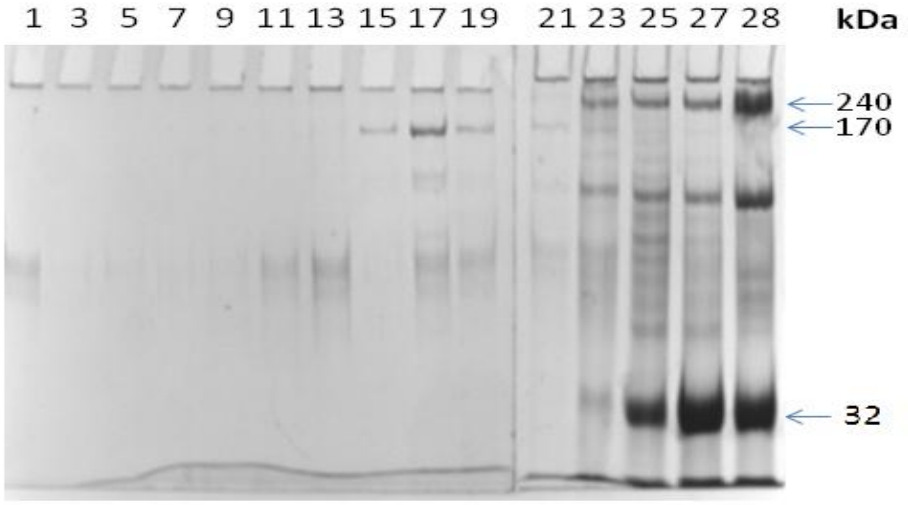

B) **Coelomic fluid**

Fraction no:

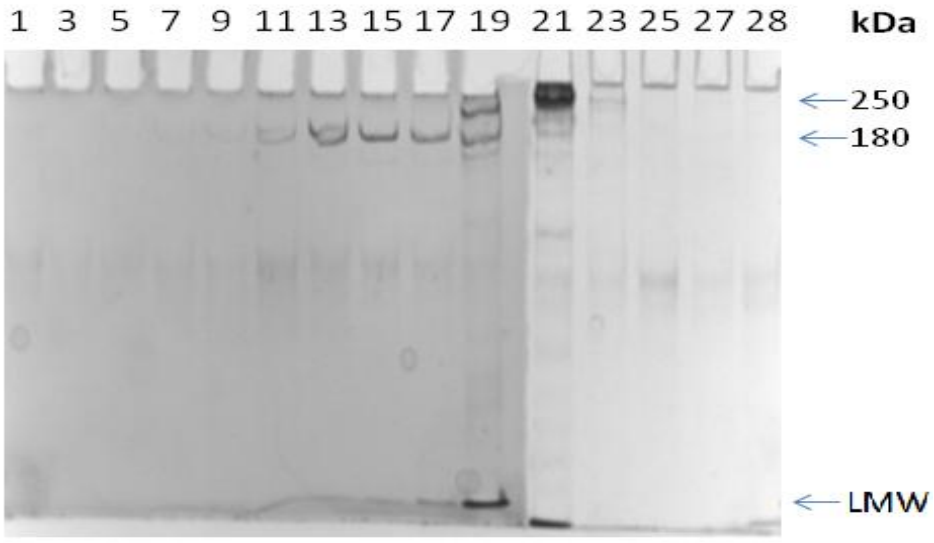

Fig. 3.5: Sodium dodecyl sulfate gel electrophoretic analysis of separated fractions of the egg and coelomic fluid extracts in the presence of 0.5% Triton X-100 after sucrose density gradient ultracentrifugation under reducing conditions.

A) Fractions collected from the egg extract after ultracentrifugation on a discontinuous sucrose gradients composed of 30%, 25%, 20% and 15% (w/v) sucrose in 20 mM Tris pH 8.0 for 18 hours at 15°C in the presence of 0.5% Triton X-100. The fractions were separated in an 8% (w/v) SDS-PAGE followed by CBB staining. The specific polypeptide bands were excised and incubated overnight with 25% (v/v) pyridine. The proteins were quantified by measuring absorbance at 650 nm. Most of the 240 kDa, 170 kDa, and 32 kDa polypeptides eluted in fraction 23, 17 and 29, respectively.

B) Fractions collected from the coelomic fluid extract after ultracentrifugation on a discontinuous sucrose gradients composed of 30%, 25%, 20% and 15% (w/v) sucrose in 20 mM Tris pH 8.0 for 18 hours at 15°C, in the presence of 0.5% Triton X-100. The fractions were separated in an 8% (w/v) SDS-PAGE followed by CBB staining. The specific polypeptide bands were excised and incubated overnight with 25% (v/v) pyridine. The proteins were quantified by measuring absorbance at 650 nm. Most of the 250 kDa, 180 kDa and a low molecular weight (LMW) polypeptide eluted in fraction 23, 17 and 21, respectively.

A)

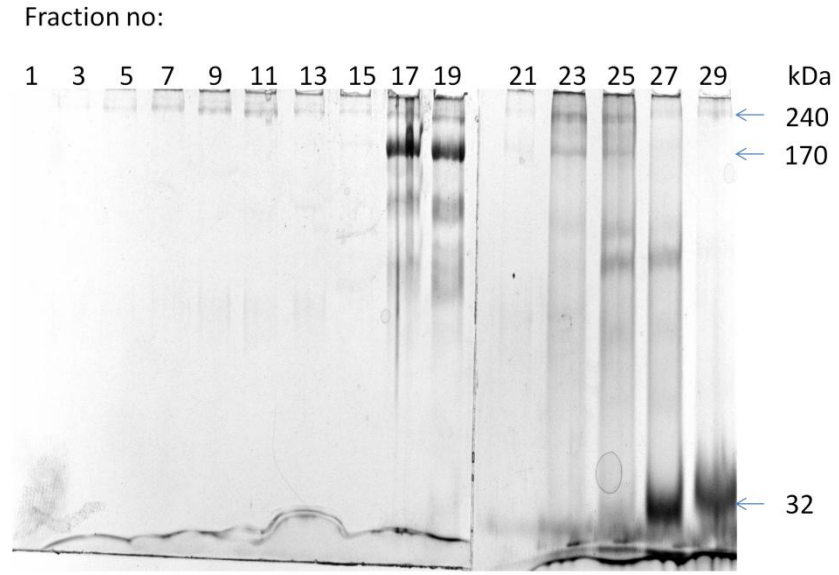
Fraction no:
1 3 5 7 9 11 13 15 17 19 21 23 25 27 29
kDa
240
170
32

B)

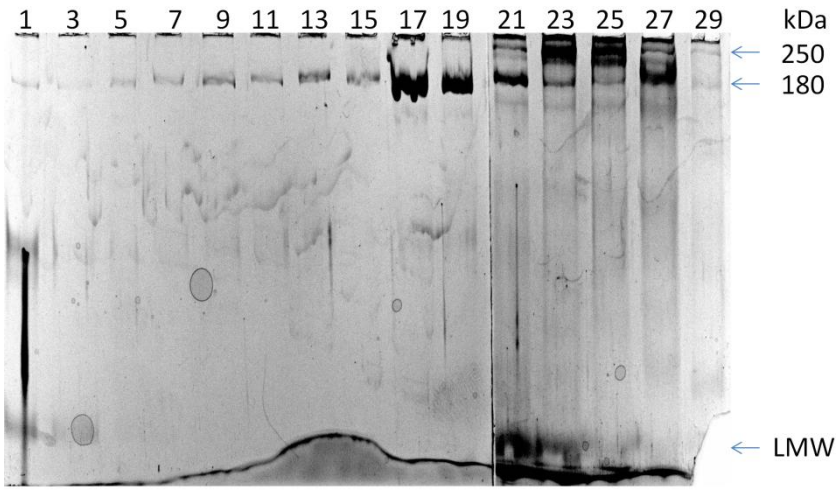
Fraction no:
1 3 5 7 9 11 13 15 17 19 21 23 25 27 29
kDa
250
180
LMW

In the presence of Triton X-100, there is a clear shift in the elution profile of the 240 kDa and 32 kDa species from the egg extract and the 250 kDa, 180 kDa and LMW species from the coelomic fluid extract (Table. 3.1). In the presence of Triton X-100, the 250 kDa and 180 kDa species eluted in the higher density fractions. In the presence of Triton X-100, the 240 kDa species eluted in the lower density fractions. The elution profile remained unchanged for the 170 kDa species in the absence and presence of Triton X-100. In the presence of Triton X-100, both the 180 kDa and 170 kDa species are eluted in fraction 17, while both the 250- and 240 kDa eluted in fraction 23.

These results indicated that there are two forms of MYP in both the egg and coelomic fluid extracts and the apparent molecular weight of the coelomic fluid MYPs are 10 kDa higher than the corresponding egg MYPs. It also suggested that the 240 kDa & 250 kDa species are not aggregates of the 170 kDa and 180 kDa species, respectively. Interestingly, all the polypeptides in both the egg and coelomic fluid extracts have unique elution profiles in the absence of Triton X-100.

3.3. Sodium dodecyl sulfate polyacrylamide gel electrophoretic analysis of the polypeptides present in the egg and coelomic fluid extracts in the presence and absence of reducing agents.

Initially, we prepared the egg and coelomic fluid extracts, enriched in the MYP. The extracts were then analyzed by SDS-PAGE both in the presence and absence of the reducing agent, DTT (Fig. 3.6).

Table. 3.1: Summery of sucrose density gradient ultracentrifugation analysis of the elution profile of proteins present in the egg and coelomic fluid extracts, both in the absence and presence of Triton X-100.

Polypeptides (kDa)	Fraction number (-Triton X-100)	Fraction number (+Triton X-100)
240	28	23
170	17	17
32	27	29
250	21	23
180	13	17
LMW	19	21

Fig. 3.6: Analysis of the eggs and coelomic fluid extracts in the presence or absence of reducing agents by SDS-PAGE followed by silver staining.

Aliquots of an egg extract (lanes 1 and 2) and a coelomic fluid extract (lanes 3 and 4) were fractionated in a 3-12% (w/v) polyacryamde gradient gel (Laemmli 1970) in the presence (lanes 1 and 3) or absence (lanes 2 and 4) of the reducing agent dithiothreitol.

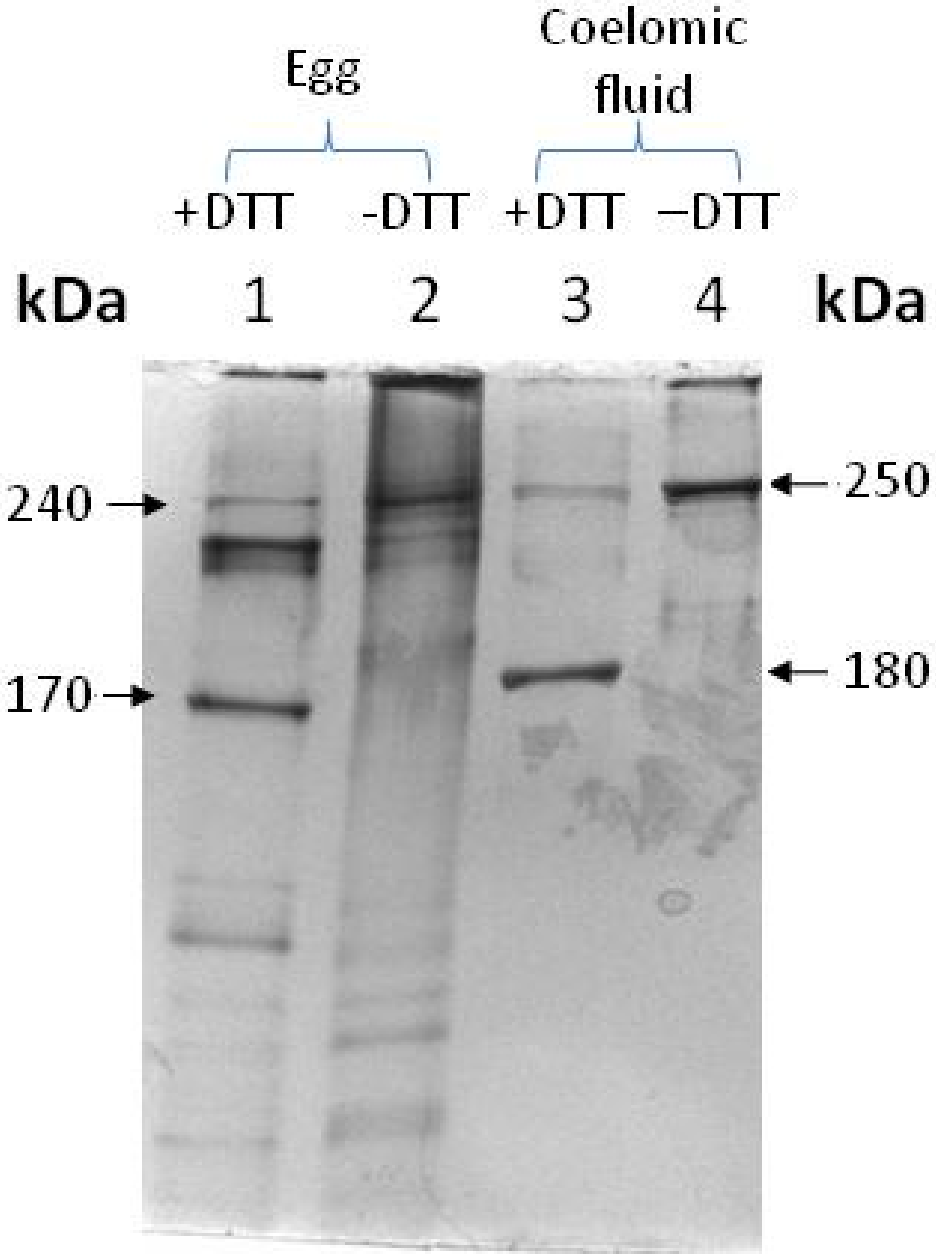
Egg
Coelomic fluid
+DTT
-DTT
+DTT
−DTT
kDa
1
2
3
4
kDa
240
170
250
180

In the presence of reducing agents, SDS-PAGE revealed that there are several polypeptide bands in the egg extract (Fig. 3.6, lane 1). One species migrated with an apparent molecular mass of 170 kDa, while a slower migrating species was seen at 240 kDa. Both species have previously been seen in preparations of the purified egg MYP (Perera et al., 2004). Interestingly, in the absence of reducing agents (Fig. 3.6, lane 2), the 170 kDa species disappeared while the 240 kDa remains. This result suggested that the 240 kDa species may represent a non-reduced form of the 170 kDa egg MYP.

Similarly, when the coelomic fluid extract was analyzed in the presence of DTT (Fig. 3.6, lane 3), two species of protein were seen with apparent molecular masses of 180 kDa and 250 kDa. In the absence of DTT (Fig. 3.6, lane 4) only the 250 kDa species was seen. These results suggested that two forms of MYP are present in both the egg and coelomic fluid extracts, one is a reducible form (170 kDa for egg and 180 kDa for coelomic fluid) and the other is a non-reducible form (240 kDa for egg and 250 kDa for coelomic fluid) of MYP. To further investigate this possibility, we did two dimensional SDS-PAGE with both the egg and coelomic fluid extracts. In the first dimension gel in the absence of DTT, only the 240 kDa and 250 kDa species of MYP were detected in the egg and coelomic fluid extracts, respectively (Fig. 3.7 A, lanes 1 and 2, respectively). The 240 kDa and 250 kDa bands were excised from the gel and incubated with DTT and SDS, and were fractionated in a second dimension SDS-PAGE gel (Fig. 3.7 B). In the presence of DTT and SDS, both the 170 kDa and 180 kDa polypeptides appeared along with the 240 kDa and 250 kDa species in the egg and coelomic fluid extracts.

Fig. 3.7: Two-dimensional SDS-PAGE analysis of the egg and coelomic fluid extracts in the presence or absence of reducing agents.

A) Aliquots of the egg extract (lane 1) and coelomic fluid extracts (lane 2) were fractionated in a 3-12% (w/v) polyacryamde gradient gel (Laemmli 1970) in the absence of the reducing agent dithiothreitol.

B) The 240 kDa and 250 kDa bands from the first dimension gel (Panel A, lanes 1 and 2, respectively) were excised, incubated in a buffer containing 50 mM Tris, 2% (w/v) SDS and 20 mM DTT, pH 6.8 for 1 hr in a shaken water bath at 37 °C and fractionated in a 3-12% (w/v) SDS-PAGE. The gel was silver stained.

A)

s

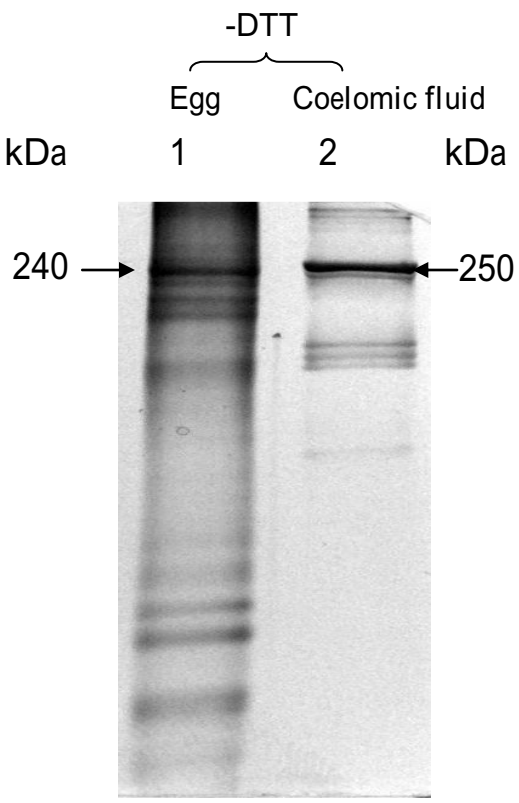
-DTT
Egg
Coelomic fluid
kDa
1
2
kDa
240
250

B)

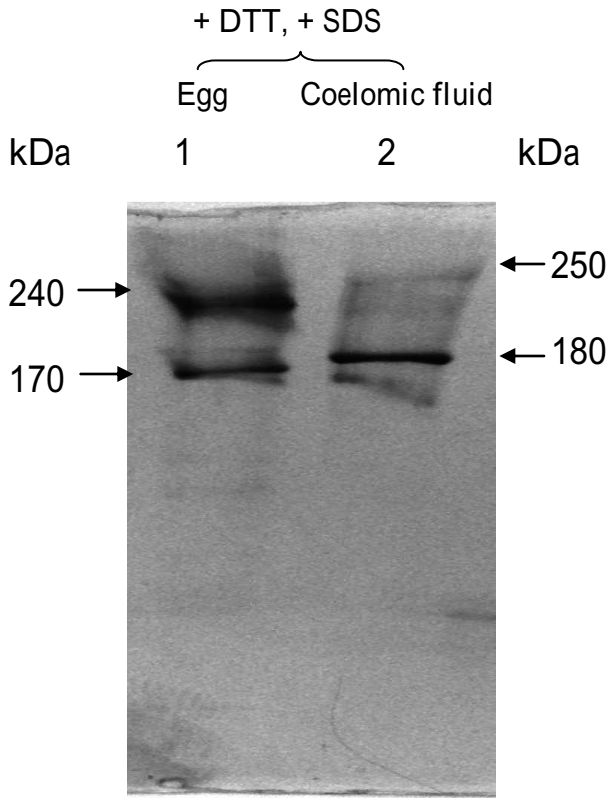
+ DTT, + SDS
Egg
Coelomic fluid
kDa
1
2
kDa
240
170
250
180

Again these results suggest that in the absence of reducing agents, a reducible form of MYP (170 kDa for egg & 180 kDa for coelomic fluid) co-migrates with the corresponding non-reducible form of the protein (240 kDa for egg and 250 kDa for coelomic fluid) in both the egg and coelomic fluid extracts. Also, the apparent molecular masses of the reducible and non-reducible forms of coelomic fluid MYPs are slightly higher than the corresponding egg MYPs.

In addition, native-PAGE was also carried out with the egg and coelomic fluid extracts to further confirm that these extracts contained the two forms of MYP. We loaded the egg and coelomic fluid extracts on a 3% (w/v) stacking gel placed on the top of a 3-12% (w/v) polyacrylamide gradient gel in the absence of SDS and DTT. Native-PAGE revealed that only a single species of MYP was present in both the egg and coelomic fluid extracts (Fig. 3.8 A, lanes 1 and 2, respectively). Both the bands were excised and incubated with DTT and SDS, and analyzed by SDS-PAGE. Sodium dodecyl sulfate polyacrylamide gel electrophoretic analysis also revealed the existence of two forms of egg MYP (240 kDa and 170 kDa) (Fig. 3.8 B, lane 1) and two forms of coelomic fluid MYP (250 kDa and 180 kDa) (Fig. 3.8 B, lane 2).

The above results lead us to conclude that under non-reducing conditions both the 170 kDa species from egg and the 180 kDa species from coelomic fluid extract co-migrates with the corresponding 240 kDa and 250 kDa species of the egg and coelomic fluid extracts, respectively. In every case, coelomic fluid MYPs are 10 kDa higher in apparent molecular mass than the corresponding egg MYPs.

Fig. 3.8: Analysis of the egg and coelomic fluid extracts by native-PAGE and SDS-PAGE.

A) Native-PAGE analysis of the egg (lane 1) and coelomic fluid extract (lane 2) in the absence of DTT and SDS on a 3-12% (w/v) polyacrylamide gradient gel with a 3% (w/v) stacking gel.

B) Second dimension SDS-PAGE analysis of the protein species appeared in panel A. The bands were excised from the native gel (Panel A), incubated with SDS and DTT and fractionated in a 3-12 % (w/v) SDS-PAGE.

A)

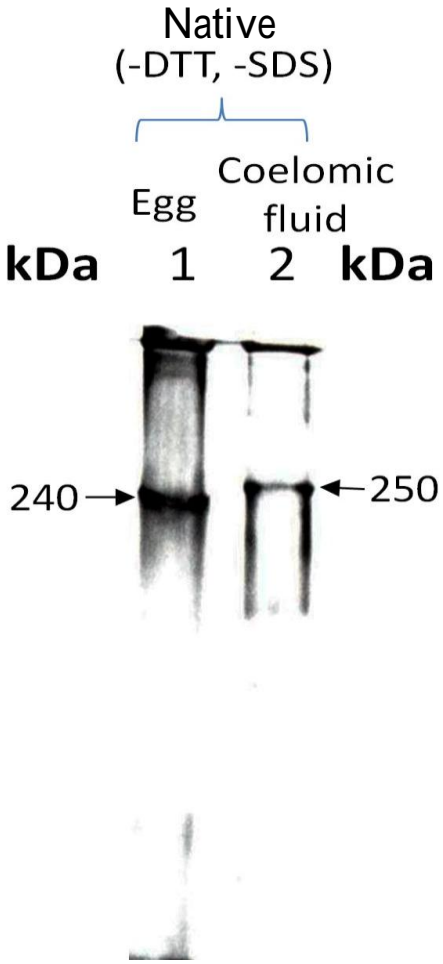
Native
(-DTT, -SDS)
Egg
Coelomic fluid
kDa
1
2
kDa
240
250

B)

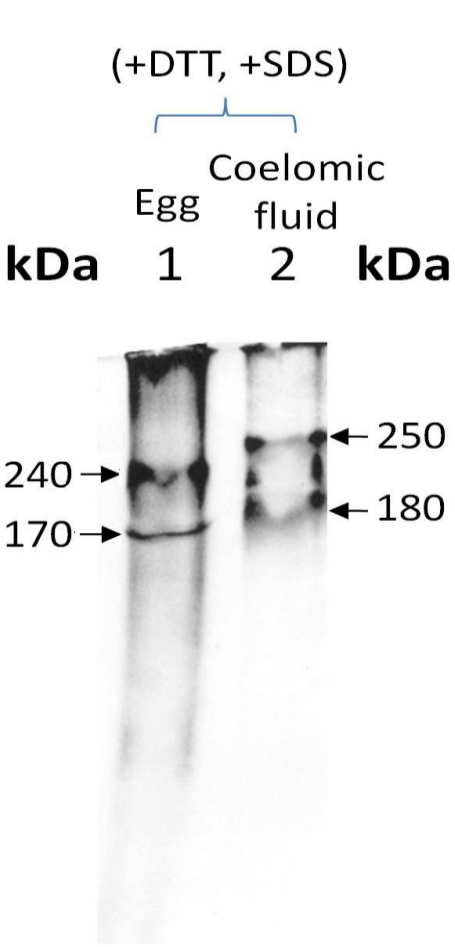
(+DTT, +SDS)
Egg
Coelomic fluid
kDa
1
2
kDa
240
170
250
180

3.4 Partial V8 protease peptide map analysis of polypeptides present in the egg and coelomic fluid extracts.

In order to explore the primary structural relationship between the different polypeptides (240-, 170-, 250- and 180 kDa) in the egg and coelomic fluid extracts, we performed a partial in gel V8 protease peptide mapping. The V8 protease is an endopeptidase that cleaves specifically at the carboxyl side of aspartate and glutamate residues. This enzyme is also known as endoproteinase Glu-C, Glu-C protease, staphylococcal serine proteinase, Staphylococcus V8 serine endopeptidase and Glutamyl endopeptidase. We used an online program ExPASy-Peptide cutter (http://web.expasy.org/peptide_cutter) to determine the number of V8 protease cleavage sites in the precursor of major yolk protein of Strongylocentrotus purpuratus. We found that it has 77 cleavage sites for V8 protease (Fig. 3.9).

Furthermore, we performed a partial in gel peptide mapping experiment by following the method of Cleveland et al. (1977) with some modifications. Polypeptides present in the egg and coelomic fluid extracts were separated by electrophoresis in a 3-12% (w/v) polyacrylamide with 3% (w/v) stacking gel under reducing conditions (Laemmli, 1970), following a brief staining with CBB. The 240 kDa and the 170 kDa species from the egg extract, and the 250 kDa and 180 kDa species from the coelomic fluid extract, were excised from the gel. All the four polypeptides were digested with different amounts of Stphylococcus aureus V8 protease following electrophoresis of the polypeptides and protease into a 3% (w/v) polyacrylamide stacking gel.

Fig. 3.9: Peptide map analysis of the major yolk protein precursor from Strongylocentrotus purpuratus by using an online program peptide cutter.

A) The amino acid sequence of the major yolk protein precursor from Strongylocentrotus purpuratus.

B) The major yolk protein precursor has 77 cleavage sites for V8 protease or Glutamyl endopeptidase.

A)

```
        10         20         30         40         50         60
MRAAILFCLV ASSMAVPSGS LGSRPGTCPP QPSDQVMIEA TRCSYVYGLT WDWNCNSQGQ

        70         80         90        100        110        120
ENYKCCQYEN DIRICVPPIP ADVDEEVGVE QPSQSVDQVR QAIQKTQDFI RKVGLYPAPD

       130        140        150        160        170        180
QRRRTTPTPD TVRWCVSSRC QMTKCQRMVS EFTYSPNMVP RKQWKCTQAT SQEQCMFWIE

       190        200        210        220        230        240
QGWADIMTTR EGQVYSANTT FNLKPIAYET TINDQQPEIQ ILKHYQNVTF ALKSSRLVNP

       250        260        270        280        290        300
NTFSELRDKT TCHAGIDMPD FDMPASFADP VCNLIKEGVI PVTGNYIESF SDFVQESCVP

       310        320        330        340        350        360
GVLNMTYNKN GTYPLSLVTL CEDQQYKYSG IKGALSCLES GKGQVTFVDQ KVIKKIMSDP

       370        380        390        400        410        420
NVRDNFQVVC RDESRPLDEE IFTDVTCHVG HTARPTIFIN KNNTQQKETD IKTLVVKMME

       430        440        450        460        470        480
LYGNTDRDVN FNIFDSSVYD CGKCQMTGKP LNKNLIFLEE SNTMKIVDDS KVYAGEVYAA

       490        500        510        520        530        540
YNVCSKLVPK PRAKICVTNV TEYEACRRFK GIAENIPEVK KVAWGCVLAN SSIECMQAVH

       550        560        570        580        590        600
NNTADLFKAN PMETFIAGKE FLLDPLMSVH RNDSVTMNHT YTRTLAVIKR SSLAKFPGLL

       610        620        630        640        650        660
SVPEGQPKYI KDLWKLKICS AGLKNFSAFH SPIGYLLANG TIPRIGSVFE SVNRYFQATC

       670        680        690        700        710        720
VPEIEPETWR LDSDLLLGRE MNWGFSSLNM YNFTGQEWLL WNTPATWNFL TYNRKVSTGL

       730        740        750        760        770        780
DIKKLIELKK QNLTSHIFNQ NLSSPRNVEL LDDLVGVEGI SDLVKGVQDT IGPEGKQKMN

       790        800        810        820        830        840
MLRDRLSNSF PNFEAVRTLS DKVDIVNKMK DARQQRLQNK DHPFGNVIQE TFQGHLMVDV

       850        860        870        880        890        900
FSKLLELRSD KISTLEEIIS HVKTIPYLTD FKDVEITTVL KHPAIMSYVE IYFPRLSQTF

       910        920        930        940        950        960
VEPFDNVELR EREFNRYTNP LWLSPKVHTY LDLVKNHQTE ITKTCNSNLP LNFKGYEGAL

       970        980        990       1000       1010       1020
RCLKSGVADL ASSTSRPSVT RTLRDTDLST GWVHLQRPPP SLPQRQVVEI DVNMDIAKVC

      1030       1040       1050       1060       1070       1080
NFGEVMNPVL VTAYNTSGSW RWNITKALMI AHQSVALPAL FGEGTVMGKD YDMLLPIAPL

      1090       1100       1110       1120       1130       1140
NQSYQPFLGS KPLRSMEAIV KASSYDWFKD QTGICYGETY TNIVKQRNET CQAIVKDVTC

      1150       1160       1170       1180       1190       1200
VGTPRMKKIS VGRFGAKQFK MIKMCSRPSK FVRKMADFQC DNGFGYLKPV ITAVACECML

      1210       1220       1230       1240       1250       1260
CEEMIEYNTS FTEDNMWSDV SNKYVLTGEQ DIYRQIPIWG NNSYFYDHTL NKNFELGNHS

      1270       1280       1290       1300       1310       1320
IIVEHVQTVV VERPSPGILS QVNSEVDPEV QVQMDSASLT KTCETVWNGQ SWLPERFQGY

      1330       1340       1350
KTSGSCVVPE TGANAKSRVD RFRQIMQRKQ QLVDHHH
```

B)

Name of enzyme	No. of cleavages	Positions of cleavage sites
Glutamyl endopeptidase	77	39 61 69 85 86 90 151 173 180 191 209 218 245 277 288 296 322 339 373 379 380 408 420 459 460 476 502 504 514 518 534 553 560 604 650 663 665 667 680 697 727 749 758 774 794 830 846 856 857 875 890 902 908 911 913 940 957 1009 1024 1063 1097 1118 1129 1197 1202 1203 1206 1213 1229 1255 1264 1272 1285 1289 1304 1315 1330

The resulting peptides were resolved in different concentrations (7-12% and 3-12%) of polyacrylamide gel and visualized by silver staining.

The resulting peptide maps showed that, the digestion patterns were almost identical between the 170 kDa and the 180 kDa species in the presence of 0.45 µg V8 protease (Fig. 3.10 A). Hence, they are highly identical proteins except the coelomic fluid form is 10 kDa higher in apparent molecular mass. Similarly, the digestion pattern was also very similar between the 170 kDa and the 240 kDa forms of egg MYP (Fig. 3.10 B). The 240 kDa species required 2.25 µg of V8 protease while the 170 kDa required 0.45 µg of V8 protease. This result indicated that the 240 kDa species is more resistant to digestion by V8 protease than the 170 kDa form of the protein.

In addition, many peptide fragments were common between the 180 kDa and 250 kDa polypeptides (Fig. 3.10 C). Here also the 180 kDa species required 0.45 µg of V8 protease but the 250 kDa species required 0.225 µg of V8 protease. Similarly, the 240- and 250 kDa species had similar peptide profile (Fig. 3.10 D). These partial digestions with V8 protease results suggested that, while they have different apparent molecular masses, all the four species of MYP in fact have the same primary structure. Moreover, the 240 kDa in the egg extract was somewhat resistant to digestion by V8 protease.

These results provided strong evidence that all the four polypeptides have the same primary structure.

Fig. 3.10: In gel partial peptide mapping of all the four species of both the egg and coelomic fluid major yolk protein with V8 protease. All the gels were silver stained.

A) V8 protease (0.45 µg) digestion of the 180 kDa and 170 kDa species in a 7-12% (w/v) SDS-PAGE followed by silver staining.

B) Digestion profiles of the 170 kDa and 240 kDa species in a 3-12% (w/v) SDS-PAGE followed by silver staining. The 240 kDa species required 2.25 µg and the 180 kDa required 0.45 µg of V8 protease.

C) Digestion profiles of the 180 kDa and 250 kDa from the coelomic fluid extract in a 3-12% (w/v) SDS-PAGE followed by silver staining and the required amount of V8 protease were 0.45 µg & 0.225 µg, respectively.

D) Digestion profiles of the 240 kDa and 250 kDa species in a 3-12% (w/v) SDS-PAGE in the presence of 2.25 µg and 0.225 µg of V8 protease, respectively.

A)

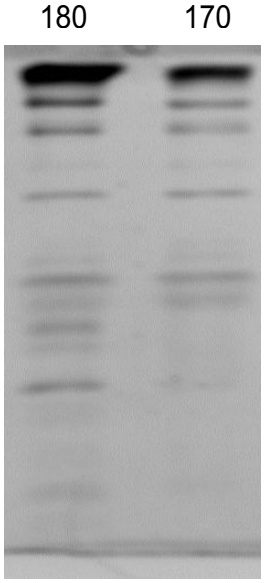

B)

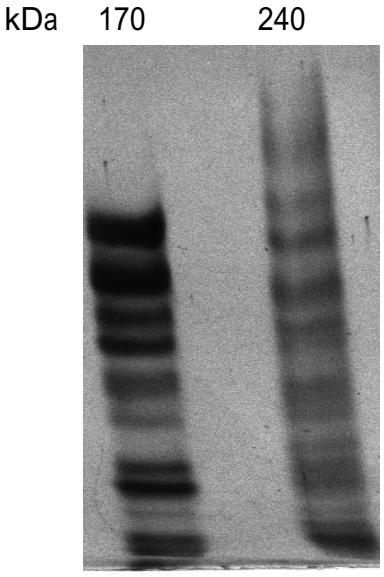

C)

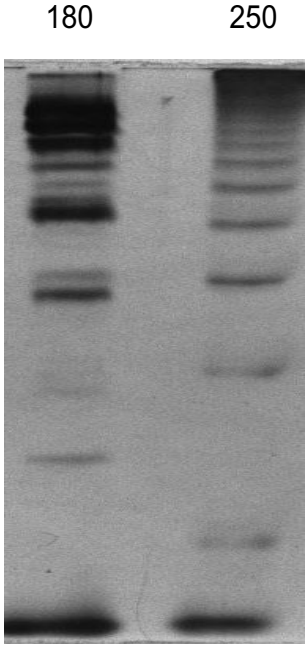

D)

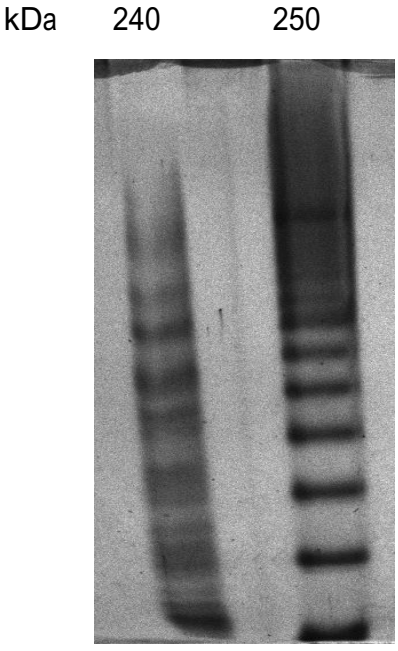

3.5. Probing the secondary structural features of the purified MYP present in the egg and coelomic fluid extracts.

Circular dichroism spectroscopy was utilized to probe the differences in secondary structural features of the purified egg and coelomic fluid MYPs. The egg MYP was previously shown to undergo structural changes in a calcium-dependent manner (Hayley et al., 2006). We examined the secondary structural features of the purified egg MYP (170 kDa) and coelomic fluid MYP (180 kDa). Ion exchange chromatography was performed using an anion exchange resin, Q-sepharose fast flow (fast-Q) (Pharmacia Biotech) to purify the 170 kDa and 180 kDa species from the egg and coelomic fluid extracts, respectively.

We calculated the molar residual elipticity (MRE) and plotted a graph of molar residual elipticity (MRE) vs wavelength. We used 20 mM Tris pH 8.0 as a blank. The MRE spectrum of purified egg MYP (170 kDa) had two negative peaks of similar magnitude at 208 nm and 219 nm (Fig. 3.11 A). Whereas, the negative peak at 219 nm was absent in purified coleomic fluid MYP (180 kDa) (Fig. 3.11 B). We used an online program k2D3 (http://www.ogic.ca/projects/k2d3) to calculate the secondary structural components of the purified 170 kDa and 180 kDa polypeptides.

The CD spectra directly reflect different types of secondary structures (alpha helix and beta sheet) present in the protein. The K2D3 program gives quantitative value of the alpha helix and beta sheet content by using a database of theoretically derived CD spectra

Fig. 3.11: Secondary structural characteristics of the purified egg MYP (170 kDa) and coelomic fluid MYP (180 kDa) between 200 nm and 300 nm CD spectra.

A) CD spectra of the purified egg MYP (170 kDa) has two negative bands (208 nm and 219 nm), whereas B) the purified coelomic fluid MYP (180 kDa) has a single negative band at 208 nm.

A) B)

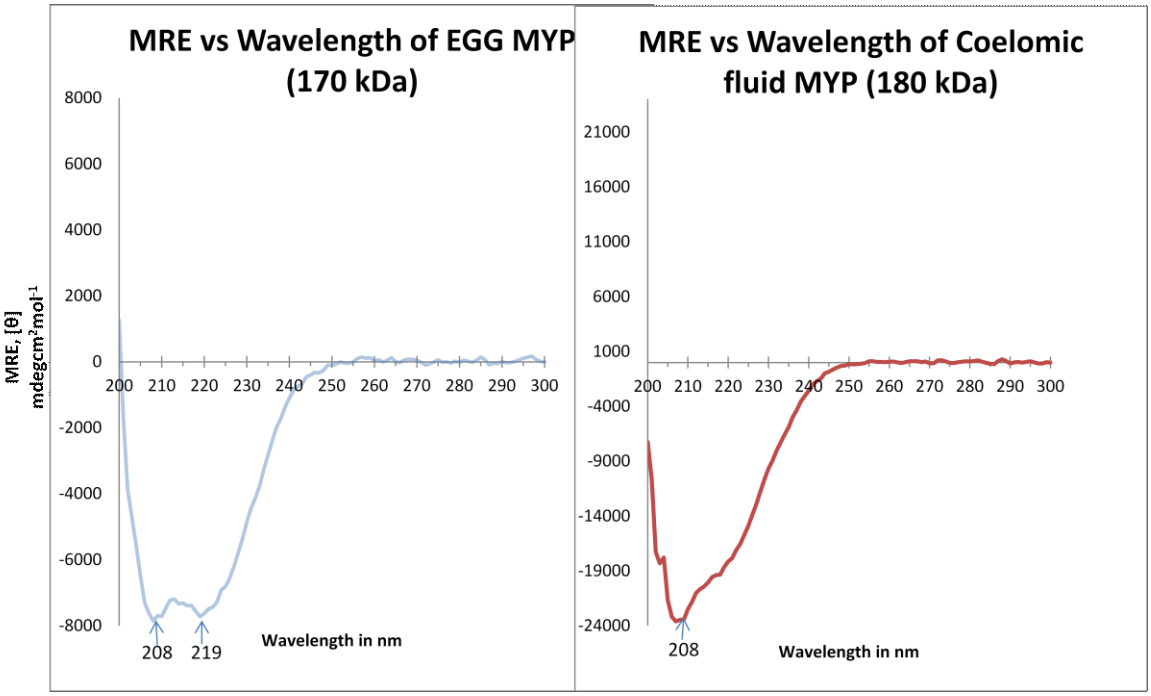
MRE vs Wavelength of EGG MYP (170 kDa)
MRE, [θ] mdegcm²mol⁻¹
8000
6000
4000
2000
0
-2000
-4000
-6000
-8000
200 210 220 230 240 250 260 270 280 290 300
208
219
Wavelength in nm
MRE vs Wavelength of Coelomic fluid MYP (180 kDa)
21000
16000
11000
6000
1000
-4000
-9000
-14000
-19000
-24000
200 210 220 230 240 250 260 270 280 290 300
208
Wavelength in nm

from the whole PDB to predict the secondary structure fractions of a protein from its CD spectrum. On the other hand, K2D3 is unreliable to give secondary structural content of 100% beta sheet protein. Our CD spectra data clearly shows that both the 170- and 180 kDa polypeptides undergo conformational change in the presence of 200 µM calcium. The α helix and β sheet contents should be viewed as differentialtion of the secondary structural features of the 170- and 180 kDa isoforms.

The K2D3 data suggested that the 170 kDa polypeptide has 5.57 ± 7.02% (n=4) α- helical and 24.27 ± 4.36% (n=4) β- sheet content, whereas the 180 kDa species has 61.71 ± 23.74 % (n=3) α-helical and 0.58 ± 0.58% (n=3) β- sheet content (Table 3.2).

Hayley et al. (2006) showed that the egg MYP undergoes a secondary structural change in the presence of 50 µM calcium and calcium concentrations above 50 µM did not induce any further change in secondary structural features. We characterized the calcium induced secondary structural changes in the 170 kDa and 180 kDa polypeptides in the presence of 200 µM calcium (Fig. 3.12 and 3.13, respectively). The MRE were quenched in both the polypeptide species in the presence of 200 µM calcium (n=3). In the presence of 200 µM calcium, the 170 kDa showed a significant quenching in the MRE values (Fig. 3.12), while the 180 kDa species showed a little or no quenching in the MRE values (Fig. 3.13). We also calculated the secondary structural components by using K2D3 after addition of 200 µM calcium. Addition of 200 µM calcium induced a secondary structural change in the 170 kDa species that resulted in a conformation containing 3.25 ± 4.66% alpha helix and 24.44 ± 5.61% beta-sheet content (Table: 3.2).

Table 3.2: Secondary structural features of the purified reducible forms of MYP in both the egg (170 kDa) and coelomic fluid (180 kDa) extracts by using K2D3 program.

Polypeptides (kDa)	Alpha-helix (%)	Beta-Sheet (%)	Random coil (%)
170	5.57 ± 7.02 (n=4)	24.27 ± 4.36 (n=4)	70.16 ± 5.16 (n=4)
170 + 200 µM Ca^{2+}	3.25 ± 4.66 (n=4)	24.44 ± 5.61 (n=4)	72.31 ± 2.02 (n=4)
180	61.71 ± 23.74 (n=3)	0.58 ± 0.58 (n=3)	37.04 ± 22.52 (n=3)
180 + 200 µM Ca^{2+}	59.45 ± 21.92 (n=3)	1.12 ± 1.16 (n=3)	39.43 ± 20.91 (n=3)

Fig. 3.12: Calcium induced secondary structural change of the purified reducible form of the egg MYP (170 kDa). In the presence of 200 μM calcium, the MRE values of both the negative peaks quenched by approximately 16000 mdeg cm^2 mol^{-2}.

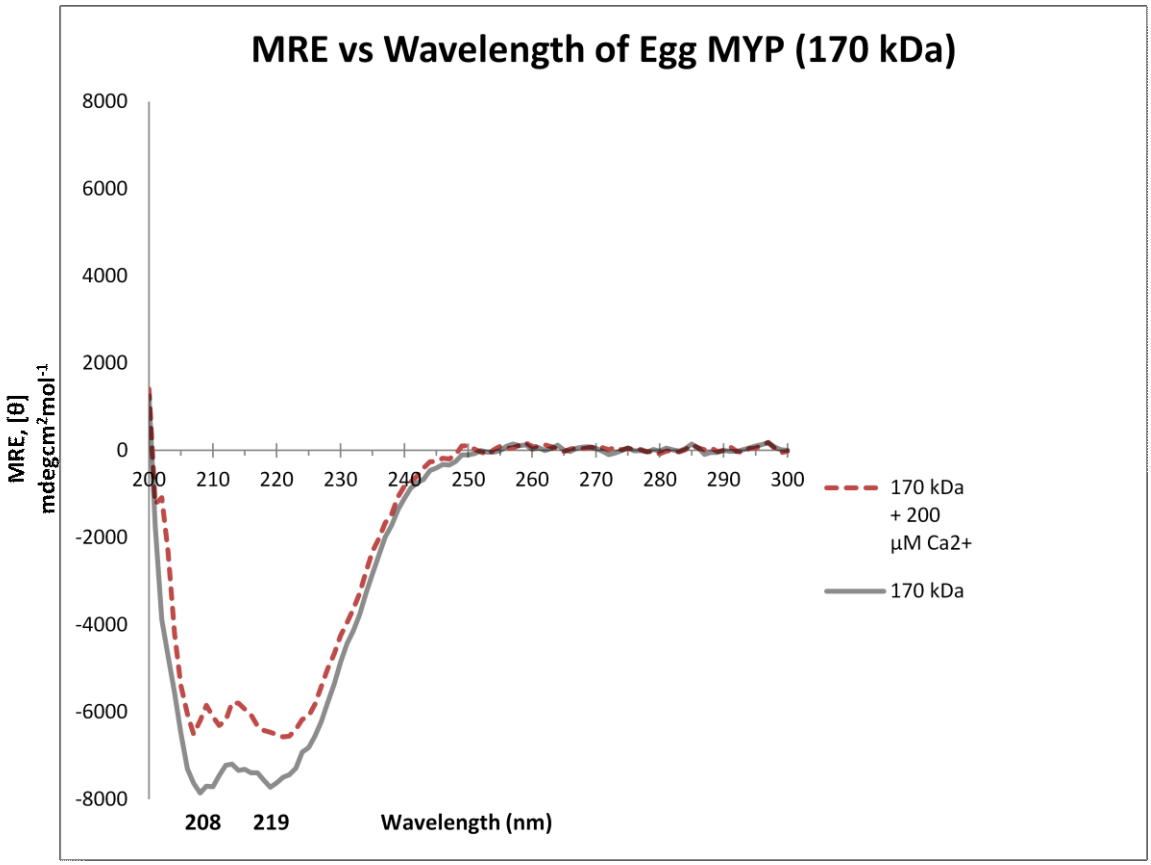
MRE vs Wavelength of Egg MYP (170 kDa)
MRE, [θ] mdegcm²mol⁻¹
8000
6000
4000
2000
0
-2000
-4000
-6000
-8000
200
210
220
230
240
250
260
270
280
290
300
208
219
Wavelength (nm)
170 kDa + 200 µM Ca2+
170 kDa

Fig. 3.13: Calcium induced secondary structural change of the purified reducible form of the coelomic fluid MYP (180 kDa). In the presence of 200 μM calcium, there was a very little or no change in the MRE values at 208 nm.

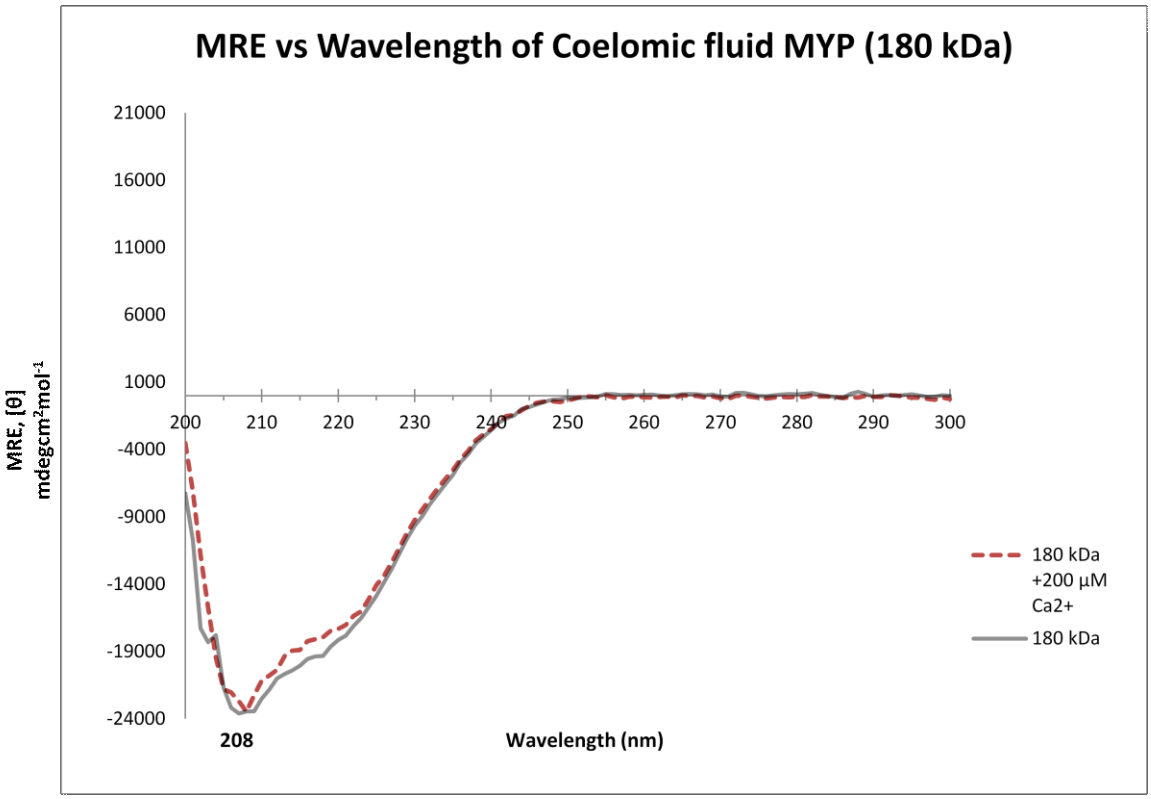
MRE vs Wavelength of Coelomic fluid MYP (180 kDa)
MRE, [θ] mdegcm²mol⁻¹
21000
16000
11000
6000
1000
-4000
-9000
-14000
-19000
-24000
200
210
220
230
240
250
260
270
280
290
300
208
Wavelength (nm)
180 kDa +200 µM Ca2+
180 kDa

In the presence of 200 µM calcium, the 180 kDa contained 59.45 ± 21.92% alpha helix and 1.12 ± 1.16% beta-sheet. These data indicated that both the 170 kDa and 180 kDa polypeptides undergo conformational changes in the presence of 200 µM calcium. We also probed the secondary structural features of the non-reducible form of coelomic fluid MYP (250 kDa) both in the absence and presence of 200 µM calcium. A single negative peak at 203 nm was evident for the 250 kDa complex in coelomic fluid (Fig. 3.14).

These results suggest that while all four species have similar primary structure they each likely possess distant secondary structural features.

3.6. Endogenous tryptophan fluorescence measurements, in the presence of different concentrations of calcium and zinc.

We next probed the tertiary structure of the purified 170 kDa (egg) and 180 kDa (coelomic fluid) polypeptides in the presence of calcium and/or zinc using endogenous tryptophan fluorescence measurements. Reports published by Hayley et al. (2006), evidenced a tertiary structural change in the egg MYP in a calcium-dependent manner. Unuma et al. (2007) showed that the MYP present in coelomic fluid has more zinc binding ability than the egg MYP and both of them can act as a zinc transporter.

Fig. 3.14: Calcium induced secondary structural change of the purified non-reducible form of the coelomic fluid MYP (250 kDa). In the presence of 200 µM calcium, there was approximately 5000 mdeg cm^2 mol^{-2} quenching in the MRE values at 203 nm.

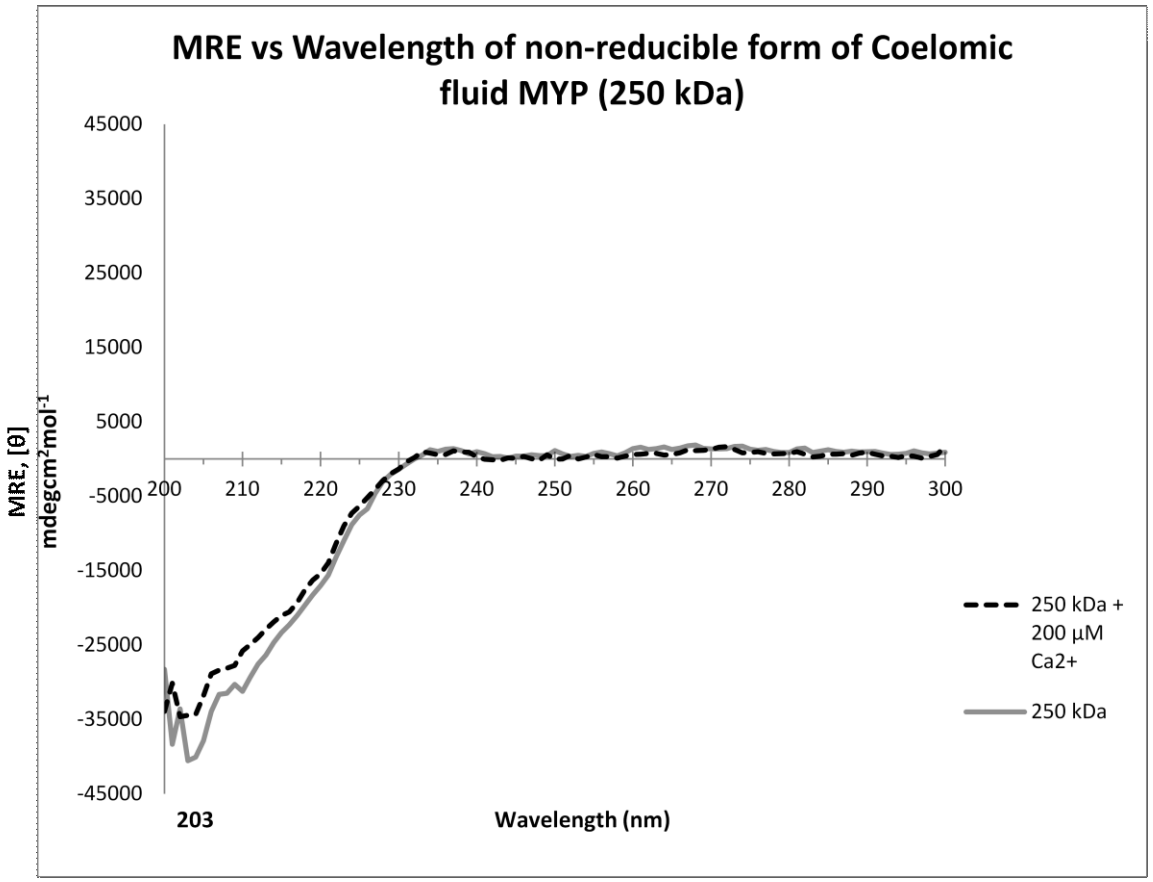
MRE vs Wavelength of non-reducible form of Coelomic fluid MYP (250 kDa)
45000
35000
25000
15000
5000
-5000
-15000
-25000
-35000
-45000
200
210
220
230
240
250
260
270
280
290
300
MRE, [θ] mdegcm²mol⁻¹
203
Wavelength (nm)
250 kDa + 200 µM Ca2+
250 kDa

In our study, the fluorescence spectra were measured by excitation at 287 nm and the emitted light was monitored between 300 and 400 nm. The maximum emission wavelength (λ_{max}) was 333 nm for both the 170 kDa and 180 kDa. The fluorescence emission spectra of both the egg MYP and coelomic fluid MYP was compared in the presence and absence of calcium (Fig. 3.15 A and B, respectively). In the presence of increasing concentrations of calcium, the emission spectrum was altered and there was a quenching in fluorescence intensity in both the 170 kDa and 180 kDa polypeptides (Fig. 3.15 A and B, respectively). However, the λ_{max} for both the egg (170 kDa) and coelomic fluid MYP (180 kDa) remained unchanged at 333 nm. The apparent dissociation constant (calcium) for the egg MYP (170 kDa) and coelomic fluid MYP (180 kDa) was 245- and 475 µM, respectively (Fig. 3.15 A and B). The fluorescence intensity was also decreased by 14% and 12% for the egg MYP (170 kDa) and coelomic fluid MYP (180 kDa), respectively.

These results suggest that, both the egg MYP (170 kDa) and coelomic fluid MYP (180 kDa) have different affinities for calcium. In addition, we also probed the tertiary structural change of both the 170 kDa and 180 kDa species in response to increasing concentrations of zinc. The emission spectrum was altered, as both protein species showed a quenching in fluorescence (Fig. 3.16 A and B, respectively). Here also the λ_{max} was at 333 nm for both polypeptide species. However, the apparent dissociation constants (zinc) were similar, 13.1- and 15.6 µM for the egg MYP (170 kDa) and coelomic fluid MYP (180 kDa), respectively (Fig. 3.16 A and B, respectively). Moreover, there was a decrease in fluorescence intensity by 17.5% for the egg MYP (170 kDa) and 16.5% for the coelomic fluid MYP (180 kDa).

Fig. 3.15: Correlation between the changes in the emitted fluorescence of the purified 170 kDa and 180 kDa polypeptides from the egg and coelomic fluid extracts, respectively as a function of calcium concentration.

A) Changes in fluorescence emission of the purified reducible form of MYP (170 kDa) from the egg extract. Aliquots of purified egg MYP (170 kDa) were incubated for 30 min at room temperature in the presence of various concentrations of calcium. The emitted fluorescence was decreased by 14% with an apparent dissociation constant (calcium) of 245 µM (K_d = 245 µM, R^2= 0.89).

B) Changes in fluorescence emission of the purified reducible form of MYP (180 kDa) from the coelomic fluid extract. Aliquots of the 180 kDa polypeptide enriched coelomic fluid were incubated for 30 min at room temperature in the presence of various concentrations of calcium. The emitted fluorescence was decreased by 12% with an apparent dissociation constant (calcium) of 475 µM (K_d = 475 µM, R^2= 0.93).

A)

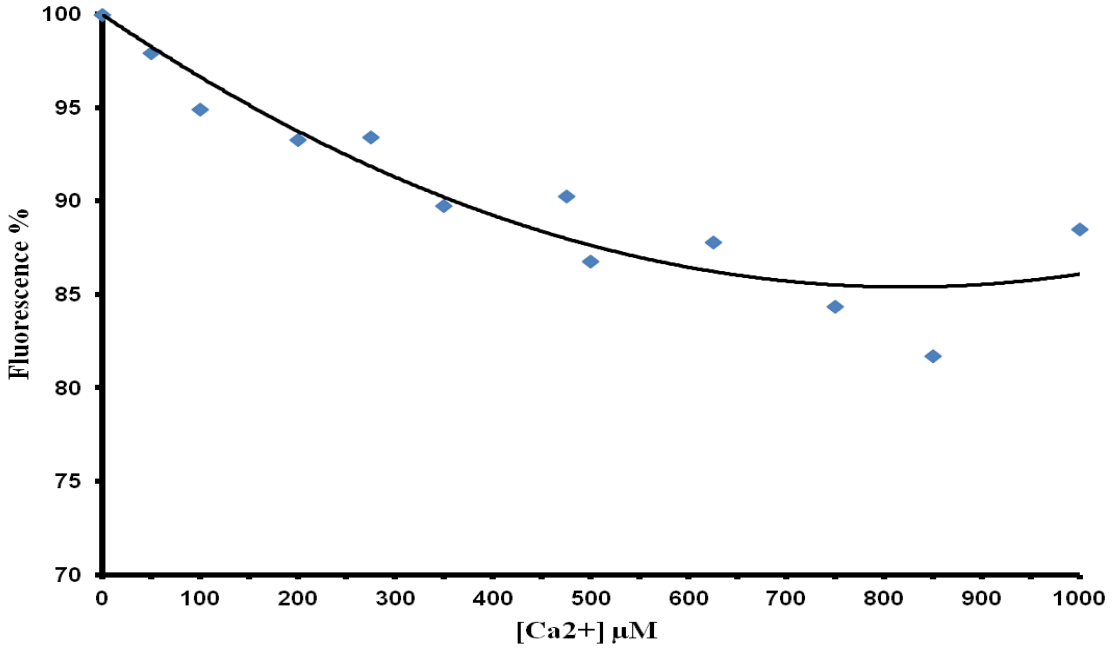
100
95
90
85
80
75
70
Fluorescence %
0
100
200
300
400
500
600
700
800
900
1000
[Ca2+] µM

B)

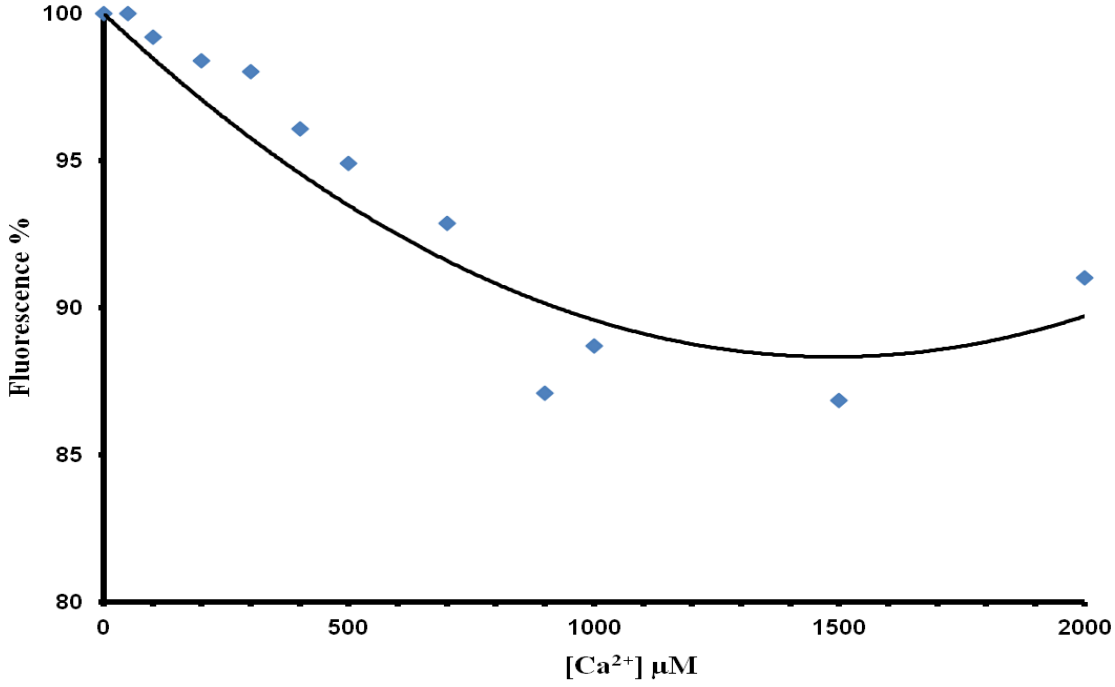
100
95
90
85
80
Fluorescence %
0
500
1000
1500
2000
[Ca2+] µM

Fig. 3.16: Correlation between the changes in the emitted fluorescence of the purified 170 kDa and 180 kDa polypeptides from the egg and coelomic fluid extracts, respectively as a function of zinc concentration.

A) Tryptophan fluorescence of the egg MYP (170 kDa) with different concentrations of zinc. Aliquots of the purified egg MYP (170 kDa) were incubated for 30 min at room temperature in the presence of various concentrations of zinc. The emitted fluorescence was decreased by 17.5% with an apparent dissociation constant (zinc) of 13.1 µM (K_d = 13.1 µM, R^2 = 0.75).

B) Tryptophan fluorescence of the coelomic fluid MYP (180 kDa) with different concentrations of zinc. Aliquots enriched with the coelomic fluid MYP (180 kDa) were incubated for 30 min at room temperature in the presence of various concentrations of zinc. The emitted fluorescence was decreased by 16.5% with an apparent dissociation constant (zinc) of 15.6 µM (K_d = 15.6 µM, R^2 = 0.75).

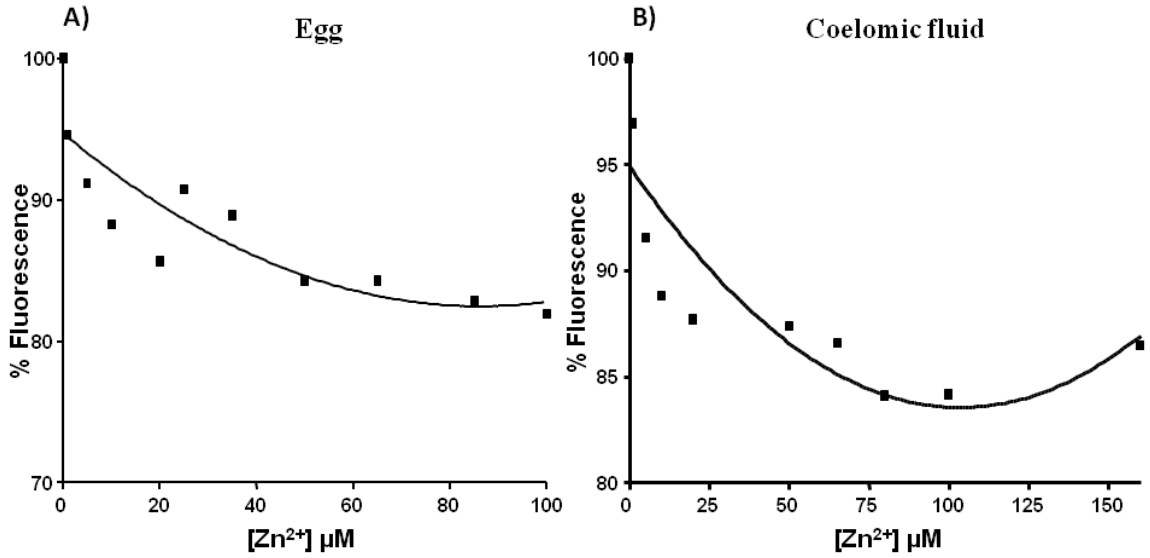
A)
Egg
100
90
80
70
% Fluorescence
0
20
40
60
80
100
[Zn2+] µM
B)
Coelomic fluid
100
95
90
85
80
% Fluorescence
0
25
50
75
100
125
150
[Zn2+] µM

These results suggest that both the egg MYP (170 kDa) and coelomic fluid MYP (180 kDa) interact with zinc in a similar manner.

3.7. Calcium-dependent liposome binding assay of the purified 170 kDa and 180 kDa polypeptides.

Peripheral membrane proteins attach temporarily to the outer portions of the biological membrane. Typically these proteins interact with the lipid head groups and sometimes top of the aliphatic chains. Their function revolves around binding and unbinding from membranes. These proteins can be involved in intracellular signaling and trafficking.

Previous studies showed that the egg MYP is peripherally associated with the plasma membrane and can promote cell-cell adhesion (Perera et al. 2004; Hayley et al., 2006, 2008). It was suggested that the egg MYP underwent structural changes during binding to liposome in a calcium-dependent manner (Hayley et al., 2006; Perera et al., 2004).

We therefore determined the ability of both the purified reducible forms of the major yolk protein present in the egg (170 kDa) and coelomic fluid MYP (180 Kda) to bind with liposomes. Liposome binding assays were employed to determine and compare liposome binding ability of the reducible forms of the MYPs in the egg (170 kDa) and coelomic fluid (180 kDa).

We quantified the calcium concentration-dependence of binding of the purified 170 kDa and 180 kDa species with multilammellar liposomes prepared using a brain lipid extract (Sigma Chemical Co.). We used the 0.25 M fraction (Fig. 3.2, Lane 5) for the purified 170 kDa and the 0.4 M fraction (Fig. 3.3, Panel B, Lane 6) for the purified 180 kDa species, eluted from the fast-Q resin and the brain lipid extract (5 µg/ ml) composed of 10% (w/v) PI, 50% (PS) and several other lipids (Sigma-Aldrich, Canada). The liposome binding assay revealed that both the 170 kDa and 180 kDa species bind with liposomes in a calcium-dependent manner (Fig. 3.17 A and B, respectively). Aliquots of the purified 170 kDa or 180 kDa species were incubated with multilammellar liposomes (5 µg/ml) in the presence of different concentrations of calcium followed by centrifugation. The unbound (supernatant) and the bound (pellet) fractions were separated by electrophoresis in an 8% (w/v) polyacrylamide gel and the gel was stained with CBB.

The bands of both of the polypeptides were excised from the gels and incubated overnight with 25% (w/v) pyridine. The polypeptides were quantified by measuring the absorbance at 650 nm. The amount of free calcium was calculated by using an online program WEBMAXCEXTENDED(http://www.leland.stanford.edu/~cpatton/webmaxc/webmaxcE.htm). The percentage of protein binding showed a positive correlation with increasing calcium concentration in both the 170 kDa and 180 kDa species (Fig. 3.18 A and B, respectively). The 170 kDa species showed a maximum percentage binding of 22% at a free calcium concentration of 160 µM, whereas the 180 kDa species showed a maximum binding of 36% at a free calcium concentration of 1000 µM.

Fig. 3.17: Liposome binding assay of the purified 170 kDa and 180 kDa polypeptides with multilammellar brain lipid liposome.

A) An aliquot of the 0.25 M fraction (Fig. 3.2, Lane 5) containing the purified 170 kDa was incubated with multilammellar liposome for 30 min at room temperature in the presence of 0 μM (lanes 1 and 2), 80 μM (lane 3 and 4), 130 μM (lane 5 and 6), 150 μM (lanes 7 and 8) and 170 μM (lanes 9 and 10) free calcium. The liposomes were pelleted by centrifugation for 30 min and both the unbound (lanes 1, 3, 5, 7 and 9, respectively) and bound fractions (lanes 2, 4, 6, 8 and 10 respectively) were fractionated in an 8% (w/v) polyacrylamide gel. The gel was stained with CBB.

B) An aliquot of the 0.4 M fraction (Fig. 3.3, Panel B, Lane 6) for the purified 180 kDa species, was incubated with multilammellar liposome for 30 min at room temperature in the presence of 0 μM (lanes 1 and 2), 100 μM (lanes 3 and 4), 300 μM (lanes 5 and 6), 500 μM (lanes 7 and 8) and 1000 μM (lanes 9 and 10) free calcium. The liposomes were pelleted by centrifugation for 30 min and both the unbound (lanes 1, 3, 5, 7 and 9, respectively) and bound fractions (lanes 2, 4, 6, 8 and 10 respectively) were fractionated in an 8% (w/v) polyacrylamide gel. The gel was stained with CBB.

A)

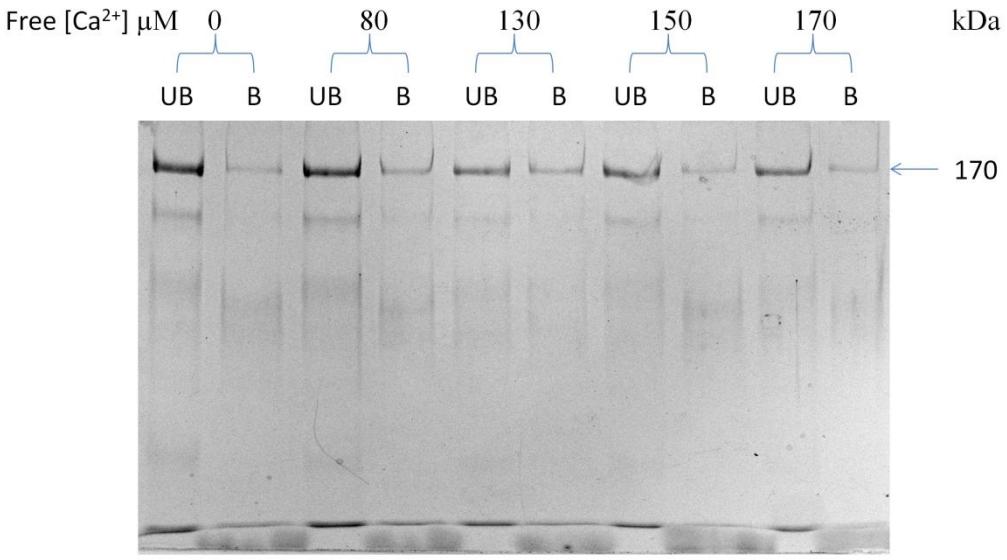
Free [Ca2+] µM
0
80
130
150
170
kDa
UB
B
170

B)

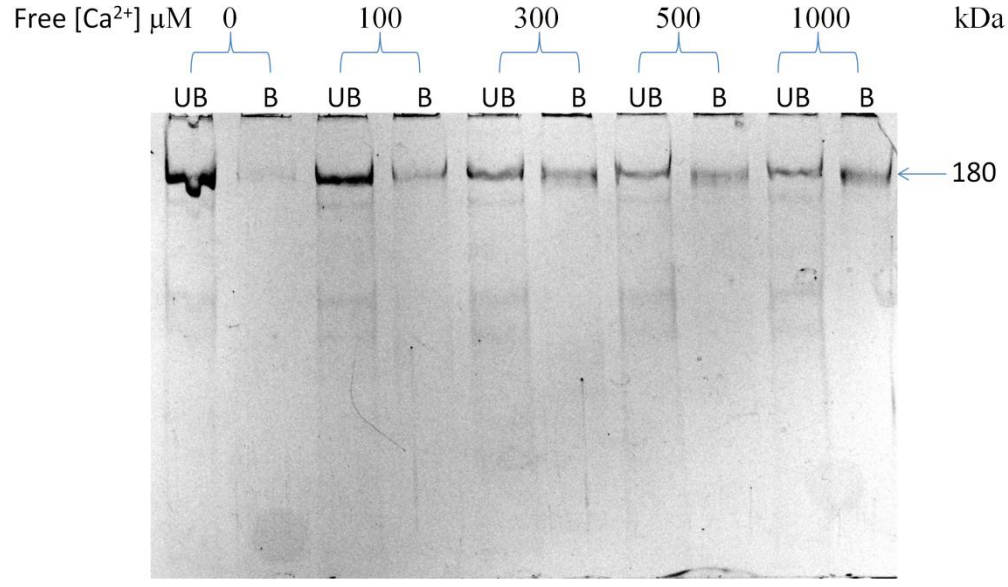
Free [Ca2+] µM
0
100
300
500
1000
kDa
UB
B
180

Fig. 3.18: Effect of calcium concentrations on both the 170 kDa and 180 kDa species binding to liposome.

A) Aliquots of 0.25 M fraction (Fig. 3.2, Lane 5) containing the purified 170 kDa was incubated with multilammellar liposome for 30 min at room temperature in the presence of different concentrations of free calcium for 30 min. The liposomes were pelleted by centrifugation for 30 min and both the unbound and bound fractions were fractionated in an 8% (w/v) polyacrylamide gel. The gel was stained with CBB. The 170 kDa bands were excised and incubated with 25% (v/v) pyridine for overnight. The percentage of bound protein to liposome was quantified by measuring absorbance at 650 nm. The apparent dissociation constant (calcium) was 10 μM (K_d = 10 μM; R^2= 0.95).

B) Aliquots of the 0.4 M fraction (Fig. 3.3, Panel B, Lane 6) for the purified 180 kDa species, was incubated with multilammellar liposome for 30 min at room temperature in the presence of different concentrations of free calcium for 30 min. The liposomes were pelleted by centrifugation for 30 min and both the unbound and bound fractions were fractionated in an 8% (w/v) polyacrylamide gel. The gel was stained with CBB. The 180 kDa bands were excised and incubated with 25% (v/v) pyridine for overnight. The percentage of bound protein to liposome was quantified by measuring absorbance at 650 nm. The apparent dissociation constant (calcium) was 290 μM (K_d = 290 μM; R^2= 0.97).

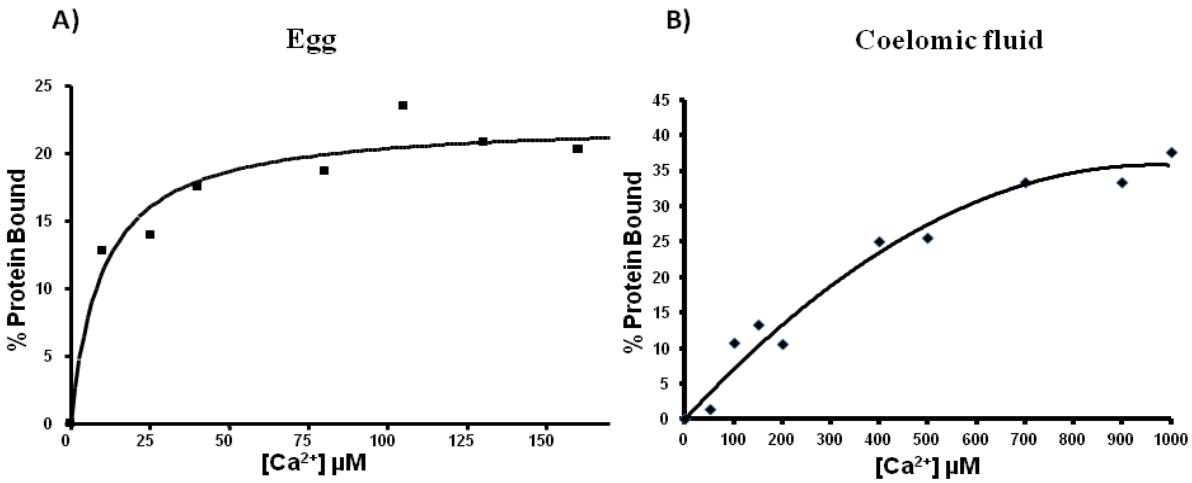
A)
Egg
% Protein Bound
[Ca2+] µM
B)
Coelomic fluid
% Protein Bound
[Ca2+] µM

The apparent dissociation constants (calcium) for the purified 170 kDa and 180 kDa species were 10- and 290 μM, respectively. The liposome binding data clearly suggested that while both proteins bind to liposomes, their calcium concentration dependencies are different.

3.8. Liposome aggregation by the egg and coelomic fluid major yolk proteins in a calcium dependent manner.

Liposome aggregation assays were performed to investigate vesicular aggregation ability of the reducible forms of the MYPs present in the egg (170 kDa) and coleomic fluid (180 kDa). The 170 kDa polypeptide was capable of driving aggregation of vesicular structures in a calcium-dependent manner. In the absence of the egg MYP, 1.5 mM calcium was able to aggregate liposome (Hayley et al., 2006).

To determine the effect of the egg MYP (170 kDa) or coleomic fluid localizd MYP (180 kDa) on liposome aggregation in a calcium-dependent manner, two sets of aggregation assays were performed. The first set involved the addition of different concentrations of calcium (below 1.5 mM) in the absence of the egg MYP (170 kDa) or the coelomic fluid MYP (180 kDa) to the liposome to demonstrate that calcium alone was not able to drive liposome aggregation. In the second set of experiment we added a fixed amount (5 μg) of the 170 kDa or 180 kDa proteins with different concentrations of calcium to liposome to determine the effect of calcium on protein-dependent liposome aggregation (Fig. 3.19 A and B, respectively).

Fig. 3.19: Determination of the effect of the egg MYP (170 kDa) or coelomic fluid MYP (180 kDa) on liposome aggregation in the presence of different concentrations of calcium.

A) Aliquots (5 µg) of 0.25 M NaCl fraction (Fig. 3.2, lane 6) enriched in the 170 kDa species were incubated for 10 min with 250-, 350-, 850- and 1000 µM of calcium. Aggregation was monitored by measuring the OD at 350 nm at one min intervals. Upon addition of multilammellar liposomes (10 mg/ml) to the aggregation buffer containing 40 mM Histidine, 300 mM sucrose, 0.5 mM $MgCl_2$, and 0.5 M KCl (pH 6.0) were monitored for 5 min. Then different concentrations of calcium were added to the liposome containing aggregation buffer and the OD were monitored for 10 min to see the effect of calcium on liposome aggregation. At 16 min, the pre-incubated protein (5 µg) with calcium was added to the aggregation buffer containing liposomes and calcium, the OD was monitored for another 10 min.

B) Aliquots (5 µg) of 0.3 M NaCl fraction (Fig. 3.3, lane 5) enriched in the 180 kDa were incubated for 10 min with 100-, 250-, 350-, 500- and 850 µM of calcium. Aggregation was monitored by measuring the OD at 350 nm at one min intervals. Upon addition of multilammellar liposomes (10 mg/ml) to the aggregation buffer containing 40 mM Histidine, 300 mM sucrose, 0.5 mM $MgCl_2$, and 0.5 M KCl (pH 6.0) were monitored for 5 min. Then different concentrations of calcium were added to the liposomes containing aggregation buffer and the OD were monitored for 10 min to see the effect of calcium on liposome aggregation. At 16 min, the pre-incubated protein (5 µg) with calcium was added to the aggregation buffer containing liposome and calcium, the OD was monitored for another 10 min

.

A)

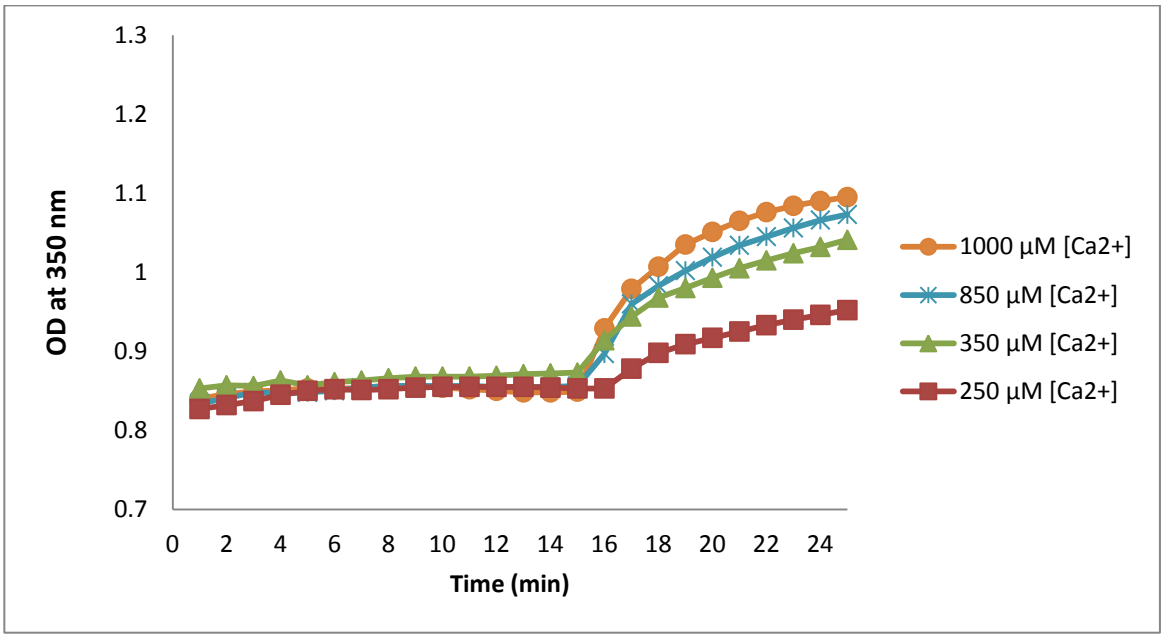
1.3
1.2
1.1
1
0.9
0.8
0.7
OD at 350 nm
0
2
4
6
8
10
12
14
16
18
20
22
24
Time (min)
1000 µM [Ca2+]
850 µM [Ca2+]
350 µM [Ca2+]
250 µM [Ca2+]

B)

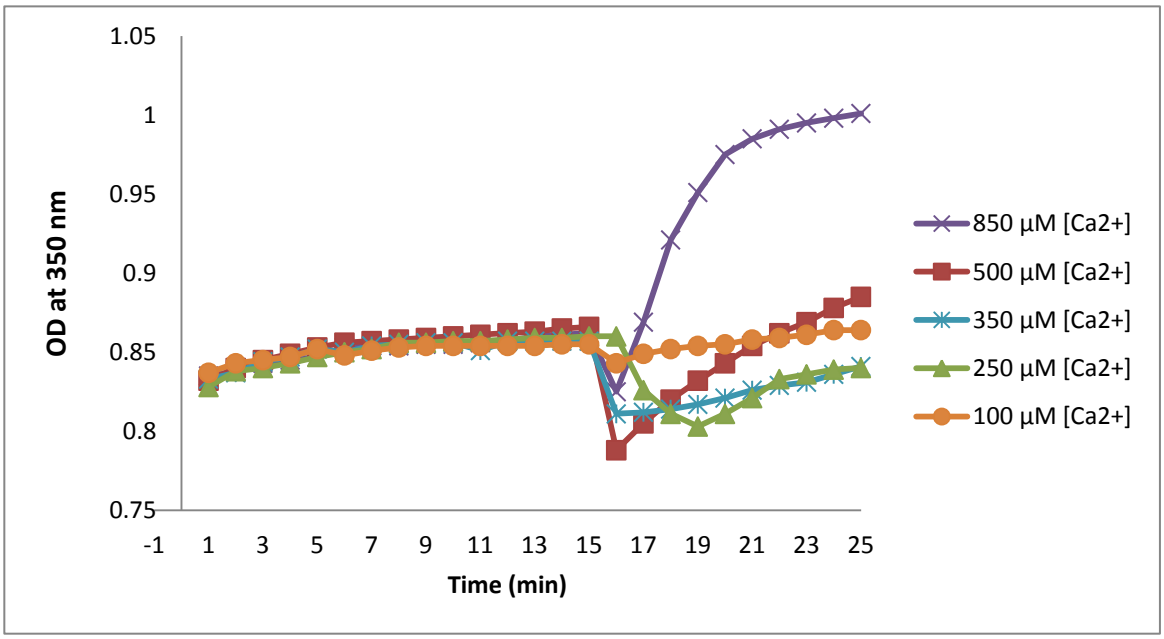
1.05
1
0.95
0.9
0.85
0.8
0.75
OD at 350 nm
-1
1
3
5
7
9
11
13
15
17
19
21
23
25
Time (min)
850 µM [Ca2+]
500 µM [Ca2+]
350 µM [Ca2+]
250 µM [Ca2+]
100 µM [Ca2+]

We used a Lowry assay to determine the concentrations of the 170 kDa and 180 kDa species in the fractions eluted from fast-Q resin. In each case, for both the 170 kDa and 180 kDa species we calculated the initial rates of aggregation and plotted them against different calcium concentrations (Fig. 3.20).

The liposome aggregation assay was then performed with the purified enriched fractions of 170 kDa species from egg extract and 180 kDa species from coelomic fluid extracts eluted from the fast-Q resin. We used the 0.25 M NaCl fraction (Fig. 3.2, lane 6) enriched in 170 kDa form in the presence of different concentrations of calcium below 1.5 mM. In each experiment we used 5 µg of 170 kDa form that was incubated for 10 min with different concentrations of calcium. We measured the absorbance of liposome in the presence of different concentrations of calcium below 1.5 mM, in a 170 kDa species independent manner for 10 min at 350 nm in one min interval and found that calcium alone could not drive liposome aggregation (Fig. 3.19 A).

In the second set, we added 5 µg of the egg MYP (170 kDa), that was pre incubated with different concentrations of calcium and took the absorbance for 10 more min at 350 nm/min. The egg MYP (170 kDa) was capable of driving liposome aggregation below 1.5 mM calcium, a concentration at which calcium alone could not drive liposome aggregation. These results indicated that in the presence of the egg MYP (170 kDa), the rate of aggregation was dependent on the calcium concentrations used in the assay. The rate of aggregation was fast and there was no effect of calcium alone used in the assay. The initial rate of aggregation for the egg MYP (170 kDa) was 2.2×10^{-5}(Fig. 3.20).

Fig. 3.20: Comparative analysis of the effect of egg MYP (170 kDa) and coelomic fluid MYP (180 kDa) on the rate of liposome aggregation.

Aggregation assays were performed by using 0.25 M NaCl fraction (Fig. 3.2, lane 6) enriched in the 170 kDa species and 0.3 M NaCl fraction (Fig. 3.3, lane 5) enriched in the 180 kDa species with multilammellar liposome in the presence of a series of calcium concentrations from 100- to 1000 µM. All the aggregation assays were performed with a fixed amount (5 µg) of protein. The initial rate of aggregation was calculated from the calcium-dependent aggregation activities of both the 170 kDa and 180 kDa species (Fig. 3.19 A and B, respectively). These initial rates of aggregation of both polypeptides were plotted against the calcium concentrations. The initial rate of aggregation for both proteins was increased with the increase of calcium concentrations. The initial rate of aggregation was 2.2×10^{-5} and 1.12×10^{-5} for the egg and coelomic fluid MYP, respectively.

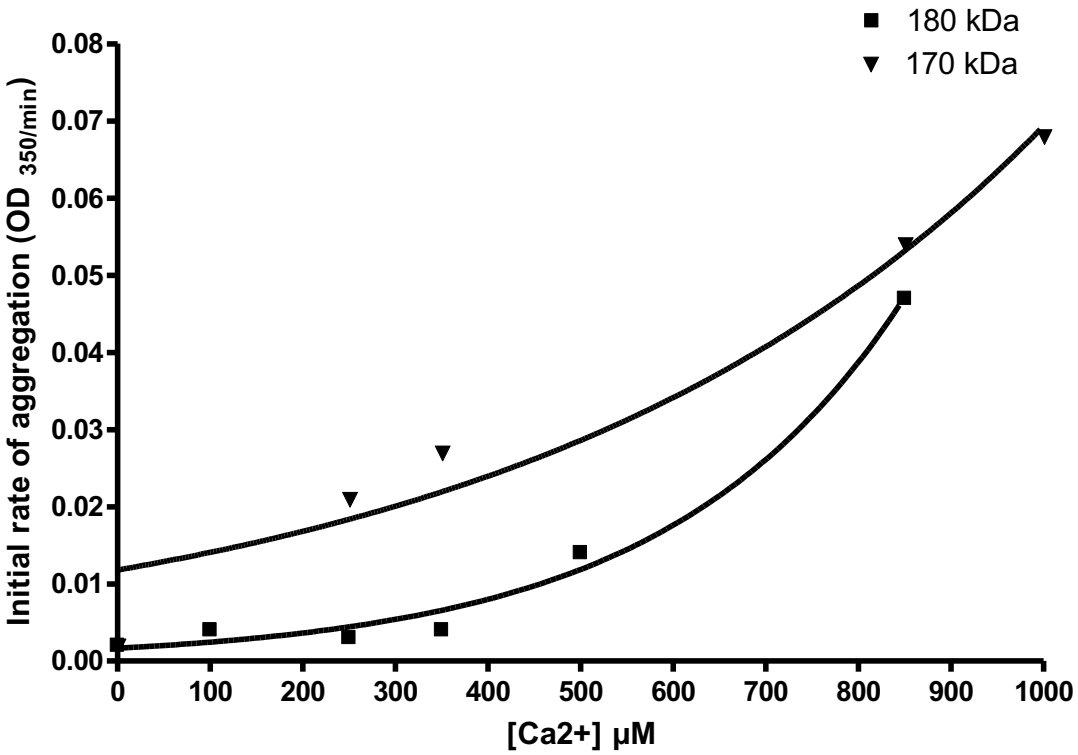
180 kDa
170 kDa
Initial rate of aggregation (OD 350/min)
0.08
0.07
0.06
0.05
0.04
0.03
0.02
0.01
0.00
0
100
200
300
400
500
600
700
800
900
1000
[Ca2+] µM

We also found a direct consistent correlation of liposome aggregation with the calcium dependent tertiary structural change of the egg MYP (170 kDa) (Fig. 3.21 A).

Similarly, a liposome aggregation assay was also performed with 5 µg of coelomic fluid MYP (180 kDa) to investigate and compare the effect of the 180 kDa species with the 170 kDa species in egg. We used 0.3 M NaCl fraction (Fig. 3.3, lane 5) enriched in 180 kDa and followed the same procedure of liposome aggregation as followed with egg MYP (170 kDa) in the presence of same concentrations of calcium below 1.5 mM (Fig. 3.19 B).

These results indicated that the coelomic fluid localized MYP (180 kDa) can also drive liposome aggregation in a calcium dependent manner. The aggregation activity was increased with the addition of higher calcium concentrations to the liposomes containing aggregation buffer in the presence of the 180 kDa species (Fig. 3.19 B). The initial rate of aggregation for the coelomic fluid MYP (180 kDa) was 1.12×10^{-5}, which is lower than the rate of vesicular aggregation driven by the egg MYP (170 kDa) (Fig. 3.20).

The MYP localized in both the egg and coelomic fluid is capable of driving vesicular aggregation in a calcium dependent manner. The egg MYP (170 kDa) has a higher capability to aggregate liposome than the coelomic fluid MYP (180 kDa). In the presence of both the egg MYP (170 kDa) and coelomic fluid MYP (180 kDa), liposome aggregation occurred in a manner consistent with the calcium concentration dependent change in tertiary structure of both polypeptides (Fig. 3.21 A and B, respectively).

Fig. 3.21: Correlation between the change in the emitted fluorescence of both the egg MYP (170 kDa) and coelomic fluid MYP (180 kDa) as a function of calcium concentration (■) and the effect of calcium dependent liposome aggregation in the presence of the170 kDa or the 180 kDa polypeptides (•).

A) In all fluorescence experiments, aliquots of the 170 kDa species were incubated for 30 min at room temperature in the presence of various concentrations of calcium followed by spectrophotometric analysis. In the liposome aggregation study, aliquots of the 170 kDa species were added to multillamellar liposomes in the presence of different concentrations of calcium. The initial rates of liposome aggregation (Δ OD_{350}/min) in the presence of the 170 kDa protein and different concentrations of calcium were calculated and plotted against the calcium concentrations.

B) In all fluorescence experiments, aliquots of the 180 kDa species were incubated for 30 min at room temperature in the presence of various concentrations of calcium followed by spectrophotometric analysis. In the liposome aggregation study, aliquots of the 180 kDa were added to multillamellar liposomes in the presence of different concentrations of calcium. The initial rates of liposome aggregation (Δ OD_{350}/min) in the presence of the 180 kDa protein and different concentrations of calcium were calculated and plotted against the calcium concentrations.

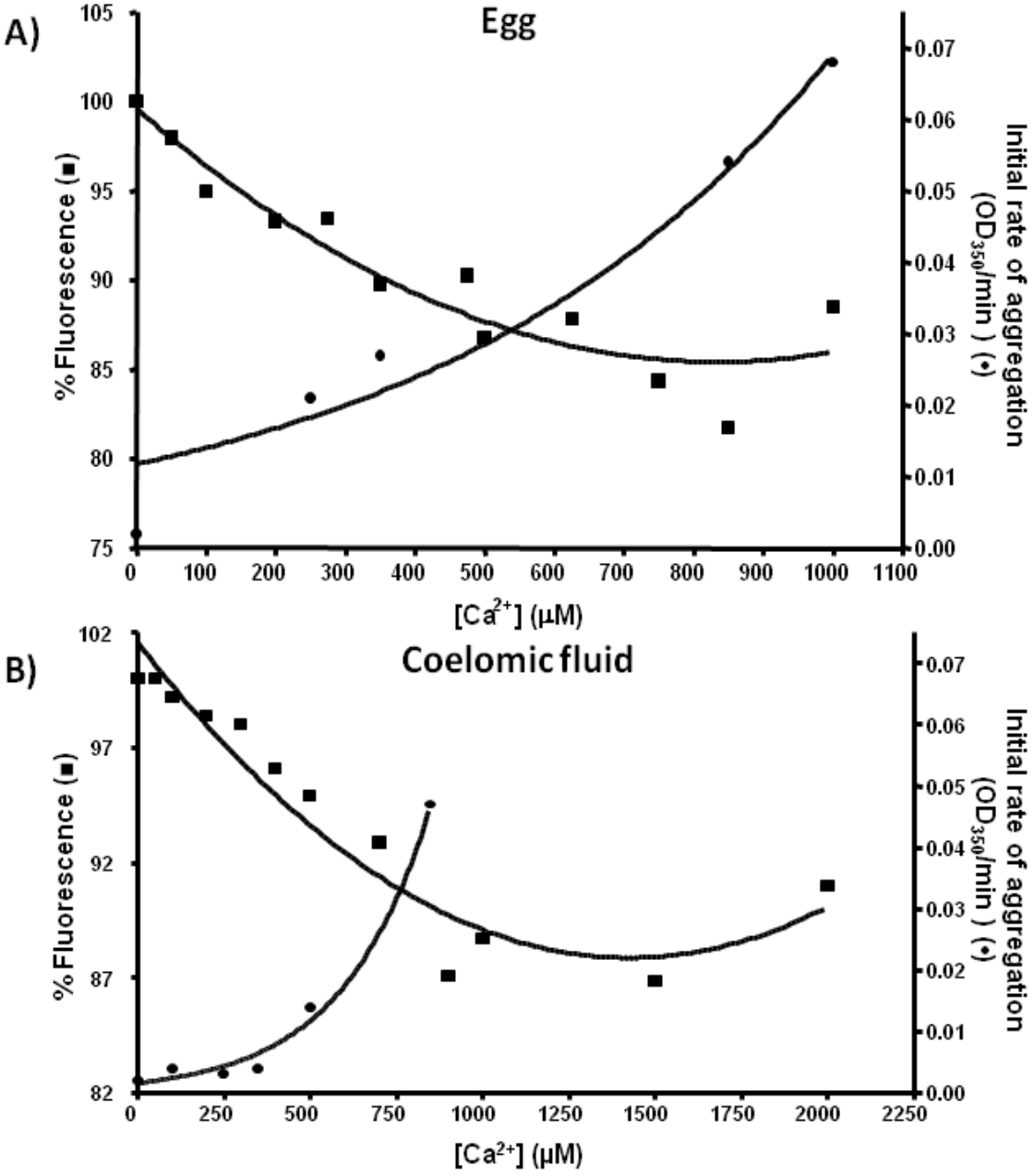
A)
Egg
% Fluorescence (■)
Initial rate of aggregation (OD350/min) (•)
[Ca2+] (µM)
B)
Coelomic fluid
% Fluorescence (■)
Initial rate of aggregation (OD350/min) (•)
[Ca2+] (µM)

These findings directly indicated that the tertiary structural change of both the egg MYP (170 kDa) and coelomic fluid MYP (180 kDa) is associated with calcium-dependent vesicular aggregation.

Chapter 4: Discussion

4.1. The major yolk protein present in the egg (170 kDa and 240 kDa) and coelomic fluid (180 kDa and 250 kDa) are the same protein, but they exhibit differences in their biological properties.

In the current study, we focused on the biochemical characterization of the major yolk protein localized in both the egg and coelomic fluid with the specific aim of identifying structural and function differences between the egg and coelom-specific forms. The egg MYP is known to be a hexameric glycoprotein characterized by intra-chain disulfide bonds and is stabilized with calcium. For our initial comparison we investigated the sucrose density gradient elution profile of the polypeptides present in the egg and coelomic fluid, both in the absence and presence of Triton X-100.

The sucrose density gradient ultracentrifugation data revealed that in the absence of Triton X-100, the egg-specific (240-, 170-kDa) and coelom-specific (250- and 180 kDa) polypeptides are unique in their elution profiles (Table. 3.1). The buoyant densities of the 170- and 180 kDa are higher than the 240- and 250 kDa. This indicated that under native conditions, both the egg MYP (240- and 170 kDa) and the coelomic fluid MYP (250- and 180 kDa) are unique in their size and/or shape. Under native conditions, the non-reducible forms of the MYP in both the egg (240 kDa) and coelomic fluid (250 kDa) are not the aggregated forms of the reduced MYPs (170 kDa in egg; 180 kDa in coelomic). Both of the coelomic fluid protein species are 10 kDa higher in molecular masses than the corresponding egg species.

In the presence of Triton X-100, there is a clear shift of elution profiles for the 240 kDa from the egg and the 250 kDa and 180 kDa species from the coelomic fluid extract (Table. 3.1). In the presence of Triton X-100, the MYP present in the coelomic fluid (250 kDa and 180 kDa) eluted in low-density fractions, while the egg MYP (240 kDa) eluted in high-density fractions, possibly because Triton X-100 induces a change in the shape of the 180-, 240- and 250 kDa polypeptides. The elution profile remains the same for the 170 kDa species both in the presence and absence of Triton X-100. Clearly, Triton X-100 does not induce any change in the shape of the reducible form of the egg MYP (170 kDa). Triton X-100 is a non-ionic detergent that induces a hydrophobic environment similar to the hydrophobic environment between the inner and outer leaflets of the lipid bilayer. This further supports the contention that the egg MYP (170 kDa) is peripherally located in the plasma membrane. Moreover, in the presence of Triton X-100, both the 240- and 250 kDa polypeptides eluted in the same fraction. Both the 170- and 180 kDa species are also eluted in the same fraction in the presence of Triton X-100. This indicated that in the hydrophobic environment all four species may exhibit same biological function.

Sodium dodecyl sulfate polyacrylamide gel electrophoresis (SDS-PAGE) and Native-PAGE studies indicated that, under reducing conditions, there are mainly two forms of major yolk protein present in both the egg (170 kDa, 240 kDa) and the coelomic fluid extracts (180 kDa, 250 kDa), and the coelomic fluid protein species are 10 kDa higher in apparent molecular masses than the corresponding egg species (Fig. 3.6, lanes 1 and 3, respectively; Fig. 3.7 B and Fig. 3.8 B). However, under non-reducing conditions, the reducible forms of the MYP in both the egg (170 kDa) and coelomic fluid (180 kDa) co-

migrated with the non-reducible forms of the MYP (240 kDa in egg; 250 kDa in coelomic fluid) (Fig. 3.6, lanes 2 and 4, respectively; Fig. 3.7 A, lanes 1 and 2, respectively and Fig. 3.8 A, lanes 1 and 2, respectively). These data indicated that the intact 240- and 250 kDa species consists of subunits characterized by intra-chain disulfide bonds. Disulfide bonds play an important role in the folding and stability of proteins, usually proteins secreted to the extracellular medium. Since most cellular compartments are reducing environments, generally disulfide bonds are unstable in the cytosol. Our data showed that, under both the reducible and non-reducible conditions, the coelomic fluid MYP is 10 kDa higher in apparent molecular mass than the egg MYP, possibly because the coelomic fluid MYP is slightly modified in molecular structure after its incorporation with the egg yolk granule. The difference in apparent molecular mass between the MYP localized in the egg and the coelomic fluid was also observed in different species of sea urchin, which indicates it may be a common phenomenon in sea urchins. All four MYP species present in both the egg and the coelomic fluid are unique in their SDS-PAGE electrophoretic mobility both under reducing and non-reducing conditions. This difference in physical property may be responsible for functional differences, which further supports the idea that the polypeptides present in the egg and coelomic fluid are unique in size. Under non-reducing conditions, both the reducible forms of the MYP in the egg (170 kDa) and coelomic fluid extract (180 kDa) co-migrated with the non-reducible forms of the MYP (240 kDa in egg; 250 kDa in coelomic fluid). This indicated that both the 170- and 240 kDa in the egg and the 180- and 250 kDa in coelomic fluid are isomers the same protein, but with a difference in their size.

To further investigate the possibility that all four polypeptides share the same primary structure, we did partial V8 protease peptide mapping. The online program ExPASy-Peptide cutter suggested that the MYP contains V8 protease digestion sites (Fig. 3.9 B). Limited V8 protease peptide mapping data also showed an identical digestion pattern between the 170 kDa and 180 kDa species (Fig. 3.10 A). The digestion pattern was also similar between the 170 kDa and 240 kDa (Fig. 3.10 B) and as well as between the 180 kDa and 250 kDa species (Fig. 3.10 C). The V8 protease digestion pattern was also somewhat similar between the non-reducible forms of the MYP present in the egg (240 kDa) and coelomic fluid (250 kDa) (Fig. 3.10 D). Although having differences in their molecular masses and different sucrose density gradient elution profiles, all four polypeptides have a similar primary structure. The V8 protease requirement was the same for the 170 kDa and 180 kDa, while the 240 kDa required high concentrations of V8 protease and the 250 kDa required lower concentrations of V8 protease. This may be because all four polypeptides are different in their molecular masses and have different shapes resulting in varying access of the V8 protease to susceptible peptide bands. This clearly indicated that all four MYP species present in both the egg and coelomic fluid are isoforms of the same protein, but may differ in their biological properties.

4.2. The reducible forms of the major yolk protein present in the egg (170 kDa) and coelomic fluid (180 kDa) undergo changes in their secondary and tertiary structure in response to calcium.

The egg MYP undergoes two calcium-concentration-dependent structural transitions: a secondary structural change responsible for membrane binding, with an apparent dissociation constant (calcium) 25 μM, followed by a tertiary structural change responsible for egg MYP-driven membrane-membrane interaction, with an apparent dissociation constant (calcium) 240 μM (Hayley et al., 2006, 2008; Perera et al., 2004).

We did a comparative analysis of both the secondary and tertiary structural changes of the egg MYP (170 kDa) and coelomic fluid MYP (180 kDa) in response to calcium concentration. Circular dichroism data suggested that, in the absence of calcium, both the egg (170 kDa) and coelomic fluid MYP (180 kDa) were unique in their secondary structural features (Fig 3.11 A and B, respectively). Their unique structural features may be due to their difference in size and/or shape. The molar residual elipticity (MRE) of the purified egg MYP (170 kDa) has a double dip (208 nm, 219 nm), whereas there is a single dip (208 nm) for the purified coelomic fluid MYP (180 kDa) species. Moreover, the purified non-reducible form of MYP (250 kDa) in the coelomic fluid also has a single dip at 203 nm (Fig. 3.14). These results further suggested that both the 170 kDa and 180 kDa species are unique in their secondary structure, hence they may also show a difference in their liposome binding ability.

In the presence of 200 μM calcium, the 170 kDa species showed a dramatic change in secondary structural features, while there was little or no evidence of structural change for the 180 kDa species in response to the same concentration of calcium (Fig. 3.12 and Fig.

3.13, respectively). This indicated that higher concentrations of calcium are required for a secondary structural change in the MYP present in the coelomic fluid (180 kDa) than the egg MYP (170 kDa). The CD data indicated that in the presence of calcium, the molar residual elipticity (MRE) of the 170 kDa species increased at 208- and 219 nm, possibly because the 170 kDa undergoes a secondary structural change by losing its α-helical structure in the presence of calcium (Fig. 3.12). Using the K2D3 data, the calcium-bound 170 kDa species is estimated to contain less α-helical structure than the calcium free protein (Table 3.2). On the other hand, there was no noticeable change in MRE of the 180 kDa species in response to 200 μM calcium (Fig. 3.13). The K2D3 data indicated that the α-helical structure of the 180 kDa species only slightly changed in the presence of 200 μM calcium (Table. 3.2). This may possibly be because the 180 kDa species requires higher concentrations of calcium to induce a conformational change. It is likely that calcium binding causes a reorganization of these polypeptides' secondary structure that is already formed in the calcium-free state. The observed change in secondary structure in response to 200 μM calcium was also evidenced with the 250 kDa species from coelomic fluid (Fig. 3.14). Here also the MRE was increased at 203 nm in the calcium bound state of the 250 kDa polypeptide. These data suggested that all three polypeptides may have a different binding affinity to calcium that causes their conformational change and thus may have differences in calcium-mediated biological functions.

In addition, the near UV region (320-260 nm) reflects the environments of the aromatic amino acid side chains (phenylalanine, tyrosine and tryptophan) and thus gives information about the tertiary structure of the protein (Kelly et al., 2000). In our study, in

the presence of 200 μM calcium, there was no dip in CD spectrum in this region, which indicated the necessity of higher concentrations of calcium to mediate tertiary structural change in the 170-, 180- and 250 kDa polypeptides. Like most of the calcium binding proteins, these three polypeptides may also play important biological functions by regulating ion transport, protein conformational change and enzyme activation.

To further analyze the effects of calcium on the tertiary conformational change of the 170 kDa and 180 kDa polypeptides, we utilized tryptophan fluorescence measurements. Calcium was found to modulate the intensity of maximal endogenous fluorescence. The effect of calcium on the egg MYP (170 kDa) species was different from the coelomic fluid MYP (180 kDa), with an apparent dissociation constant of 245- and 475 μM for the 170 kDa and 180 species, respectively (Fig. 3.15 A and B, respectively). These data indicated that the 170 kDa species is more sensitive to tertiary conformational change in response to calcium than the 180 kDa species. There was a characteristic calcium-mediated 14% and 12% maximum quenching of fluorescence in both the 170 kDa and 180 kDa polypeptides because the tryptophan residues of both the polypeptides are exposed to a more polar environment. The decrease in fluorescence also indicated that both the proteins undergo a transition from the folded state to an unfolded state in response to high calcium concentrations. This also indicated that the calcium-mediated tertiary structural change may play an important biological role. The calcium requirements for tertiary structural change in both the 170 kDa and 180 kDa were higher than was required for the secondary structural change. This indicated that both the

polypeptides undergo a calcium-mediated two step structural change that may modulate their biological function.

In addition, the endogenous tryptophan fluorescence study showed that, in the presence of 200 µM calcium, only a 2.5% decrease in fluorescence was evident in the 180 kDa species, while an approximate 7% decrease was evident with the 170 kDa polypeptide (Fig. 3.15 A and B, respectively). This also supported the idea that the 170 kDa species is more sensitive to a calcium-dependent secondary structural change than the 180 kDa species (Fig. 3.12 and Fig. 3.13, respectively). Both the 170- and 180 kDa induce two-step structural changes in a calcium-dependent manner. In the first step, both the proteins undergo a secondary structural change in the presence of calcium. In the second step, both the polypeptides undergo a tertiary structural change in the presence of higher concentrations of calcium. The 180 kDa requires more calcium than the 170 kDa to undergo a conformational change, possibly because the polypeptides may have a different calcium binding affinity, which may further modulate their biological functions.

We further characterized the metal binding capacity of these proteins by analyzing the effects of zinc on the tertiary conformation of 170 kDa and 180 kDa polypeptides. Both the 170 kDa and 180 kDa polypeptides induce a tertiary conformational change in response to zinc, characterized by a maximum quenching in fluorescence by 17.5% and 16.5%, respectively (Fig. 3.16 A and B, respectively). The apparent dissociation constant (zinc) was 13.1- and 15.6 µM for the 170 kDa and 180 kDa, respectively. These data indicated that the 170- and 180 kDa species have the same weak affinity for zinc, but both

the proteins were nevertheless able to induce a zinc-mediated tertiary structural change. In contrast, the study conducted by Unuma et al., (2007) concluded that the 180 kDa species contains more zinc-binding sites than 170 kDa and may act as a zinc transporter. However, our results suggested that both polypeptides have the same affinity to zinc.

4.3. The calcium-driven structural transitions of the reducible forms of the major yolk protein present in the egg (170 kDa) and coelomic fluid (180 kDa) are required to mediate liposome binding and vesicular aggregation.

In this study, we first compared the liposome binding ability of both the reducible forms of MYP present in the egg (170 kDa) and coelomic fluid (180 kDa) in a calcium-dependent manner. We found that both the MYP (170 kDa and 180 kDa) undergo structural changes in a calcium-dependent manner that could further mediate membrane-membrane interaction. The egg MYP drives a calcium-dependent secondary and tertiary structural change that is responsible for binding with liposome and vesicular aggregation (Hayley et al., 2006; Perera et al., 2004). Most of the proteins involved in membrane aggregation, fusion and intracellular transportation belong to the family of annexins, which are involved in binding with the acidic phospholipids in a calcium-dependent manner (Grewal et al., 2000; Filipenko and Wasiman, 2000; Mailliard et al., 1995; Boustead et al., 1993 & Spenneberg et al., 1998). Calcium binding provides positive charges for proteins, which can mediate acidic phospholipid binding (Lee et al., 1997; Spenneberg et al., 1998; Boustead et al., 1993; Filipenko and Waisman, 2000). Acidic and amide amino acids and the carbonyl oxygen atoms in peptide bonds are responsible

for calcium binding. Moreover, with a very weak affinity, the egg MYP binds with calcium and the calcium mediates a secondary structural change that facilitates interactions between the egg MYP and the phosphoserine head group (Hayley et al., 2006). These weak-affinity binding sites are occupied by calcium and actively modulate the biological functions of the MYP by modulating the structure of the MYP. Again, the sequence analysis study showed that the major yolk protein in the egg does not have any known high-affinity calcium-binding motifs, but did reveal a 27.11 M percentage content of acidic and amide residues, all potential low affinity calcium binding sites (Brooks & Wessel 2002).

The egg MYP (240 kDa) undergoes vesicular aggregation through embryonic development (Perera et al., 2004). We were interested in biochemically characterizing and comparing the phospholipid binding and vesicular aggregating activities of the reducible form of MYP present in both the egg (170 kDa) and the coelomic fluid (180 kDa). There is a high likelihood that the calcium binds with both the egg MYP (170 kDa) and coelomic fluid MYP (180 kDa) followed by a structural change that drives both the proteins to bind and aggregate liposomes.

Perera et al., (2004) and Hayley et al. (2006) showed that a maximum binding of 25% was observed at a calcium concentration of 200 μM, with an apparent dissociation constant (calcium) of 25 μM and the percentage of bound protein remained constant at 25% in the presence of calcium concentrations above 200 μM. In our study we also found evidence of binding between the reducible form of egg MYP (170 kDa) and

liposome in a calcium-dependent manner, with an apparent dissociation constant (calcium) of approximately 10 μM (Fig. 3.18 A). This difference in apparent dissociation constant (calcium) with the previous studies is possibly because of different species of sea urchins. In the presence of 40 μM calcium, maximum 22% of the egg MYP (170 kDa) was bound to liposomes. This result supports the data published by Perera et al., (2004) and Hayley et al. (2006). On the other hand, in the presence of 800 μM calcium, a maximum 38% of the coelomic fluid MYP (180 kDa) was bound to liposomes, with an apparent dissociation constant (calcium) 290 μM (Fig. 3.18 B). The MYP localized in the egg and coelomic fluid were unable to bind with liposome in the absence of calcium, which indicated that a calcium responsive structural change is required to have binding between the liposome and the MYP localized in both the egg and the coelomic fluid. This result clearly indicated that the egg MYP (170 kDa) is more sensitive than the coelomic fluid MYP (180 kDa) to calcium. Probably calcium binding mediated a secondary structural change of the egg MYP (170 kDa) and the coelomic fluid MYP (180 kDa) followed by opening a secondary binding site for the phospholipid head groups. Moreover, the egg MYP interacts peripherally with the membrane, thus a calcium mediated tertiary structural change was required for the process of membrane aggregation.

This idea was supported by our data that indicated higher concentrations of calcium were required for a secondary structural change in the coelomic fluid MYP (180 kDa) than the egg MYP (170 kDa) to show binding with liposomes. Again, membrane binding may also promote rearrangement, dissociation, or conformational changes within many protein

structural domains, resulting in an activation of their biological activity. Both the egg MYP (170 kDa) and the coelomic fluid MYP (180 kDa) may have a difference in their calcium binding affinity, and thus may also have different biological functions.

In general, the net charge of the polar head group seems to be important for recruiting proteins to the membrane. However, the molecular interactions of the lipid head group with the protein also influence the affinity with which the protein binds with the lipid. In our liposome binding study we used brain lipid extract containing 50% (w/w) phosphatidyl serine. The egg yolk granule also contains 18.3% phosphatidyl serine (PS). Therefore, the difference in calcium induced liposome binding ability may also be because the coelomic fluid MYP (180 kDa) has less affinity to bind with the phosphatidyl serine (PS) head group than the egg MYP (170 kDa). In addition, as both the 170- and 180 kDa required different calcium concentrations to bind with liposomes, this also suggests that both the proteins can respond to a different spectrum of calcium concentration changes induced by different stimuli.

Moreover, in the absence of the egg MYP (240 kDa), liposome aggregation did not occur at calcium concentrations below 1.25 mM, while in the presence of the egg MYP (240 kDa), liposome aggregation occurred at greatly reduced concentrations of calcium (Perera et al., 2004; Hayley et al., 2006). The aggregation was mediated by the calcium dependent tertiary structural changes of the egg MYP (240 kDa) with an apparent dissociation constant of 240 μM.

We also determined and compared the effect of calcium on liposome aggregation in the presence of the egg (170 kDa) or the coelomic fluid MYP (180 kDa). We found that in the absence of calcium, both the egg MYP (170 kDa) and the coelomic fluid MYP (180 kDa) were not able to aggregate liposomes (Fig. 3.19 A and B, respectively). The initial rate of liposome aggregation was exponentially increased with the increase of calcium concentrations for both the 170- and 180 kDa species (Fig. 3.20 A and B, respectively). Again, the egg MYP (170 kDa) showed more sensitivity to the increasing amount of calcium than the coelomic fluid MYP (180 kDa). The initial rate of aggregation was higher for the egg MYP (170 kDa) than the coelomic fluid MYP (180 kDa), which indicated that the MYP localized in coelomic fluid (180 kDa) required higher concentrations of calcium than the MYP localized in egg (170 kDa) to induce the conformational change required for membrane-membrane interactions. The coelomic fluid MYP may have required more calcium for its translocation to the membrane. It is also possible that the coelomic fluid MYP (180 kDa) required higher concentrations of calcium to induce tertiary structural change. In our study, we found that in the presence of both the egg (170 kDa) and the coelomic fluid MYP (180 kDa) with different concentrations of calcium, there is a steady increase in aggregation activity until a plateau is reached (Fig. 3.19 A and B, respectively). Again, Kanungo, (1982) showed that in vitro coelomocyte clumping in sea stars is mediated by an unknown factor present in the coelomic fluid that requires calcium and/or magnesium. The coelomocytes were unable to aggregate in the presence of 0.23 mM calcium and 0.50 mM magnesium. In the presence of 0.45 mM calcium coelomocytes undergo biphasic aggregation, consisting of a fast phase followed by a slow phase. We assume that the unknown factor is the MYP

localized in the coelomic fluid (180 kDa), which required high concentrations of calcium to induce tertiary structural change to mediate liposome aggregation. According to our study, the coelomic fluid MYP (180 kDa) mediated liposome aggregation rate was high at a calcium concentration of 500- and 850 μM, which supports the idea of Kanungo (1982) (Fig. 3.19 B). The liposome aggregation buffer contains 0.5 mM magnesium. However, the egg MYP (240 kDa) does not have any interaction with magnesium (Hayley et al., 2008). This indicates a need for further comparative analysis of the effect of magnesium on egg MYP (170 kDa) and coelomic fluid MYP (180 kDa).

In our study, we also found that both the MYP localized in egg (170 kDa) and coelomic fluid (180 kDa) drives two-phase liposome aggregation in a calcium dependent manner. In an initial phase occurring during the first 4-minute period after adding protein, the liposome aggregation rate is high. this is followed by a slow occurring second phase during the last 6-minute period. This is possible because the interactions between the MYP localized in the egg (170 kDa) or coelomic fluid (180 kDa) with liposome may affect the structural and dynamic properties of the lipid bilayer.

A positive correlation was also observed between the change in tertiary structure of the MYP present in egg (170 kDa) and coelomic fluid (180 kDa) with the liposome aggregation activity driven by both polypeptides in a calcium dependent manner (Fig. 3.21 A and B, respectively). This data further confirms that a change in the tertiary structure of the egg MYP (170 kDa) and the coelomic fluid (180 kDa) is required to mediate membrane-membrane interactions.

4.4. Conclusion.

The research carried out by Hayley et al. (2006, 2008) and Perera et al. (2004) clearly demonstrated that the major yolk protein present in the egg undergoes a calcium-driven structural transition which may mediate membrane-membrane interaction. Again, major yolk proteins are also localized in the coelomic fluid of the adult sea urchin, which contains coelomocytes. Reports suggested that coelomocytes play an immune effector role, such as in the formation of cellular clots, phagocytosis, encapsulation, wound repair, etc; all of which require an adhesive activity (Matranga. 1996; Matranga et al., 2005). Moreover, sea water is a very hostile environment which contains 10 mM calcium. Injury occurring in the plasma membrane is a common event in sea water, and requires resealing to maintain cell viability. The influx of 10 mM calcium is more than enough to induce secondary and tertiary structural change in both the egg MYP (170 kDa) and coelomic fluid MYP (180 kDa), and thus may facilitate membrane-membrane interaction to repair the plasma membrane.

We have identified and compared the biochemical characteristics of the major yolk proteins present in the egg and coelomic fluid of the Strongylocentrotus droebachiensis. The results presented here for the egg MYP (170 kDa) support the findings of Hayley et al. (2006, 2008) and Perera et al. (2004). Our results show that the reducible forms of the MYP present in the egg (170 kDa) and the coelomic fluid (180 kDa) have the ability to bind with calcium. Both the 170 kDa and 180 kDa polypeptides have the ability to bind and aggregate liposomes in a calcium-dependent manner, so that they may participate in

signaling pathways that regulate key cellular processes. Kanungo (1982) suggested that the in vitro coelomocyte aggregation is mediated by an unknown factor in the presence of calcium. Coelomocyte clumping is a defense mechanism in sea star and sea urchin during stress conditions. We think that the coelomic fluid MYP may also participate in coelomocyte aggregation in response to stress conditions and play an immune effector role in the sea urchin. However, the 180 kDa protein is more dependent on calcium concentrations than the 170 kDa one. Low concentrations of calcium induce a change in secondary structure of both the egg MYP (170 kDa) and the coelomic fluid MYP (180 kDa) that facilitates binding with phospholipids. Both the 170 kDa and 180 kDa polypeptides were able to aggregate liposomes in the presence of higher concentrations of calcium. Moreover, higher concentrations of calcium can induce a tertiary structural change in both the egg MYP (170 kDa) and coelomic fluid MYP (180 kDa) which are correlated with the ability to facilitate membrane-membrane interactions. Our study suggested that under physiological conditions, the biological functions of both the 170 kDa and 180 kDa can be regulated by calcium. We suggest that, under stress conditions, the coelomic fluid MYP may incorporate with the coelomocyte membrane in a calcium-dependent manner and plays an immune effector role by mediating membrane-membrane interactions.

In summary, we can conclude that the coelomic fluid MYP and the egg MYP are different from each other regarding their affinity for lipids and calcium. Both of them may be involved in a wide range of intra- and extracellular biological processes for example,

membrane trafficking, membrane-cytoskeleton interaction, ion channel activity and regulation, as well as antiinflammatory and anticoagulant activities.

4.5. Future directions.

In our observation, both the egg MYP (170 kDa) and coelomic fluid MYP (180 kDa) bind and aggregate liposomes in a calcium-dependent manner. Both the proteins may participate in calcium-regulated cell adhesions, plasma membrane repair, endocytosis, cell signaling, etc. The egg MYP (170 kDa) is peripherally located with the plasma membrane, and thus may also participate in membrane fusion events, export pathways, vesicle trafficking and ion channel formation. Both the egg MYP (170 kDa) and coelomic fluid MYP (180 kDa) undergo a conformational change during membrane-membrane interactions in a calcium-dependent manner. There may be two possible mechanisms by which the MYP present in the egg and coelomic fluid can induce membrane-membrane interactions: A) both the polypeptides may generate a second binding site for the protein of the opposing membrane, thus mediating protein-protein interaction, and allowing the opposing membranes to interact; or B) both the polypeptides may expose a second membrane binding site in a calcium-dependent manner. Future experiments can be designed to investigate the mechanism of MYP-mediated membrane-membrane interaction. We can utilize cryo-electron microscopy of aggregated lipid vesicles in the presence of the egg MYP or the coelomic fluid MYP, both in the presence and in the absence of calcium.

Our study showed that the initial rate of liposome aggregation is higher in the egg MYP than the coelomic fluid MYP in a calcium-dependent manner. Again phosphorylation and proteolysis negatively regulate vesicular aggregation in annexin family proteins (Kaetzel et al., 2001). In the future we can investigate the effect of phsophorylation and proteolysis on biological functions of the MYP localized in the egg and coelomic fluid. We can induce phosphorylation in both the egg MYP and coelomic fluid MYP by using protein kinase C and then investigate their regulation on membrane-membrane interactions. We can also compare the trypsin digestion patterns of free and vesicle-bound proteins between the egg MYP and coelomic fluid MYP both in the absence and in the presence of calcium. These will also further prove that both the proteins undergo conformational changes in the course of vesicle binding and aggregation.

In our study, we found that the coelomic fluid MYP is more dependent on calcium for liposome binding and aggregation than the egg MYP. The phospholipid composition of the egg yolk granule may be different than the coelomocytes. To determine whether phsopholipid composition had an effect on aggregation, vesicles composed of different phospholipids, such as vesicles containing brain or synthetic PS, or 1,2-di-(9Z-octadecenoyl)-sn-glycero-3-phosphate (DOPA) or 1,2-dioleoyl-sn-glycero-3-[phospho-rac-(1-glycerol)] (DOPG), can be incubated with both the egg MYP and the coelomic fluid MYP and assayed for aggregation.

Our data showed that the coelomic fluid MYP (180 kDa) required higher concentrations of calcium to induce secondary and tertiary structural change to facilitate liposome

binding and aggregation. We can do a comparative analysis between the egg MYP and coelomic fluid MYP by quantifying the calcium binding sites on the MYP present in the egg and in the coelomic fluid. The egg MYP also binds with magnesium, barium, cadmium and manganese as well as iron in vitro (Brooks and Wessel, 2002; Hayley et al., 2008). We can also perform endogenous tryptophan fluorescence study with the coelomic fluid MYP incubated with magnesium, barium, cadmium and manganese.

Our data suggested that the coelomic fluid MYP (180 kDa) undergoes little or no change in the presence of 200 μM calcium and it required higher concentrations of calcium than the egg MYP (170 kDa) for tertiary structural change, liposome binding and vesicular aggregation. To determine the calcium concentration dependency effect on the secondary structural change of both the egg MYP (170 kDa) and the coelomoic fluid MYP (180 kDa), and to correlate between the secondary structural change and liposome binding, we can perform CD analysis by using different concentrations of calcium.

In addition, we know that the near UV region (320-260 nm) reflects the environments of the aromatic side chains and, thus gives information about the tertiary structure of the protein. Circular dichroism spectroscopy can be utilized to determine the tertiary conformational changes of the egg MYP and coelomic fluid MYP in the presence of higher concentrations of calcium than are required for secondary structural changes. In addition, our data suggested that the 240-, 250- and 180 kDa species induce changes in shape in the presence of Triton X-100, which may involve a change in their secondary and/or tertiary structures. Circular dichrosim can be performed to probe the

conformational changes of the egg MYP and coelomic fluid MYP in the presence of Triton X-100.

Nuclear magnetic resonance studies can be used to determine the site of interaction of the coelomic fluid MYP with the coelomocyte membrane. As each of the MYP required different amounts of calcium for their biological functions, this indicated that both the polypeptides may act as an intracellular calcium sensor with a regulatory role to other signaling pathways.

To determine the ability of calcium to modulate the stability of the egg MYP (reducible and non-reducible form), we can perform a thermal denaturation study. We can then compare the thermal stability of both the egg MYP (both reducible and non-reducible forms) and the coelomic fluid MYP (both reducible and non-reducible forms) in the presence and absence of calcium.

Plasma membrane disruption is a common form of cell injury, which occurs due to stress. As both the MYP are able to bind and aggregate liposomes, both of the polypeptides may also play an important role in membrane repair. A redistribution of the egg MYP and coelomic fluid MYP may also occur at the disruption site. Therefore, in future to confirm the biological role of the egg MYP and the coelomic fluid MYP, we can utilize an in vivo comparative analysis by using live embryos, coelomocytes, or cultured cells, which express egg MYP and coelomic fluid MYP. Perera et al. (2004) showed that anti-egg MYP antibodies can inhibit phospholipid binding and vesicular aggregation. We can use

this anti-egg MYP or anti-coelomic fluid MYP antibody in in vivo assays by using wounded or ruptured cells to observe their effect on the cells. We can also localize the MYP presence on the wounded site by immunostaining.

Coelomocytes play an immune effector role in the sea urchin. There is a possibility that the coelomic fluid MYP may also modulate anti-inflammatory responses induced by lipopolysaccharide. In future, we can employ an in vivo assay by using cultured coelomocytes to discover how coelomic fluid MYP modulates the MAPK/ERK pathways.

References

Angerer, L., Hussain, S., Wei, Z., & Livingston, B. T. (2006). Sea urchin metalloproteases: A genomic survey of the BMP-1/tolloid-like, MMP and ADAM families. Developmental Biology, 300(1), 267-281. doi:10.1016/j.ydbio.2006.07.046

Armant, D. R. D. (1986). Characterization of yolk platelets isolated from developing embryos of arbacia punctulata. BMC Developmental Biology, 113(2), 342-355.

Baker, E. N., & Lindley, P. F. (1992). New perspectives on the structure and function of transferrins. Journal of Inorganic Biochemistry, 47(3-4), 147-160.

Baker, E. E. (1987). Transferrins: Insights into structure and function from studies on lactoferrin. Trends in Biochemical Sciences (Amsterdam.Regular Ed.), 12, 350-353.

Baker, H. M., Anderson, B. F., & Baker, E. N. (2003). Dealing with iron: Common structural principles in proteins that transport iron and heme. Proceedings of the National Academy of Sciences of the United States of America, 100(7), 3579-3583. doi:10.1073/pnas.0637295100

Bartfeld, N. S., & Law, J. H. (1990). Isolation and molecular cloning of transferrin from the tobacco hornworm, manduca sexta. sequence similarity to the vertebrate transferrins. The Journal of Biological Chemistry, 265(35), 21684-21691.

Becker, J., & Craig, E. A. (1994). Heat-shock proteins as molecular chaperones. European Journal of Biochemistry, 219(1-2), 11-23. doi:10.1111/j.1432-1033.1994.tb19910.x

Bertheussen, K. K. (1978). Echinoid phagocytes in vitro. Experimental Cell Research, 111(2), 401-412.

Boldt, D. H. (1999). New perspectives on iron: An introduction. The American Journal of the Medical Sciences, 318(4), 207-212.

Boustead, C. M., Brown, R., & Walker, J. H. (1993). Isolation, characterization and localization of annexin V from chicken liver. The Biochemical Journal, 291 (Pt 2), 601-608.

Brooks, J. M., & Wessel, G. M. (2002). The major yolk protein in sea urchins is a transferrin-like, iron binding protein. Developmental Biology, 245(1), 1-12. doi:10.1006/dbio.2002.0611

Brooks, J. M., & Wessel, G. M. (2003). Selective transport and packaging of the major yolk protein in the sea urchin. Developmental Biology, 261(2), 353-370.

Brooks, J. M., & Wessel, G. M. (2004). The major yolk protein of sea urchins is endocytosed by a dynamin-dependent mechanism. Biology of Reproduction, 71(3), 705-713. doi:10.1095/biolreprod.104.027730

Buchner, J. (1996). Supervising the fold: Functional principles of molecular chaperones. FASEB Journal : Official Publication of the Federation of American Societies for Experimental Biology, 10(1), 10-19.

Cervello, M., Arizza, V., Lattuca, G., Parrinello, N., & Matranga, V. (1994). Detection of vitellogenin in a subpopulation of sea urchin coelomocytes. European Journal of Cell Biology, 64(2), 314-319.

Cervello, M., & Matranga, V. (1989). Evidence of a precursor-product relationship between vitellogenin and toposome, a glycoprotein complex mediating cell adhesion. Cell Differentiation and Development : The Official Journal of the International Society of Developmental Biologists, 26(1), 67-76.

Cho, W. L., Tsao, S. M., Hays, A. R., Walter, R., Chen, J. S., Snigirevskaya, E. S., & Raikhel, A. S. (1999). Mosquito cathepsin B-like protease involved in embryonic degradation of vitellin is produced as a latent extraovarian precursor. The Journal of Biological Chemistry, 274(19), 13311-13321.

Cleveland, D. W., Fischer, S. G., Kirschner, M. W., & Laemmli, U. K. (1977). Peptide mapping by limited proteolysis in sodium dodecyl sulfate and analysis by gel electrophoresis. The Journal of Biological Chemistry, 252(3), 1102-1106.

Cooper, A. D., & Crain, W. R. (1982). Complete nucleotide sequence of a sea urchin actin gene.Nucleic Acid Research, 10 (13),4081-4092.

Costello, D. P. (1939). The volumes occupied by the formed cytoplasmic components in marine eggs. Physiological Zoology, 12(1), 13-21.

Cox, K. H., Angerer, L. M., Lee, J. J., Davidson, E. H., & Angerer, R. C. (1986). Cell lineage-specific programs of expression of multiple actin genes during sea urchin embryogenesis. Journal of Molecular Biology, 188(2), 159-172.

Crain, W. R.,Jr, Durica, D. S., & Van Doren, K. (1981). Actin gene expression in developing sea urchin embryos. Molecular and Cellular Biology, 1(8), 711-720.

Crichton, R. R., & Charloteaux-Wauters, M. (1987). Iron transport and storage. European Journal of Biochemistry, 164(3), 485-506. doi:10.1111/j.1432-1033.1987.tb11155.x

Cleveland, D.W., Fischer, S.G., Kirschner, M.W. & Laemmli, U.K. (1977). Peptide mapping by limited proteolysis in sodium dodecyl sulfate and analysis by gel electrophoresis. Journal of Biological Chemistry, 252(3), 1102.

Davidson, E. H., Rast, J. P., Oliveri, P., Ransick, A., Calestani, C., Yuh, C. H., Minokawa, T., Amore, G., Hinman, V., Arenas-Mena, C. et al. (2002). A genomic regulatory network for development. Science 295, 1669-1678.

Dheilly, N. M., Nair, S. V., Smith, L. C., & Raftos, D. A. (2009). Highly variable immune-response proteins (185/333) from the sea urchin, strongylocentrotus purpuratus: Proteomic analysis identifies diversity within and between individuals. Journal of Immunology, 182(4), 2203-2212. doi:10.4049/jimmunol.07012766

Falchuk, K. H., & Montorzi, M. (2001). Zinc physiology and biochemistry in oocytes and embryos. Biometals : An International Journal on the Role of Metal Ions in Biology, Biochemistry, and Medicine, 14(3-4), 385-395.

Fasoli, E., D'Amato, A., Righetti, P. G., Barbieri, R., & Bellavia, D. (2012). Exploration of the sea urchin coelomic fluid via combinatorial peptide ligand libraries. The Biological Bulletin, 222(2), 93-104.

Fausto, A. M., Gambellini, G., Mazzini, M., Cecchettini, A., Masetti, M., & Giorgi, F. (2001). Yolk granules are differentially acidified during embryo development in the stick insect carausius morosus. Cell and Tissue Research, 305(3), 433-443.

Filipenko, N. R., Kang, H. M., & Waisman, D. M. (2000). Characterization of the Ca2+-binding sites of annexin II tetramer. The Journal of Biological Chemistry, 275(49), 38877-38884. doi:10.1074/jbc.M004125200

Fuji, A. (1960). Studies on the biology of the sea urchin: I: Superficial and histological gonadal changes in gametogenic process of two sea urchins, Strongylocentrotus nudus and S. intermedius. Bull. Fac. Fish. Hokkaido University, 11(1), 1-14.

Gerardi, P., Lassegues, M., & Canicatti, C. (1990). Cellular distribution of sea urchin antibacterial activity. Biology of the Cell, 70(3), 153-157. doi:10.1016/0248-4900(90)90372-A

Giga, Y., & Ikai, A. (1985). Purification and physical chemical characterization of 23S glycoprotein from sea urchin (Anthocidaris crassipinia) eggs. Journal of Biochemistry, 98(1), 237-243.

Giorgi, F., Yin, L., Cecchettini, A., & Nordin, J. H. (1997). The vitellin-processing protease of blattella germanica is derived from a pro-protease of maternal origin. Tissue & Cell, 29(3), 293-303.

Gratwohl, E. K., Kellenberger, E., Lorand, L., & Noll, H. (1991). Storage, ultrastructural targeting and function of toposomes and hyalin in sea urchin embryogenesis. Mechanisms of Development, 33(2), 127-138.

Grewal, T., Heeren, J., Mewawala, D., Schnitgerhans, T., Wendt, D., Salomon, G., Enrich, C., Beisiegel, U., Jäckle, S. (2000). Annexin VI stimulates endocytosis and is involved in the trafficking of low density lipoprotein to the prelysosomal compartment. The Journal of Biological Chemistry, 275(43), 33806-33813. doi:10.1074/jbc.M002662200

Gross, P. R., Philpott, D. E., & Nass, S. (1960). Electron microscopy of the centrifuged sea urchin egg, with a note on the structure of the ground cytoplasm. The Journal of Biophysical and Biochemical Cytology, 7(1), 135-142.

Gross, P. S., Al-Sharif, W. Z., Clow, L. A., & Smith, L. C. (1999). Echinoderm immunity and the evolution of the complement system. Developmental and Comparative Immunology, 23(4), 429-442. doi:10.1016/S0145-305X(99)00022-1

Haley S.A, & Wessel G.M. (1999). The cortical granule serine protease CGSP1 of the sea urchin, strongylocentrotus purpuratus, is autocatalytic and contains a low-density lipoprotein receptor-like domain. Developmental Biology, 211(1), 1-10. doi:10.1006/dbio.1999.9299

Harrington, F. E., & Ozaki, H. (1986). The major yolk glycoprotein precursor in echinoids is secreted by coelomocytes into the coelomic plasma. Cell Differentiation, 19(1), 51-57.

Harrington, F. F. (1982). A putative precursor to the major yolk protein of the sea urchin. Developmental Biology, 94(2), 505-508.

Harvey, E. N. (1932). Physical and chemical constants of the egg of the sea urchin, arbacia punctulata. Biological Bulletin, 62(2), 141-154.

Haug, T., Kjuul, A. K., Styrvold, O. B., Sandsdalen, E., Olsen, Ø. M., & Stensvåg, K. (2002). Antibacterial activity in strongylocentrotus droebachiensis (echinoidea), cucumaria frondosa (holothuroidea), and asterias rubens (asteroidea). Journal of Invertebrate Pathology, 81(2), 94-102. doi:10.1016/S0022-2011(02)00153-2

Hayley, M., Perera, A., & Robinson, J. J. (2006). Biochemical analysis of a Ca2+-dependent membrane-membrane interaction mediated by the sea urchin yolk granule protein, toposome. Development, Growth & Differentiation, 48(6), 401-409. doi:10.1111/j.1440-169X.2006.00872.x

Hayley, M., Sun, M., Merschrod, E. F., Davis, P. J., & Robinson, J. J. (2008). Biochemical analysis of the interaction of calcium with toposome: A major protein component of the sea urchin egg and embryo. Journal of Cellular Biochemistry, 103(5), 1464-1471. doi:10.1002/jcb.21531

Himmelman, J. H. (1975). Phytoplankton as a stimulus for spawning in three marine invertebrates. Journal of Experimental Marine Biology and Ecology, 20(2), 199-214. doi:10.1016/0022-0981(75)90024-6

Howard-Ashby, M., Materna, S. C., Brown, C. T., Chen, L., Cameron, R. A., & Davidson, E. H. (2006). Gene families encoding transcription factors expressed in early development of strongylocentrotus purpuratus. Developmental Biology, 300(1), 90-107. doi:10.1016/j.ydbio.2006.08.033

Ichio, I., Deguchi, K., Kawashima, S., Endo, S., & Ueta, N. (1978). Water-soluble lipoproteins from yolk granules in sea urchin eggs. I. isolation and general properties. Journal of Biochemistry, 84(4), 737-749.

Infante, A. A., & Nemer, M. (1968). Heterogeneous ribonucleoprotein particles in the cytoplasm of sea urchin embryos. Journal of Molecular Biology, 32(3), 543-565. doi:10.1016/0022-2836(68)90342-2

Kaetzel, M. A., Mo, Y. D., Mealy, T. R., Campos, B., Bergsma-Schutter, W., Brisson, A., Dedmen, J.R., Seaton, B. A. (2001). Phosphorylation mutants elucidate the

mechanism of annexin IV-mediated membrane aggregation. Biochemistry, 40(13), 4192-4199. doi:10.1021/bi002507s

Kanungo, K. (1982). In vitro studies on the effects of cell-free coelomic fluid, calcium, and/or magnesium on clumping of coelomocytes of the sea star asterias forbesi (echinodermata: Asteroidea). Biological Bulletin, 163(3), 438-452.

Kari, B. E., & Rottmann, W. L. (1985). Analysis of changes in a yolk glycoprotein complex in the developing sea urchin embryo. Developmental Biology, 108(1), 18-25.

Kato, K. H., & Ishikawa, M. (1982). Flagellum formation and centriolar behavior during spermatogenesis of the sea urchin, hemicentrotus pulcherrimus. Acta Embryologiae Et Morphologiae Experimentalis ("Halocynthia" Association"), 3(1), 49-66.

Kelly, S. M., & Price, N. C. (2000). The use of circular dichroism in the investigation of protein structure and function. Current Protein & Peptide Science, 1(4), 349-384.

Kobayashi, N. (1980). Comparative sensitivity of various developmental stages of sea urchins to some chemicals. Marine Biology, 58(3), 163-171.

Kurama, T., Kurata, S., & Natori, S. (1995). Molecular characterization of an insect transferrin and its selective incorporation into eggs during oogenesis. European Journal of Biochemistry, 228(2), 229-235.

Laemmli, U. K. (1970). Cleavage of structural proteins during the assembly of the head of bacteriophage T4. Nature, 227(5259), 680-685.

Lambert, L. A., Perri, H., & Meehan, T. J. (2005). Evolution of duplications in the transferrin family of proteins. Comparative Biochemistry and Physiology.Part B, Biochemistry & Molecular Biology, 140(1), 11-25. doi:10.1016/j.cbpc.2004.09.012

Smith, L.C., Rast, J.P., Brockton, V., Terwilliger, D.P., Nair, S.V., Buckley, K.M., & Majeske, A.J. (2006). The sea urchin immune system. Invertebrate Survival Journal, 3(1), 25-39.

Lee, G., & Pollard, H. B. (1997). Highly sensitive and stable phosphatidylserine liposome aggregation assay for annexins. Analytical Biochemistry, 252(1), 160-164. doi:10.1006/abio.1997.2311

Lee, G. F., Fanning, E. W., Small, M. P., & Hille, M. B. (1989). Developmentally regulated proteolytic processing of a yolk glycoprotein complex in embryos of the sea urchin, strongylocentrotus purpuratus. Cell Differentiation and Development : The Official Journal of the International Society of Developmental Biologists, 26(1), 5-17.

Lee, J. J., Shott, R. J., Rose, S. J., Thomas, T. L., Britten, R. J., & Davidson, E. H. (1984). Sea urchin actin gene subtypes. Journal of Molecular Biology, 172(2), 149-176. doi:10.1016/S0022-2836(84)80035-2

Legrand, D., Mazurier, J., Montreuil, J., & Spik, G. (1988). Structure and spatial conformation of the iron-binding sites of transferrins. Biochimie, 70(9), 1185-1195.

Li, C., Haug, T., Styrvold, O. B., Jørgensen, T. Ø., & Stensvåg, K. (2008). Strongylocins, novel antimicrobial peptides from the green sea urchin, strongylocentrotus droebachiensis. Developmental and Comparative Immunology, 32(12), 1430-1440. doi:10.1016/j.dci.2008.06.013

Liao, Y. D., & Wang, J. J. (1994). Yolk granules are the major compartment for bullfrog (rana catesbeiana) oocyte-specific ribonuclease. European Journal of Biochemistry, 222(1), 215-220.

Louis-Jeune, C., Andrade-Navarro, M. A., & Perez-Iratxeta, C. (2011). Prediction of protein secondary structure from circular dichroism using theoretically derived spectra. Proteins,80, 374-381 doi:10.1002/prot.23188; 10.1002/prot.23188

Lowry, O.H., Rosebrough, N.J., Farr, A.L., & Randall, R.J. (1951). Protein measurement with the folin phenol reagent. The Journal of Biological Chemistry, 193(1), 265-275.

Majeske, A. J., Bayne, C. J., & Smith, L. C. (2013). Aggregation of sea urchin phagocytes is augmented in vitro by lipopolysaccharide. PloS One, 8(4), e61419. doi:10.1371/journal.pone.0061419

Malkin, L. L. (1965). A crystalline protein of high molecular weight from cytoplasmic granules in sea urchin eggs and embryos. Developmental Biology, 12(3), 520; 520-542; 542.

Mallya, S. K., Partin, J. S., Valdizan, M. C., & Lennarz, W. J. (1992). Proteolysis of the major yolk glycoproteins is regulated by acidification of the yolk platelets in sea urchin embryos. The Journal of Cell Biology, 117(6), 1211-1221.

Mann, K., Wilt, F. H., & Poustka, A. J. (2010). Proteomic analysis of sea urchin (strongylocentrotus purpuratus) spicule matrix. Proteome Science, 8(1), 33. doi:10.1186/1477-5956-8-33

Masuda, R. (1977). Studies on the annual reproductive cycle of the sea urchin and the acid phosphatase activity of relict ova. The Biological Bulletin (Lancaster), 153(3), 577-590.

Matranga, V., Bonaventura, R., & Di Bella, G. (2002). Hsp70 as a stress marker of sea urchin coelomocytes in short term cultures. Cellular and Molecular Biology (Noisy-Le-Grand, France), 48(4), 345-349.

Matranga, V., Kuwasaki, B., & Noll, H. (1986). Functional characterization of toposomes from sea urchin blastula embryos by a morphogenetic cell aggregation assay. The EMBO Journal, 5(12), 3125-3132.

Matranga, V., Pinsino, A., Celi, M., Bella, G. D., & Natoli, A. (2006). Impacts of UV-B radiation on short-term cultures of sea urchin coelomocytes. Marine Biology, 149(1), 25-34. doi:10.1007/s00227-005-0212-1

Matranga, V., Pinsino, A., Celi, M., Natoli, A., Bonaventura, R., Schroder, H. C., & Muller, W. E. (2005). Monitoring chemical and physical stress using sea urchin immune cells. Progress in Molecular and Subcellular Biology, 39, 85-110.

Matranga, V., Toia, G., Bonaventura, R., & Muller, W. E. (2000). Cellular and biochemical responses to environmental and experimentally induced stress in sea urchin coelomocytes. Cell Stress & Chaperones, 5(2), 113-120.

Mayne, J., & Robinson, J. J. (1998). The sea urchin egg yolk granule is a storage compartment for HCL-32, an extracellular matrix protein. Biochemistry and Cell Biology = Biochimie Et Biologie Cellulaire, 76(1), 83-88.

Mayne, J., & Robinson, J. J. (2002). Localization and functional role of a 41 kDa collagenase/gelatinase activity expressed in the sea urchin embryo. Development, Growth & Differentiation, 44(4), 345-356.

McNeil, P. L., & Steinhardt, R. A. (1997). Loss, restoration, and maintenance of plasma membrane integrity. The Journal of Cell Biology, 137(1), 1-4.

McNeil, P. L., Vogel, S. S., Miyake, K., & Terasaki, M. (2000). Patching plasma membrane disruptions with cytoplasmic membrane. Journal of Cell Science, 113 (Pt 11), 1891-1902.

Medina, M., Leon, P., & Vallejo, C. G. (1988). Drosophila cathepsin B-like proteinase: A suggested role in yolk degradation. Archives of Biochemistry and Biophysics, 263(2), 355-363.

Monroy, A., & Maggio, R. (1964). Biochemical studies on the early development of the sea urchin. Advances in Morphogenesis, 4, 95-145.

Morale, A., Coniglio, L., Angelini, C., Cimoli, G., Bolla, A., Alleteo, D., Russo, C. & Falugi, C. (1998). Biological effects of a neurotoxic pesticide at low concentrations on sea urchin early development. A terathogenic assay. Chemosphere, 37(14-15), 3001-3010.

Moss, C. (1998). Patterns of bromodeoxyuridine incorporation and neuropeptide immunoreactivity during arm regeneration in the starfish asterias rubens. Philosophical Transactions.Biological Sciences, 353(1367), 421-436.

Nappi, A. J., & Vass, E. (2000). Iron, metalloenzymes and cytotoxic reactions. Cellular and Molecular Biology (Noisy-Le-Grand, France), 46(3), 637-647.

Nishioka, D., Marcell, V., Cunningham, M., Khan, M., Von Hoff, D. D., & Izbicka, E. (2003). The use of early sea urchin embryos in anticancer drug testing. Methods in Molecular Medicine, 85, 265-276. doi:10.1385/1-59259-380-1:265

Noll, H., Alcedo, J., Daube, M., Frei, E., Schiltz, E., Hunt, J., Humphries, T., Matranga, V., Hochstrasser, M., Aebersold, R., Lee, H. & Noll, M. (2007). The toposome, essential for sea urchin cell adhesion and development, is a modified iron-less calcium-binding transferrin. Developmental Biology, 310(1), 54-70. doi:10.1016/j.ydbio.2007.07.016

Noll, H., Matranga, V., Cervello, M., Humphreys, T., Kuwasaki, B., & Adelson, D. (1985). Characterization of toposomes from sea urchin blastula cells: A cell organelle mediating cell adhesion and expressing positional information. Proceedings of the National Academy of Sciences of the United States of America, 82(23), 8062-8066.

Noll, H., Matranga, V., Palma, P., Cutrono, F., & Vittorelli, L. (1981). Species specific dissociation into single cells of live sea urchin embryos by fab against membrane components of paracentrotus lividus and arbacia lixula. Developmental Biology, 87(2), 229-241.

Nomura, K., Hoshino, K., & Suzuki, N. (1999). The primary and higher order structures of sea urchin ovoperoxidase as determined by cDNA cloning and predicted by homology modeling. Archives of Biochemistry and Biophysics, 367(2), 173-184. doi:10.1006/abbi.1999.1219

Overbeek, P. A., Merlino, G. T., Peters, N. K., Cohn, V. H., Moore, G. P., & Kleinsmith, L. J. (1981). Characterization of five members of the actin gene family in the sea urchin. Biochimica Et Biophysica Acta, 656(2), 195-205.

Ozaki, H. (1980). Yolk proteins of the sand dollar dendraster-excentricus. Development, Growth & Differentiation, 22(3), 365-372.

Ozaki, H. (1986). A glycoprotein in the accessory cell of the echinoid ovary and its role in vitellogenesis. Wilhelm Roux's Archives of Developmental Biology, 195(1), 74-79.

Ozretic, B., & Krajnovic-Ozretic, M. (1985). Morphological and biochemical evidence of the toxic effect of pentachlorophenol on the developing embryos of the sea urchin. Aquatic Toxicology, 7(4), 255-263. doi:10.1016/0166-445X(85)90043-8

Pancer, Z. (2000). Dynamic expression of multiple scavenger receptor cysteine-rich genes in coelomocytes of the purple sea urchin. Proceedings of the National Academy of Sciences of the United States of America, 97(24), 13156-13161. doi:10.1073/pnas.230096397

Parcellier, A., Gurbuxani, S., Schmitt, E., Solary, E., & Garrido, C. (2003). Heat shock proteins, cellular chaperones that modulate mitochondrial cell death pathways. Biochemical and Biophysical Research Communications, 304(3), 505-512. doi:10.1016/S0006-291X(03)00623-5

Pederson, T. (2006). The sea urchin's siren. Developmental Biology, 300 (1), 9-14.

Perera, A., Davis, P., & Robinson, J. J. (2004). Functional role of a high mol mass protein complex in the sea urchin yolk granule. Development, Growth & Differentiation, 46(2), 201-211. doi:10.1111/j.1440-169X.2004.00737.x

Petrunkevitch, A., 1875-1964.Morphology of invertebrate types, by alexander petrunkevitch Macmillan company.

Pinsino, A., Thorndyke, M. C., & Matranga, V. (2007). Coelomocytes and post-traumatic response in the common sea star asterias rubens. Cell Stress & Chaperones, 12(4), 331-341.

Poccia, D., Lieber, T., & Childs, G. (1989). Histone gene expression during sea urchin spermatogenesis: An in situ hybridization study. Molecular Reproduction and Development, 1(3), 219-229. doi:10.1002/mrd.1080010310

Ramos, I., & Wessel, G. M. (2013). Calcium pathway machinery at fertilization in echinoderms. Cell Calcium, 53(1), 16-23. doi:10.1016/j.ceca.2012.11.011; 10.1016/j.ceca.2012.11.011

Rast, J. P., Smith, L. C., Loza-Coll, M., Hibino, T., & Litman, G. W. (2006). Genomic insights into the immune system of the sea urchin. Science, 314(5801), 952-956. doi:10.1126/science.1134301

Reunov, A. A., Yurchenko, O. V., Kalachev, A. V., & Au, D. W. T. (2004). An ultrastructural study of phagocytosis and shrinkage in nutritive phagocytes of the sea

urchin anthocidaris crassispina. Cell and Tissue Research, 318(2), 419-428. doi:10.1007/s00441-004-0901-y

Russo, R., Zito, F., Costa, C., Bonaventura, R., & Matranga, V. (2010). Transcriptional increase and misexpression of 14-3-3 epsilon in sea urchin embryos exposed to UV-B. Cell Stress and Chaperones, 15(6), 993-1001. doi:10.1007/s12192-010-0210-1

Schuel, H. H. (1974). Sulfated acid mucopolysaccharides in the cortical granules of eggs. Experimental Cell Research, 88(1), 24-30.

Schuel, H. H. (1975). Heterogeneous distribution of "lysosomal" hydrolases in yolk platelets isolated from unfertilized sea urchin eggs by zonal centrifugation. Developmental Biology, 46(2), 404-412.

Schuler, M. A., McOsker, P., & Keller, E. B. (1983). DNA sequence of two linked actin genes of sea urchin. Molecular and Cellular Biology, 3(3), 448-456.

Sconzo, G., Romancino, D., Fasulo, G., Cascino, D., & Giudice, G. (1995). Effect of doxorubicin and phenytoin on sea urchin development. Die Pharmazie, 50(9), 616-619.

Scott, L. B., Leahy, P. S., Decker, G. L., & Lennarz, W. J. (1990). Loss of yolk platelets and yolk glycoproteins during larval development of the sea urchin embryo. Developmental Biology, 137(2), 368-377.

Scott, L. B., & Lennarz, W. J. (1989). Structure of a major yolk glycoprotein and its processing pathway by limited proteolysis are conserved in echinoids. Developmental Biology, 132(1), 91-102.

Semenova, M. N., Kiselyov, A., & Semenov, V. V. (2006). Sea urchin embryo as a model organism for the rapid functional screening of tubulin modulators. Biotechniques, 40(6), 765-774. doi:10.2144/000112193

Shyu, A. B., Raff, R. A., & Blumenthal, T. (1986). Expression of the vitellogenin gene in female and male sea urchin. Proceedings of the National Academy of Sciences of the United States of America, 83(11), 3865-3869.

Smith, L. C., Chang, L., Britten, R. J., & Davidson, E. H. (1996). Sea urchin genes expressed in activated coelomocytes are identified by expressed sequence tags. complement homologues and other putative immune response genes suggest immune system homology within the deuterostomes. Journal of Immunology, 156(2), 593-602.

Sodergren, E, Weinstock, G.M., Davidson, E.H., Cameron, R.A., Gibbs, R.A, et al. (2006) The genome of the sea urchin Strongylocentrotus purpuratus. Science 314, 941–952.

Somers, C. E., Battaglia, D. E., & Shapiro, B. M. (1989). Localization and developmental fate of ovoperoxidase and proteoliaisin, two proteins involved in fertilization envelope assembly. Developmental Biology, 131(1), 226-235.

Spenneberg, R., Osterloh, D., & Gerke, V. (1998). Phospholipid vesicle binding and aggregation by four novel fish annexins are differently regulated by Ca^{2+}. Biochimica Et Biophysica Acta (BBA) - Molecular Cell Research, 1448(2), 311-319. doi:10.1016/S0167-4889(98)00131-1

Stabili, L., Pagliara, P., & Roch, P. (1996). Antibacterial activity in the coelomocytes of the sea urchin paracentrotus lividus. Comparative Biochemistry and Physiology, Part B, 113(3), 639-644. doi:10.1016/0305-0491(95)02080-2

Starr, M., Himmelman, J., & Therriault, J. (1992). Isolation and properties of a substance from the diatom phaeodactylum-tricornutum which induces spawning in the sea-urchin strongylocentrotus-droebachiensis. Marine Ecology Progress Series, 79(3), 275-287.

Tamm, L. K., Crane, J., & Kiessling, V. (2003). Membrane fusion: A structural perspective on the interplay of lipids and proteins. Current Opinion in Structural Biology, 13(4), 453-466.

Terasaki, M., Miyake, K., & McNeil, P. L. (1997). Large plasma membrane disruptions are rapidly resealed by Ca^{2+}-dependent vesicle-vesicle fusion events. The Journal of Cell Biology, 139(1), 63-74. doi:10.1083/jcb.139.1.63

Terwilliger, D. P., Buckley, K. M., Mehta, D., Moorjani, P. G., & Smith, L. C. (2006). Unexpected diversity displayed in cDNAs expressed by the immune cells of the

purple sea urchin, strongylocentrotus purpuratus. Physiological Genomics, 26(2), 134-144. doi:10.1152/physiolgenomics.00011.2006

Tominaga, A., & Takashima, Y. (1987). Ultracytochemical study on the behavior of the nurse cell giant granules in the sea urchin ovary. Acta Histochemica Et Cytochemica, 20(5), 569-579. doi:10.1267/ahc.20.569

Tsukahara, J. (1971). Electron microscopic studies on the behavior of glycogen particles during oogenesis in the sea urchin. Development, Growth & Differentiation, 13(4), 367-378.

Unuma, T., Ikeda, K., Yamano, K., Moriyama, A., & Ohta, H. (2007). Zinc-binding property of the major yolk protein in the sea urchin - implications of its role as a zinc transporter for gametogenesis. The FEBS Journal, 274(19), 4985-4998. doi:10.1111/j.1742-4658.2007.06014.x

Unuma, T., Konishi, K., Kiyomoto, M., Matranga, V., Yamano, K., Ohta, H., & Yokota, Y. (2009). The major yolk protein is synthesized in the digestive tract and secreted into the body cavities in sea urchin larvae. Molecular Reproduction and Development, 76(2), 142-150. doi:10.1002/mrd.20939; 10.1002/mrd.20939

Unuma, T., Nakamura, A., Yamano, K., & Yokota, Y. (2010). The sea urchin major yolk protein is synthesized mainly in the gut inner epithelium and the gonadal nutritive phagocytes before and during gametogenesis. Molecular Reproduction and Development, 77(1), 59-68. doi:10.1002/mrd.21103; 10.1002/mrd.21103

Unuma, T., Sawaguchi, S., Yamano, K., & Ohta, H. (2011). Accumulation of the major yolk protein and zinc in the agametogenic sea urchin gonad. The Biological Bulletin, 221(2), 227-237.

Unuma, T., Yamamoto, T., Akiyama, T., Shiraishi, M., & Ohta, H. (2003). Quantitative changes in yolk protein and other components in the ovary and testis of the sea urchin pseudocentrotus depressus. The Journal of Experimental Biology, 206(Pt 2), 365-372.

Unuma, T. (2001). Cloning of cDNA encoding vitellogenin and its expression in red sea urchin, pseudocentrotus depressus. Zoological Science, 18(4), 559-565.

Unuma T. (2002). Gonadal growth and its relationship to aquaculture in sea urchins. In: YokotaY, MatrangaV, SmolenickaZ, editors.The sea urchin: From basic biology to aquaculture. Lisse: Swets & Zeitlinger. pp. 115–127.

Unuma, T., K. Konishi, H. Furuita, T. Yamamoto, and T. Akiyama. 1996. Seasonal changes in gonads of cultured and wild red sea urchin, Pseudocentrotus depressus. Suisanzoshoku 44(2): 169-175.

Unuma, T., Suzuki, T., Kurokawa, T., Yamamoto, T., & Akiyama, T. (1998). A protein identical to the yolk protein is stored in the testis in male red sea urchin, pseudocentrotus depressus. Biological Bulletin, 194(1), 92-97.

Walker, C.W. (2007). Edible sea urchins: Biology and ecology chapter 2 gametogenesis and reproduction of sea urchins. Developments in Aquaculture and Fisheries Science, 37, 11-33.

Walker, C.W., Harrington, L.M., Lesser, M.P., & Fagerberg, W.R. (2005). Nutritive phagocyte incubation chambers provide a structural and nutritive microenvironment for germ cells of strongylocentrotus droebachiensis, the green sea urchin. The Biological Bulletin, 209(1), 31-48.

Walker,C.W. 1982. Nutrition of gametes. In: JangouxM, LawrenceJM, editors. Echinoderm nutrition. Rotterdam: Balkema. pp.449–468.

Wang, J. J., Tang, P. C., Chao, S. H., Cheng, C. H., Ma, H. J., & Liao, Y. D. (1995). Immunocytochemical localization of ribonuclease in yolk granules of adult rana catesbeiana oocytes. Cell and Tissue Research, 280(2), 259-265.

Ward, R.D., & Nishioka, D. (1993). Seasonal changes in testicular structure and localization of a sperm surface glycoprotein during spermatogenesis in sea urchins. The Journal of Histochemistry and Cytochemistry : Official Journal of the Histochemistry Society, 41(3), 423-431. doi:10.1177/41.3.8429205

Wessel, G.M., Berg, L., Adelson, D.L., Cannon, G., & McClay, D.R. (1998). A molecular analysis of hyalin--a substrate for cell adhesion in the hyaline layer of the sea urchin embryo. Developmental Biology, 193(2), 115-115. doi:10.1006/dbio.1997.8793

Wessel, G.M., Zaydfudim, V., Hsu, Y.J., Laidlaw, M., & Brooks, J.M. (2000). Direct molecular interaction of a conserved yolk granule prostein in sea urchins. Development, Growth & Differentiation, 42(5), 507-517.

William S. Mailliard, Harry T. Haigler, & David D. Schlaepfer. (1996). Calcium-dependent binding of S100C to the N-terminal domain of annexin I. Journal of Biological Chemistry, 271(2), 719-725. doi:10.1074/jbc.271.2.719

Yamaguchi, S., Miura, C., Kikuchi, K., Celino, F. T., Agusa, T., Tanabe, S., & Miura, T. (2009). Zinc is an essential trace element for spermatogenesis. Proceedings of the National Academy of Sciences of the United States of America, 106(26), 10859-10864. doi:10.1073/pnas.0900602106; 10.1073/pnas.0900602106

Yokota, Y. (1993). Morphological and biochemical-studies on yolk degradation in the sea-urchin, hemicentrotus-pulcherrimus. Zoological Science, 10(4), 661-670.

Yokota, Y., Unuma, T., Moriyama, A., & Yamano, K. (2003). Cleavage site of a major yolk protein (MYP) determined by cDNA isolation and amino acid sequencing in sea urchin, hemicentrotus pulcherrimus. Comparative Biochemistry and Physiology.Part B, Biochemistry & Molecular Biology, 135(1), 71-81.

Yokota, Y., & Kato, K. H. (1988). Degradation of yolk proteins in sea urchin eggs and embryos. Cell Differentiation, 23(3), 191-199. doi:10.1016/0045-6039(88)90071-1

Yoshiga, T., Georgieva, T., Dunkov, B. C., Harizanova, N., Ralchev, K., & Law, J. H. (1999). Drosophila melanogaster transferrin. cloning, deduced protein sequence, expression during the life cycle, gene localization and up-regulation on bacterial infection. European Journal of Biochemistry, 260(2), 414-420.

Zito, F., Burke, R. D., & Matranga, V. (2010). Pl-nectin, a discoidin family member, is a ligand for ßC integrins in the sea urchin embryo. Matrix Biology, 29(5), 341-345. doi:10.1016/j.matbio.2010.02.005